SCALABLE CULTURE SYSTEMS FOR EXPANSION AND DIRECTED DIFFERENTIATION OF RAT MULTIPOTENT ADULT PROGENITOR CELLS

A DISSERTATION

SUBMITTED TO THE FACULTY OF THE GRADUATE SCHOOL

OF THE UNIVERSITY OF MINNESOTA

BY

Yonsil Park

IN PARTIAL FULFILLMENT OF THE REQUIREMENTS

FOR THE DEGREE OF

DOCTOR OF PHILOSOPHY

Adviser: Wei-Shou Hu and Catherine Verfaillie

May 2010

Acknowledgements

I am heartily thankful to my advisers, Prof. Wei-Shou Hu and Prof. Catherine Verfaillie, whose encouragement, guidance and support from the initial to the final level enabled me to develop an understanding of stem cell science and engineering. I would like to also thank Prof. Meri Firpo for being a mentor at SCI. Her practical advice helped me go on to a next level.

It was an honor for me to work with many great people. I would like to thank former and current Hu group members for their help and support. Especially Kartik and Jason have been such wonderful lab mates who taught me how to carefully set up experiments and critically evaluate data throughout discussion. Also, without people at SCI, my study here would have not been easily started or continued. I thank April, SM, and Yeuhua for getting me started on stem cell experiments, and many others for making their help available in many ways.

For those who are outside the lab and school but still supported to make this thesis possible, I thank my parents for always listening and supporting so close from the other side of the earth, my brother for sharing crazy thoughts and stimulating me to challenge for something new, and my friends especially DH, DK and Y^2 for being there for me whenever I would like to laugh and discuss life with them.

Lastly, I send my regards and blessings to all of those who supported me in any respect during the completion of the project.

Yonsil Park

Dedication

To

My Family

For their support, for their understanding, and for their love

Abstract

Advances in stem cell science have stimulated the prospect of stem cells as therapeutics. For the translation of stem cell research to technology, robust and efficient expansion and differentiation is essential. Rat multipotent adult progenitor cells (rMAPCs) are a type of adult stem cells isolated from the rodent bone marrow. MAPCs can be expanded *in vitro* without obvious senescence, and are capable of differentiating into cell types of mesoderm, endoderm, and ectoderm *in vitro*. They are typically maintained surface adherent at low cell densities of 100-300 cells/cm^2 in order to maintain their broad potency, which would make scale-up for further clinical applications cumbersome. In this study, we explored different cultivation methods to investigate the feasibility of scalable culture systems for rMAPCs: (1) high density 2D culture, stirred bioreactor culture as (2) 3D aggregates and (3) on microcarriers.

Culturing cells under hypoxic condition (5% O_2) during the isolation, has yielded rMAPC expressing high levels of the embryonic stem cell specific transcription factor *Oct4*, which is associated with their greater potency. First, the effect of oxygen tension and cell density on the growth rate and potency of MAPC were examined. MAPC exhibited an increased growth rate at hypoxic conditions (5%) than at normoxic conditions (21%). Furthermore, when inoculated at a cell density of 1000 cells/cm^2, MAPC exhibited a small but significant increase in growth rate compared to cells seeded at 300 cells/cm^2 at both oxygen levels, though the difference was more pronounced under hypoxic

conditions. The Oct4 mRNA or protein expression level and the ability of MAPC to differentiate towards endothelium- and hepatocyte-, and neuroectoderm-like cells were shown to be unaffected by cultivation at a higher cell density and/or oxygen tension for 48 days (1000 cells/cm^2; 21% O_2; with subculturing every 48 hr). The results provide evidence that MAPC isolated under hypoxic conditions and expressing high levels of Oct4 can be readily cultured at a higher cell density without any apparent loss of potency.

Encouraged by MAPCs ability to grow at high density, we explored aggregate formation of MAPC for cell expansion as well as differentiation. Culture in aggregates may be an ideal method to allow large scale expansion, if combined with bioreactor cultures. Time lapse microscopy revealed three stages during the initial period of aggregate formation: agglomeration, compaction, and expansion. Compared to cells from adherent culture, significantly more cells from 3D culture are in G0/G1 phase and fewer in S phase suggesting a partial restriction in cell proliferation possibly due to spatial restriction in aggregates. There was no significant difference in *Oct4* level and aggregate size when aggregation was at 5% or 21% O_2 after 4 day culture. However, aggregation at 21% O_2 increased the percent of cells in G0/G1 and increased expression of early differentiation markers such as *Flk1* and *Afp*. Cultivation of MAPC aggregates in stirred bioreactor lead to a 70-fold expansion in six days with final cell densities of about 10^6 cells/ml. Importantly, the MAPC aggregates recovered from stirred bioreactors could be differentiated to hepatocyte-like cells that expressed *Albumin*, *Aat*, *Tat* transcripts and also secreted albumin and urea.

We then employed a microcarrier culture system for the expansion of undifferentiated MAPC as well as for directed differentiation of these cells to hepatocyte-like cells. During the four-day expansion culture, cell concentration increased by 85-fold while expression level of pluripotency markers were maintained, as well as the MAPC differentiation potential. Directed differentiation into hepatocyte-like cells on the microcarriers themselves gave comparable results as that observed with cells cultured in static cultures. The cells expressed several mature hepatocyte-lineage genes and asialoglycoprotein receptor-1 (ASGPR-1) surface protein, and secreted albumin and urea.

Lastly, the experience with MAPC microcarrier culture was extended to human embryonic stem cell (hESC) microcarrier culture. hESCs as small clumps were attached to Matrigel-coated microcarriers and expanded 10-fold during 4 day static culture. The level of pluripotency-related genes, *OCT4* and *SOX2*, were maintained compared to day 0 cells. The cells expanded on microcarriers underwent hepatic differentiation to increase hepatic genes such as *AFP* and *ALBUMIN*.

Both aggregate and microcarrier cultivation methods for scalable expansion combined with differentiation can potentially be used to generate large numbers of MAPC and MAPC-derived differentiated cells. These culture systems thus offer the potential of large-scale expansion and differentiation of stem cells in a more controlled bioreactor environment.

Table of Contents

List of Tables

List of Figures

CHAPTER 1. INTRODUCTION

1.1. Stem cells

1.1.1. Definition

A stem cell is defined by its unique ability to (1) self-renew, (2) have the potential to differentiate into multiple cell types, and (3) functionally reconstitute and maintain a given tissue *in vivo* [1]. Common conception of stem cells can be explained by their self-renewal characteristic of dividing indefinitely without senescence and by differentiation capability of providing a large numbers of progeny. The types of progeny determine the developmental potential, or potency, of a stem cell: totipotency, pluripotency, multipotency, or unipotency. Totipotency is the capacity to generate all cell types found in the embryo including the extra-embryonic components such as trophoblast and placenta [2]. Pluripotency is the capacity to generate all somatic and germ cells types found in embryonic and adult organisms [3]. Embryonic stem cells (ESCs), induced pluripotent stem cells (iPSCs), and some rare adult stem cells are pluripotent stem cells. Multipotency is the limited capacity to develop multiple differentiated cell types, but typically all within a particular tissue. Adult stem cells such as hematopoietic stem cells (HSCs), neural stem cells (NSCs), and mesenchymal stem cells (MSCs) belong to the category of multipotent stem cells. Lastly, unipotent cells such as endothelial precursor cells or skeletal muscle stem cells can produce only one cell type [2, 4]. Pluripotency or multipotency is an important characteristic to demonstrate during stem cell derivation or isolation and is what makes stem cells a promising resource for regenerative medicine and biotechnology applications.

1.1.2. Types of stem cells

1.1.2.1. Embryonic stem cells (ESCs)

ESCs are pluripotent cells that proliferate extensively and are capable of generating all three somatic germ layers of ectoderm, mesoderm and endoderm. ESCs were first derived from the inner cell mass (ICM) of blastocyst stage in murine embryo in the early 1980s [5], and human ESCs were first derived in 1998 [6]. Mouse and human ESCs (m/h ESCs) are usually derived and maintained with the co-culture of irradiated mouse embryonic fibroblasts (MEFs) as a feeder layer. They grow in colonies; small size, compactness, a clear boundary of colonies, and a high nucleus to cytoplasm ratio are morphological indications of undifferentiated ESC colonies. To date, many transcription factors, regulators, and genes have found to regulate and maintain ESC pluripotency. Undifferentiated ESCs express a set of cell surface antigens such as SSEA1 (mouse), SSEA3, SSEA4, TRA1-60, and TRA1-81 (human), and the intrinsic transcription factors such as *Oct4*, *Sox2*, and *Nanog*. These three transcription factors are important markers to demonstrate and regulate pluripotent identity of ESCs. *Oct4*, or *Pou5F1*, is one of the most important factors indicative of ESC pluripotency. It is highly expressed in the ICM of the early blastocyst *in vivo*, and becomes down-regulated as the embryo development proceeds [7]. In adult, *Oct4* is expressed in oocytes and spermatogonial germ cells. *In vitro*, *Oct4* expression level should be maintained within a certain range in order to maintain undifferentiated ESCs. More than two-fold up-regulation in *Oct4* level induces commitment of mESC to primitive endoderm and mesoderm while more than two-fold down-regulation causes decrease in potency and differentiation including commitment to

trophectodetm [8]. For mESCs, the extrinsic signal from the cytokine leukemia inhibitory factor (LIF) is also needed. LIF is a member of the interleukin-6-related cytokine family. LIF binds with low-affinity to the LIFRß, which then heterodimerize with gp130 to for the high-affinity and signaling-competent complex [9]. LIF/LIFRß induces phosphorylation of tyrosine kinase, Janus Kinase (JAK), and this leads to the phosphorylation of Singal transducer and activator of transcription-3 (STAT3). STAT3 phosphorylation further induces target genes such as *c-Myc* which has anti-apoptotic and pro-mitogenic properties [10]. STAT3 phosphorylation is essential and sufficient to maintain mouse ESC pluripotency in serum contained medium [11]. However, LIF does not maintain pluripotency of hESCs. The differential effect may be due to the different developmental stage upon derivation of mESCs or hESCs [12].

Upon the removal of signals that keep ESCs undifferentiated, in the culture environment preventing cell-surface adherence, ESCs spontaneously aggregate into embryoid bodies (EBs), and then differentiate into three germ layers recapitulating embryonic development [13]. Similarly, when injected *in vivo* and uncontrolled in immunodeficient mice, ESCs differentiate and develop into multi-cellular masses forming teratocarcinomas. Another differentiation method is to induce directed differentiation without forming EBs. A monolayer of ESCs alone or with the support of extracellular matrix (ECM) proteins or stromal cells undergoes differentiation guided by signals including soluble factors, cell-cell contact, and/or mechanical stimuli. Although pluripotency of ESCs is clearly a benefit to produce different types of cells of all three

germ layers, it also makes the design of differentiation to a specific cell lineage more difficult. Combinations of many growth factors, which are adopted from developmental and cell culture studies, are supplemented to direct ESCs into a specific pathway over another. Selection of a cell type of interest during or after differentiation process is another challenge. For clinical applications, techniques to avoid adverse immune response and teratoma formation need to be investigated.

1.1.2.2. Induced pluripotent stem cells (iPSCs)

Induced pluripotent stem cells (iPSCs) are cells produced by reprogramming of somatic cells to ESC-like cells by introducing forced expression of defined set of transcription factors and by culturing the cells under ESC culture condition. Initially cells were transduced with set of four transcription factors-*Oct4*, *Sox2*, *c-Myc* and *Klf4*- using murine retroviruses [14]. These retroviruses are naturally silenced in ESCs and iPSCs resulting iPSCs which maintain their pluripotency on their own after reprogramming. These four factors have been introduced to many types of human and mouse somatic cells such as fibroblasts, liver and stomach cells to produce iPSCs [14-19]. Other combinations of genes (*Oct4, Sox2, Klf4*; *Oct4, Sox2, n-Myc, Klf4*; *Oct4, Sox2, Lin28, Nanog*) were also applied mostly to substitute *Myc* and *Klf4* and also proven to induce iPSCs [19-21].

Oct4, *Sox2*, and *Nanog* have been known to play an important role in maintaining pluripotency. *c-Myc*, a target gene of STAT3 and many others, promotes DNA replication which allows relaxation of the chromatin structure and provides an opportunity for the somatic genome to reset its epigenetic state. *Klf4* directly represses p53 which is known

to suppress *Nanog* during ESC differentiation [22, 23]. *Klf4* also binds to the proximal promoters of *Oct4* target genes, such as *Lefty1*, and helps to activate *Oct4* and *Sox2* [24]. *c-Myc* and *Klf4* may allow cancer-like transformation of somatic cells by endowing cells an immortalized growth and rapid proliferation properties [25]. Elimination of *c-Myc* or *Klf4* still produced iPSCs with some modifications but with markedly lower efficiency [18, 21, 26, 27]. LIN28, an RNA binding protein, was found to be highly expressed in hESC, and down-regulated upon differentiation [28].

With the various option of starting cells, iPSC technology opens a new possibility of patient-specific cell therapy and avoids ethical dilemma of destroying human embryos. However, more studies should be followed to identify the yet undefined state of iPSCs compared to other types of stem cells and to overcome technical challenges that iPSCs face currently.

One of the critical issues of current iPSC study is to find how iPSCs are different from or similar to ESCs. Although some gene expression studies show that fully reprogrammed iPSCs are in a developmentally comparable stage as ESCs [16, 27], there exist differences in hESC lines and among different iPSC lines. More investigation is needed on how these differences would affect the stability of iPSCs in long term culture and differentiation.

Also, the derivation of iPSCs produces innumerable partially reprogrammed cells. While we want to reduce the partial integration of introduced transcription factors to increase

the derivation efficiency of fully reprogrammed iPSCs, it is also worthwhile to extensively study those partially reprogrammed cells to define their states. It is not known yet whether partially reprogrammed iPSCs fall in a developmental state or a non-developmental state [29]. If partially reprogrammed iPSCs truly belong somewhere along the developmental process between a somatic cell and an ESC, partially reprogrammed cells which already have some characteristics of a desired cell type may be more preferable for late stage differentiation than fully reprogrammed or primitive iPSCs. Therefore, as a choice, instead of creating iPSCs, reprogramming into adult cells or progenitor cells of a certain tissue could be more beneficial for cell therapy. Vierbuchen et al. recently showed that defined neural-lineage-specific TFs (*Ascl1*, *Brn2*, and *Myt1l*) can be used to directly induce rapid and efficient conversion of mouse embryonic and postnatal fibroblasts to functional neurons *in vitro* [30].

In addition to studying the various states of iPSC cell lines, there are several obstacles to overcome in regards to the efficiency and safety of iPSC production. Initial iPSCs were induced by retroviral transduction. Mice generated through the iPSC injection to blastocysts displayed a high prevalence of tumorigenesis, likely to be assicoated with the reactivation of c-Myc transgene expression [17]. For clinical applications, iPSCs should be free of any adverse potential from viral integration such as viral-mediated gene transfer and permanent integration of activated oncogenes. In order to solve the safety concern, non-viral carriers such as plasmids and small molecules have been studied to transfect iPSCs [16, 31]. Okita et al. used the repeated transfection of cells with two

expression plamids [31]. Kaji et al. tried the excision the transgenes after reprogramming [32].

Both selection and transfection efficiency should be improved. So far, identifying iPSC colonies are dependent on selection markers which are pre-integrated into starting cells. Morphological criteria and gene expression patterns alone have been used to select iPSC colonies [20, 33]. Stem cells such as NSCs could be reprogrammed with better efficiency to produce iPSCs. NSCs, which endogeneously express *Sox2*, *c-Myc*, *Klf4*, alkaline phosphatase and SSEA-1, were shown to be more rapidly reprogrammed upon the four factor transduction [34]. In addition, *Oct4* alone was sufficient to induce the pluripotency [34].

1.1.2.3. Adult stem cells

Although most cells are committed to different cell types by the end of fetal development or shortly after birth, many adult tissues also undergo *in vitro* self-renewal in order to maintain homeostasis during life time. Adult stem cells are a type of stem cells that are isolated from different organs and tissues such as bone marrow, liver, skin, brain, peripheral blood, blood vessels and skeletal muscle. Compared to ESCs, most adult stem cells have limited self-renewal and differentiation capabilities. Being quiescent most of the time in tissues, adult stem cells interact with their tissue specific niche to produce and accept signals for maintenance or onset of differentiation. Hematopoietic stem cells (HSCs) are isolated from bone marrow and the most extensively studied adult stem cells. They differentiate into different blood cell types. Neural stem cells (NSCs) are isolated

from the central nervous system and the peripheral nervous system and cultured in neurosphere culture systems. NSCs have been shown to develop into neurons, astocytes, and oligodendrytes. Mesenchymal stem cells (MSCs) are another type that is mainly accessible from bone marrow. MSCs have a potential to differentiate into cell types of a connective tissue such as osteocytes, chondrocytes, myoblasts, fibroblasts, and adipocytes.

Lineage restriction of adult stem cells has been a commonly accepted thought, but some studies showed plasticity of stem cells that adult stem cells can also be differentiated into different lineages when placed in a particular microenvironment. HSCs may have the potential to differentiate into hepatocytes, myocytes, or neurons. Three mechanisms explain the plasticity. First, culture conditions may induce dedifferentiation or transdifferentiation of differentiated cells. Second, fusion with differentiated cells may give rise to the false appearance of plasticity. Third, there may be pluripotent stem cells persisting in adult tissues [2].

A number of adult stem cell populations with more extensive differentiation capacities have been reported to be isolated from bone marrow and other tissues. Human bone marrow derived stem cells (hBMSCs), marrow isolated adult multilineage inducible (MIAMI) cells, multipotent adult progenitor cells (MAPCs), and non-hematopoietic/endothelial SSEA-1^{pos} cells are isolated from the bone marrow, multipotent renal progenitor cells (MRPCs) from kidney, and very small ES like (VSEL)

cells and unrestricted somatic stem cells (USSCs) from cord blood. These cells are shown to have extended potency, but whether these cells pre-exist *in vivo* or are a culture phenomenon is yet to be determined. Nevertheless, obtaining cells with broad differentiation capacity from somatic tissues, without the need for addition of exogenous genes, may offer an alternative source of cells to study or compare self-renewal, differentiations and reprogramming mechanisms.

hBMSCs were clonally expanded cells from human BM, differentiate into the three germ layers and regenerate myocardium after myocardial infarction [35]. hBMSCs have been expanded for more than 140 population doublings without loss of multipotency. They are cultured in media containing 17% FBS and maintained at cell densities 4000-8000 cells/cm^2 on fibronectin coated plates. hBMSC do not express OCT4 and markers typical for MSCs such as CD90, CD117, CD105, MHC-I and II. The cells differentiate *in vitro* to cells with phenotype of neural and hepatic lineages. When transplanted to a myocardial infartion site, cells engrafted and expressed markers of cardiomyocytes, endothelial cells, and smooth muscle cells.

MIAMI cells are obtained by plating whole BM initially in media containing 5% fetal bovine serum (FBS) and are subsequently maintained in media containing 2% FBS in fibronectin coated dishes, at 3% O_2, and at cell densities between 1300-1400 cells/cm^2. MIAMI cells express high levels of CD29, CD63, CD81, CD122, CD164, hepatocyte growth factor receptor (cMET), Bone morphogenetic protein receptor 1B (BMPR1B), and Neurotrophic tyrosine kinase receptor 3 (NTRK3) and were negative for CD34,

CD36, CD45, CD117 (cKITR) and HLADR. They retain *Oct4*, *Rex1* expression, and telomerase, and can be expanded for more than 50 population doublings in culture. MIAMI cells are able to differentiate into osteoblasts, chondrocytes, adipocytes, neural cells, and attachment-independent spherical clusters expressing pancreatic islets-associated genes [36].

VSELs have been identified from murine BM and human cord blood by applying multi-parameter cell sorting to obtain a highly enriched cell population. They are SCA-$1^{pos}$with $CXCR4^{pos}$, $OCT4^{pos}$ and SSEA-1^{pos}(murine)/SSEA-4^{pos}(human) and LIN^{neg} and $CD45^{neg}$. VSEL express pluripotent stem markers such as *Oct4*, *Rex1* and *Nanog* as well as early tissue specific markers of the liver (*Afp*, *CK19*), muscle (*MyoD, Myf5*), neurons (*Gfap*), intestinal epithelium, skin epidermis, and endocrine pancreas. They are small cells with high nuclei to cytoplasm ratio, and have open-type chromatin (euchromatin) which is typical for ESCs. Murine VSEL are present the highest in BM of young mice, and cannot be expanded *ex vivo*. VSEL differentiate *in vitro* into all three germ layer lineages. Interestingly, these cells, like mESCs, respond by chemotaxis to SDF-1, HGF/SF and LIF gradients [37, 38].

USSCs, isolated from human cord blood, are $CD45^{neg}$, HLA class II^{neg} mononuclear cells with fibroblastic morphology. The cells were maintained for 40 population doublings without spontaneous differentiation. *In vitro* and *in vivo* studies have shown that USSCs differentiate into osteoblasts, chondroblasts, adipocytes, hematopoetic, hepatic, and

neural cells. [39].

Using an approach similar to MAPC, MRPCs were isolated from rat kidneys. They are spindle-shaped, expanded more than 200 population doublings without obvious senescence, and express *Vimentin*, *CD90*, *Pax2*, and *Oct4*. The high Oct4 MRPC clones differentiated into cells that have phenotypic features of endothelial, hepatocyte and neural lineages *in vitro* and into cells with the phenotype of renal tubular epithelium in both uninjured as well as injured kidneys *in vivo* [40].

In 2007, it was reported that non-hematopoietic/endothelial SSEA-1^{pos} (0.5-1% of all MSC) cells were isolated from the mesenchymal compartment of murine BM and defined as the primitive mesenchymal progenitor cells. The cells were selected, based on negative depletion of CD45/CD11b from adherent cultures or LIN/CD45/$CD31^{neg}$ from the whole BM, and the expression of SSEA-1^{pos}. They express *Oct4*, *Nanog*, and *Rex1*. Alternatively, the SSEA-1^{pos} cells could also be sorted from uncultured BM and were shown to express Oct4 and Nanog mRNA and protein. Similar to MAPCs, they differentiate at a single cell level into cells of the three germ layers *in vitro* and into multiple mesodermal cell types *in vivo*. MAPC culture conditions were used to maintain the cell phenotype and differentiation capabilities *in vitro*. In addition, SSEA-1^{pos} cells give rise to SSEA-1^{neg} fraction where as the reverse does not happen. It suggests that the Oct4 expressing cells were not the result of re-programming by culture conditions [41].

MAPCs are derived from rodent BM and have almost pluripotent characteristics. MAPCs

express high levels of the ESC-specific transcription factors such as *Oct4* and *Rex1* and differentiate into cells of mesoderm, ectoderm, and endoderm lineages. Since MAPCs are the main cell type that was studied in this thesis, it will be more extensively described in the next section.

Although many have reported *OCT4* expression in a number of adult stem cells and differentiated cells, these results should be carefully analized in order to link the expression to truly functional *OCT4* expression because of its pseudogenes. *OCT4* pseudogenes have been identified in human as well as in mouse [42-45]. Other pluripotenccy-related genes such as *NANOG* are also known to have several pseudogenes [46, 47]. Thus, there have been controversial arguments that *OCT4* and *NANOG* expression previously assessed by RT-PCR may be due to the artifacts from its pseudogenes. Tools that can clearly distinguish between isoforms and pseudogenes still need to be further investigated. *OCT4* expressions in mouse and human somatic tissues were clarified by newly designed primers, which can exclude amplification of its pseudogenes [48, 49].

1.2. Multipotent Adult Progenitor Cells (MAPC)

In 2002, multipotent adult progenitor cells (MAPCs) were isolated from rat, mouse and human bone marrow and were shown to have the capacity to self-renew without senescence, to differentiate at a clonal level to cells of the mesoderm, neuroectoderm and endoderm *in vitro*, and to contribute to functional reconstitution of somatic cells *in vivo*. In addition to bone marrow, mMAPCs have also been isolated from muscle and brain [50]. Isolation, characterization, and differentiation capacity of MAPCs are discussed in the following sections.

1.2.1. Isolation of MAPCs

1.2.1.1. Human MAPC isolation

Human MAPCs are isolated from bone marrow mononuclear cells by magnetic column depletion of $CD45^{pos}$ and $GLYA^{pos}$ cells and then plated on to fibronectin coated surface in MAPC culture medium (described in detail in method section of other chapters) until small colonies of adherent cells were observed after 7 to 21 days in culture [51].

1.2.1.2. Rodent MAPC isolation

Isolation of MAPC from rodent bone marrow is a labor intensive and lengthy procedure taking about three months. Every BM isolation does not guarantee the successful derivation of a qualified MAPC cell line. Rodent MAPCs are isolated based on a similar protocol as hMAPC isolation, where bone marrow cells were magnetic column depleted of $CD45^{pos}$ and $TER119^{pos}$ cells and subcloned in the MAPC medium at 5-10 cells/well.

Since the initial isolation of MAPCs, there have been changes in the isolation methods, most notably decreasing the ambient oxygen levels to 5% during the isolation process. The modified protocol consists of plating the bone marrow cells at high density on the fibronectin coated plates in 5% O_2 and 6% CO_2 for 1 month before column depletion and then subcloned at 1-5 cells/well [52]. This change yielded cells with more stable phenotype and genotype for prolonged periods of culture *in vitro*. In addition, MAPCs expressed significantly higher levels of Oct4 than the cells isolated under normoxic conditions. In addition, more modifications have been made to better define the isolation process [53]. rMAPC-1 and rMAPC-2, used in this thesis, were isolated using the modified isolation protocol.

rMAPC lines have been isolated from Fisher rats. The isolation process can be subdivided into three steps: BM cell expansion, column depletion of BM cells, and expansion of the cells at low cell density to identify MAPC. Figure 1 describes the schematic of rMAPC isolation process. The third step, the expansion of the column depleted cells is critical and requires some expertise. During the expansion, several candidate cell populations are selected based on morphology. Cells should look small, compact and not fibroblastic. Selected cells are cultured at low cell density to separate the cell colonies and detect the rise of MAPC-like cell colonies after 4-6 weeks of expansion. Different cell lines undergo series of assays to be identified as MAPC.

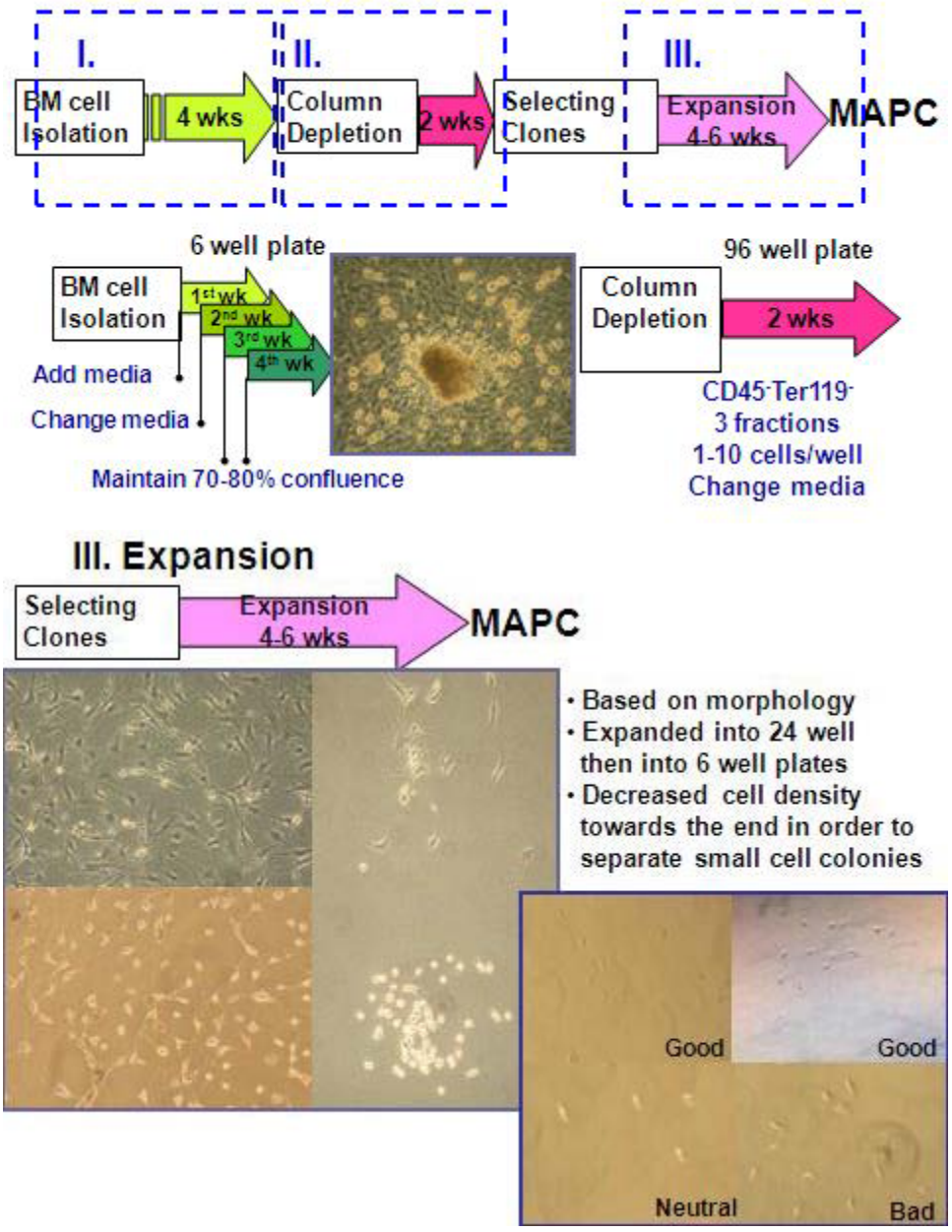

Figure 1. Schematic of rMAPC isolation process and morphologies of different cell populations observed during the isolation. I. Expansion of BM cells; II. Column depletion; III. Expansion of cells.

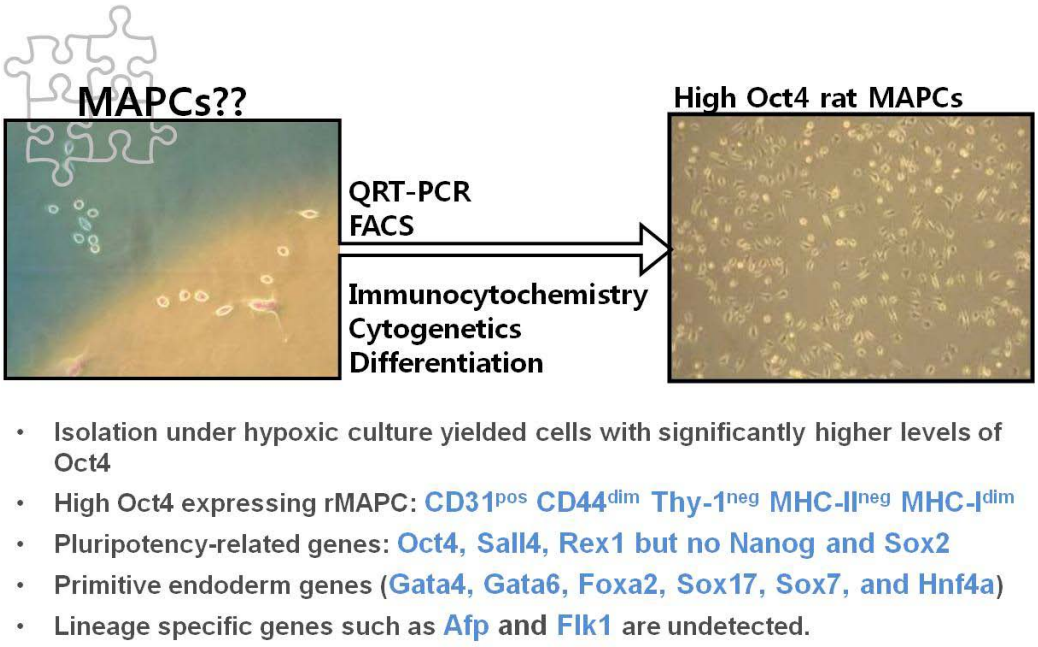

Figure 2. Phenotype of high Oct4 expressing rMAPC.

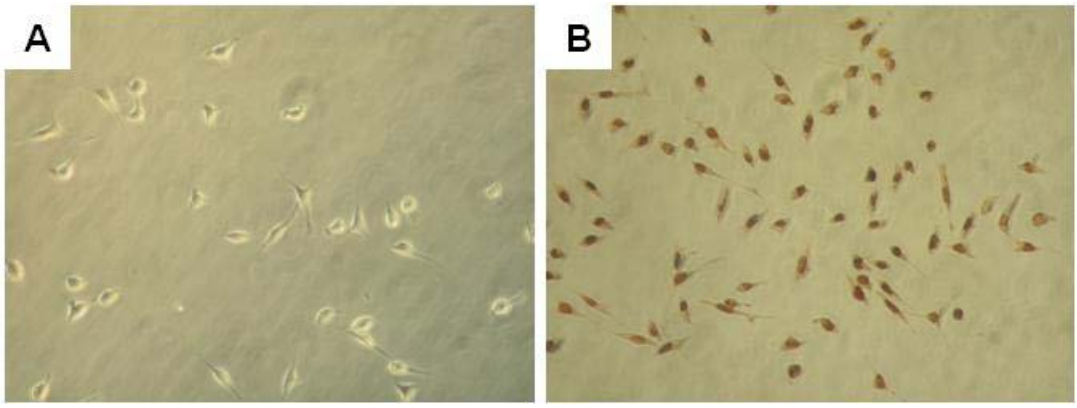

Figure 3. Immunocytochemical staining for intracellular OCT4 protein in rMAPC-2. (a) Isotype control. (b) OCT4 antibody.

1.2.2. Characterization of MAPC

Several expandable cell lines are obtained during the isolation process, but they are not identical. *Oct4* expression varies between deltaCT to *Gapdh* of 5 to 15. MAPC express high levels of Oct4 at the mRNA and protein level, but do not express *Nanog* or *Sox2*. For rat MAPCs, the phenotype is $CD44^{neg}$, $CD45^{neg}$, MHC-I^{neg} and MHC-II^{neg}, but $CD31^{pos}$. The phenotype of mouse MAPCs is $B220^{neg}$, $CD3^{neg}$, $CD15^{neg}$, $CD31^{neg}$, $CD34^{neg}$, $CD44^{neg}$, $CD45^{neg}$, $CD105^{neg}$, $THY1.1^{neg}$, $SCA\text{-}1^{neg}$, $E\text{-}CADHERIN^{neg}$, MHC-I^{neg} and MHC-II^{neg}, $EPCAM^{dim}$ and C-KIT^{pos}, VLA-6^{pos} and $CD9^{pos}$. MSC-like cells isolated under similar conditions express no or low levels of OCT4 and $CD44^{pos}$ and MHC-I^{pos} and C-KIT^{neg} (mouse) and $CD31^{neg}$ (rat). This clearly indicates the difference in phenotype between MAPCs and the closely related MSCs isolated under similar culture conditions.

A transcriptome analysis was performed to compare MAPCs with ESC, MSC and neurospheres (NS) in an attempt to identify a relationship between gene expression pattern and potency of MAPC and to obtain potential surface markers for MAPC[54]. Multivariate analysis techniques showed that MSCs and MSC-like cells isolated under MAPC conditions cluster closely together and significantly more distant from ESCs and NSCs than high Oct4 expressing MAPCs are from ESCs and NSCs. Pluripotency-related genes such as *Klf2*, *Klf4*, and *c-Myc* are expressed in MAPCs. Further, MAPCs express tissue committed genes such as transcripts of primitive endoderm (*Gata4*, *Gata6*, *Foxa2*, *Sox17*, *Sox7*, *Hnf4α*), also described in extra-embryonic cells lines [55], and mesoderm

(*Tefc*, *Myocd*, *Pitx2*). While some endoderm genes such as *Ttr* are expressed at low levels, the earliest primitive/definitive endoderm gene, Alpha-fetoprotein (*Afp*) is undetected in undifferentiated MAPC.

1.2.3. Differentiation of MAPCs to different lineages

Since the initial isolation of MAPCs in 2002, there were several reports on the differentiation of MAPCs to cells of the three germ layers: endoderm, ectoderm and mesoderm. MAPCs can differentiate to neuroectodermal cells [56], hepatocyte-like cells [57] and endothelial progenitors [51]. Subsequent to these, additional studies have shown that MAPCs can differentiate to various cell types, including arterial and venous specified endothelial cells, hepatocyte-like cells, beta-like cells, functional smooth-muscle cells and can reconstitute the hematopoietic system.

VEGF-A (vascular endothelial growth factor) treatment induced hMAPCs to differentiate to both arterial and venous endothelium *in vitro* and *in vivo*. This shows stem cell plasticity that adult stem cells differentiate into different types of endothelial cells. Similarly, in rat and mouse MAPC, robust specification to arterial and lymphatic endothelium was seen [58].

Since the initial publication in the differentiation of MAPC to hepatocyte-like cells, additional studies demonstrated that on a sequential treatment of sets of cytokines and growth factors: Activin, Wnt3a, bFGF, BMP4, FGF1, FGF4, FGF8, HGF, Follistatin and dexamethasone, cells express higher level mature hepatic markers and functional

characteristics of hepatocytes (Pauwelyn et al., manuscript submitted).

MAPCs were shown to differentiate to functional smooth muscle cells (SMCs). MAPCs were treated with TGFβ1 and PDGF in a serum free medium resulting in the induction of transcripts and proteins that recapitulate smooth muscle development. MAPC-derived SMCs adopted functional characteristics like functional L-type calcium channels, showed entrapment in vascular fibrin molds and generated force in response to KCl and cyclic distention as neonatal SMCs [59].

In vitro differentiation of HSCs, MAPCs in co-culture with fetal liver feeder AFT-24, with VEGF and BMP4, resulted in the expression of *Gata2*, *Scl* and *CD45* transcripts. Up to 1% of cells expressed CD45 by FACS. MAPCs grafted in sublethally irradiated mice, give rise to HSCs that can reconstitute multilineage hematopoietic engraftment in secondary/tertiary recipients and that can lead to myeloid and lymphoid progenitor cells as well as all mature white blood cells, including mature functional lymphocytes [60].

The large numbers of tissues derived from MAPCs make MAPCs useful not just for prospective cell therapies but also for elucidating fundamental questions of stem cell biology.

1.3. Liver development

The liver is the largest organ in the body, contributing about 1/50 of the total body. The basic functional unit of liver is the liver lobule which composed principally of many hepatic cellular plates with hepatocytes. Liver functions in many different ways including filtration and storage of blood; metabolism of carbohydrates, proteins, fats, hormones, and foreign chemicals; formation of bile; storage of vitamins and iron; and formation of coagulation factors [61].

1.3.1. Murine liver development in embryo

Understanding the molecular signals favoring liver development is essential to develop a rationale for *in vitro* differentiation of pluripotent stem cells towards the hepatic fate. The liver is developed through four distinct successive steps during embryo development : (1) gastrulation of the epiblast with the formation of first primitive streak/mesendoderm and the definitive endoderm, (2) specification of definitive endoderm into a primitive gut tube that is subdivided into foregut, midgut and hindgut endoderm, (3) specification of ventral foregut endoderm towards hepatoblasts, and (4) outgrowth of the liver bud and terminal differentiation into either hepatocytes or cholangiocytes (Figure 4 and 5).

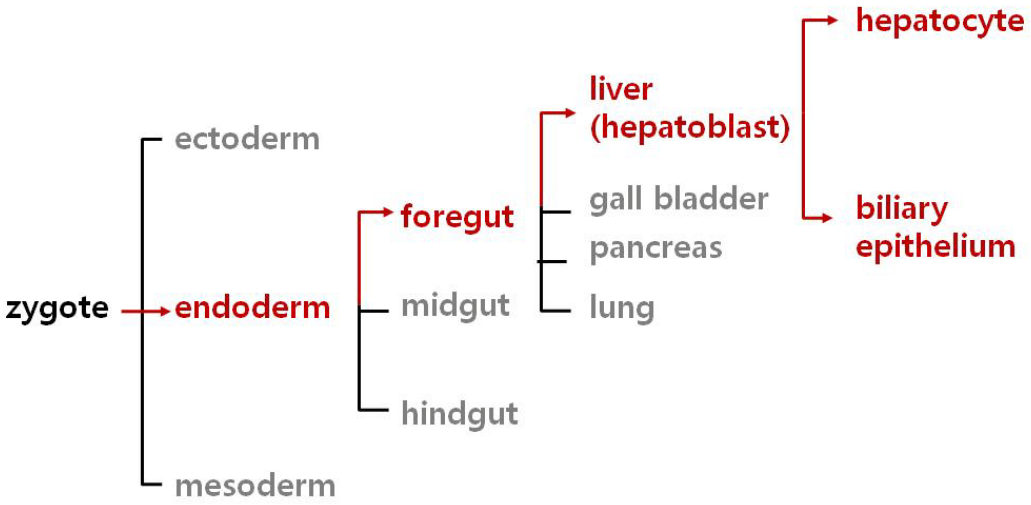

Figure 4. Illustration of hepatic cell development in embryo (modified from [62]). Hepatic development in red.

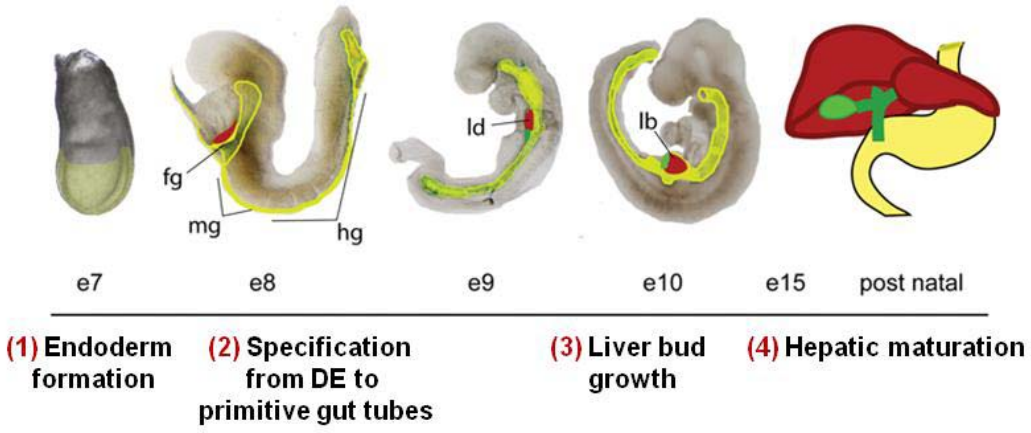

Figure 5. Time line of mouse liver development (modified from [62]). Non-liver endoderm; liver; gall bladder.

1.3.1.1. Gastrulation of the epiblast

After fertilization, the embryo undergoes cell division from the diploid zygote stage to

the blastocyst stage. The blastocyst initially consists of two types of cells: (1) the inner cell mass (ICM), which gives rise to the embryo, associated yolk sac, allantois and amnion, and (2) the trophectoderm, which gives rise to extra-embryonic ectoderm and trophoblast to provide nutrients to the embryo and comprises a large part of the placenta. The ICM segregates into an inner layer, epiblast and an outer layer, primitive endoderm (E3.5-4.5). The epiblast generates the actual embryo, and the hypoblast or the primitive endoderm give rise to extra-embryonic endoderm which forms the yolk sac.

The epiblast divide, differentiate, and rearrange through a process called gastrulation (E6.0-7.5) which results in the three germ lineages: ectoderm, mesoderm and endoderm. Shortly after the anterior movement of the distal visceral endoderm (E6.0-6.5), epiblast cells at the embryonic and extra-embryonic junction start to move to opposite (posterior end) side of the anterior visceral endoderm and undergo epithelial-mesenchymal transformation to generate the primitive steak (PS) (expressing *Mixl1*, *Eomes*, *Lhx1*, *Brachyury*, *Gsc*, *Foxa2*). PS, which consists of a posterior, middle and anterior regions, elongates from the rim of the cup to its distal tip, and the cell emigrating through the PS give rise to the definitive endoderm, mesoderm, and extra-embryonic mesoderm. Especially the definitive endoderm formation begins with the migration of endoderm precursor cells through the anterior PS region, expressing *Cer1*, *Gsc*, and *Foxa2*. It generates the node and the definitive endoderm. The node further generates axial mesoderm and part of the foregut endoderm.

The primitive streak and the node (anterior region of the primitive streak) produce a number of signaling via factors including members of the Transforming growth factor beta (TGFβ), Fibroblast growth factor (FGF) and Wnt families and also the morphogen, retinoic acid that influences cell fate. FGF4 is required for the initial outgrowth of the epiblast. TGFβ growth factor Nodal and SMAD2 are necessary for epiblast pre-pattering and formation of primitive streak [63-65]. Nodal affects endoderm and mesoderm formation in a dose-dependent manner; low doses induce mesoderm while higher doses induce endoderm [66, 67]. BMP4 is required later in gastrulation for mesoderm differentiation as BMP4 is highly expressed in both posterior and extra-embryonic mesoderm from the posterior epiblast [68].

1.3.1.2. Definitive endoderm to foregut endoderm

After gastrulation, cells in a single-cell-thick sheet move into the inside of the developing embryo and form a primitive gut tube (E7.5-8.5). The gut tube is patterned along the anterior-posterior (A-P) axis into foregut, midgut, and hindgut. The foregut endoderm ($HHEX^{pos}$) later gives rise to liver, ventral pancreas, lungs and thyroid by ventral foregut endoderm and esophagus, stomach, dorsal pancreas, and duodenum by dorsal foregut endoderm. Midgut (PDX^{pos}) forms to small intestine and hindgut (CDX^{pos}) to large intestine. Temporal and spatial gradients of FGF, BMP, Wnt, and retinoic acid from adjacent mesoderm take parts in patterning the endoderm [69-75]. Recent studies in chick and xenopus suggest that FGF4 and Wnts inhibit the foregut formation but promote hindgut formation [70, 72, 76]. The E8.5 embryo now has a dorsal-ventral axis (D-V)

with the foregut and hindgut cavities.

1.3.1.3. Hepatic endoderm specification

During hepatic endoderm specification (E8.25-9.5), liver-specific genes can be detected in portions of the endoderm which proliferate out of the endoderm layer as a newly specified hepatic endoderm to further form a liver bud and mature [77, 78]. Intrinsic hepatic potential of this region may be due to the expression transcription factors including *Foxa2*, *Gata4-6*, and *Hhex*. At this stage, binding sites for a number of transcription factors (*Foxa2* and *Gata4*) are sufficiently occupied. Subsequently, more transcription factors such as *C/EBPβ* (CCAAT/enhancer binding protein-β) and NF1 (nuclear factor-1) become engaged along with the promoter and the cells of the domain acquire the competence to begin expressing liver-specific genes. Activation of liver specific genes occurs earlier than morphological signs of liver differentiation [79]. There is an activation of *Albumin* and *Afp* expression in the ventral endoderm [77]. *Afp* and *Ttr* are expressed in gut endoderm [80]. Signals from adjacent mesodermal cells play a significant role in tissue specification. FGFs from the cardiac mesoderm and BMPs from the adjacent septum transversum mesenchyme (STM) induce the liver gene expression in the ventral foregut endoderm while blocking the pancreatic program [77, 81, 82]. Negative signals from dorsal mesoderm and ectoderm, on the other hand, restricts hepatogenesis [79].

1.3.1.4. Liver bud formation and specification to hepatocytes and cholangiocytes

After the hepatic endoderm speficication, the epithelium begins to express *Albumin*, *Afp*,

and *Hnf4α* and proliferate as the columlar epithelium [83]. Then the columnar epithelium migrates into the adjacent STM in the process of liver bud morphogenesis. *Hhex* (hematopoietically expressed homeobox) is required for hepatoblast delamination [83]. *Prox1*, *Oc1* (*Hnf6*) and *Oc2* also regulate hepatoblst delamination but act later than *Hhex*. *Prox1* (prospero-related homeobox 1) and *Oc1* also help to down-regulate *E-cadherin* expression on hepatoblasts. At E9.0, endothelial precursor cells are present between the hepatic epithelium and the STM. Primitive endothelial cells, or angioblasts, exist close to the liver bud by E9.5 and provide a crucial growth signal to the hepatic bud even before the hematopoietic cells invasion and vascularization occur [84, 85].

The liver bud grows and becomes the major site of fetal hematopoiesis. At E10.5, the liver bud becomes a vascularized organ and hematopoietic progenitor cells increase [86]. During E14-16, hepatoblasts are characterized by the expression of *Prox1*, *Afp*, *Albumin*, *CK19*. Mesenchymal signals come in to promote hepatoblast migration, and proliferation. FGF and BMP signaling assist liver bud growth [87, 88]. HGF, through its interaction with C-MET (HGF receptor) on hepatoblasts, protects the cells against apoptotic stimuli [89]. *Hlx*, specific to the STM, positively regulates the synthesis of a paracrine factor for hepatoblasts growth [90, 91]. Other TGF-β family members like SMAD2/SMAD3, expressed on hepatoblasts, have been shown to act in parallel with HGF, which converge on regulation of integrin-β1 levels and extracellular matrix interactions [92]. Moreover, there are many genes such as *c-Jun*, *Xbp1*, *K-ras*, *Tbx3* that encode components of signaling pathways and transcription factors such as *Tnfα* and *Nfκβ* that prevent

hepatocyte apoptosis [93-100].

Bipotential hepatoblasts give rise to hepatocytes and cholangiocytes (E13.5). Adult hepatocytes are $PROX1^{pos}CK19^{neg}CK7^{neg}AFP^{neg}$, and cholangiocytes are $PROX1^{neg}CK19^{pos}CK7^{pos}AFP^{neg}$ [101]. During mid-gestation, the hematopoietic cells in the liver secrete Oncostatin M (OSM) that promotes hepatic differentiation in coordination with glucocorticoid hormones, HGF, and Wnt [24, 100, 102-104]. *Hnf4α* (Hepatocyte nuclear factor 4) directly promotes hepatocyte gene expression and hepatocyte epithelial morphology, independently of and through *Hnf1α* activation. *Hnf6* inhibits cholangiocyte differentiation through the activation of *Hnf1β*. Important liver enriched transcription factors are *C/EBPα and β, Gata4, Gata6, Hlx, Hnf3β, Hnf6,* and *Prox1* [105].

By E17, hepatocytes begin to adopt a cuboidal epithelial morphology after making a transition from an epithelium (hepatic endoderm) via a non-polarized hepatoblast stage. At mid- and late-gestation, the fetal liver functions as the hematopoietic organ lacking metabolic functions of the adult liver. Towards the end of gestation and during the early post-natal phase, the fetal liver prepares to make the shift from a hematopoietic support role to normal adult liver functions including metabolic functions, glucogenesis, urea synthesis, cholesterol and bile production, and detoxification.

1.3.2. Stem cell differentiation towards the hepatic lineage

For liver regeneration therapies, the use of adult human hepatocytes is ideal. However, lack of donors limits their availability. Hepatocytes have limited proliferation potential, and lose function and viability in *ex vivo* culture. Stem cells or progenitor cells are a promising candidate for cell therapies with more availability and better proliferation potential.

1.3.2.1. Intrahepatic progenitor cells

As for progenitor cells, fetal and adult hepatic progenitor cells (hepatoblasts and oval cells respectively) have been used to generate primary hepatocytes or cholangiocytes [106-108]. Hepatoblasts are found in the early fetal liver bud and comprised ~0.1% of first trimester fetal liver mass [109]. Hepatoblasts express *Afp, Albumin, Ck19, delta-like kinase (Dlk),* and *Epcam* [110-112]. Activin A/TGFß signaling regulates hepatoblast differentiation to biliary epithelium [113]. TFs *Hnf6* and *Oc2* prevent Activin A/ TGFß signaling from undergoing hepatocyte differentiation [114].

Hepatic oval cells are present in the bile ductules and the canals of Hering in the liver [115], consisting about 0.3-0.7% of liver mass [109]. When replication of mature hepatocytes is inhibited by liver injury, hepatocyte progenitor cells are activated and differentiate to mature hepatocytes. They are phenotypically similar to hepatoblasts; activated cells are bipotential, expressing markers of *Ck7* and *Ck19* and *Afp* [116]. HGF, which level is known to increase during oval cell proliferation [117], with stem cell factor

(SCF), which acts in the proliferation and stem cell migration to injured liver site [118], has been shown to expand hepatic progenitor cells isolated from fetal livers [119]. Hepatocyte progenitor cells have been isolated from rodent livers, but they are still low in number for large-scale expansion, and the phenotype is still unclear.

1.3.2.2. Pluripotent stem cells

With the unlimited self-renewal capacity and the potential for endoderm differentiation, pluripotent stem cells such as ESCs, iPSCs, and MAPCs are a prominent cell source to study liver differentiation. Hepatic differentiation protocols for these cells focus on recapitulating the liver development process in order to guide the cells through selected pathway over many others. In this section, hepatic differentiation of ESCs will be mainly discussed since ESCs constitute, at present, the best *in vitro* hepatocyte differentiation model and their differentiation knowledge can be easily extended to differentiate other type of stem cells.

Many approaches have been used to differentiate ESCs into functional hepatocyte-like cells. ESCs differentiate spontaneously via EB formation towards the hepatic lineage upon removal of the factors that maintain the undifferentiated state [120-122]. Directed differentiation has been demonstrated with exposure of ESC to the appropriate cytokines [123-127]. The stochastic differentiation via EB formation results in the formation of mixed cell types, and thus additional ways to improve the efficiency such as addition of growth factors corresponding to hepatic developmental stage, and purification of differentiated cells are studied. Genetically modified ESCs that purify primitive streak-

like cells [128] and cell sorting markers such as asialoglycoprotein receptor (ASGPR), which selects cells with mature hepatic functions, have been proposed to address this issue [129].

Directed differentiation usually adopts multi-step protocols which recapitulate intracellular and extracellular signaling during liver development. The first step of hepatocyte-like cells generation is efficient generation of definitive endoderm cells. High concentration treatment with Activin induces m/h ESCs into definitive endoderm-like cells [130-132]. The cells temporarily express mesendoderm genes and then later definitive endoderm genes such as *Sox17* and *Foxa2*. The exposure of ESC to Activin A and Wnt3a signaling was recently found to improve hepatocyte functionality [133]. Many studies generated hepatic cells with various protocols involving FGF and BMP for hepatic induction and HGF, OSM, FGF and dexamethasone for hepatoblast proliferation and hepatocyte maturation [123-125, 133-137].

Mouse ESCs cultured as hanging drops to induce embryoid body (EB) formation and plated on collagen have been shown to express *Transthyretin (Ttr), Afp, α-1-antitrypsin (Aat)* and *Albumin*. Further, expression of mature markers *like tyrosine aminotransferase (Tat)* and *glucose-6-phosphatase (G6p)* was observed on addition of aFGF, HGF, oncostatin, and dexamethasone [138]. Ishizaka et al. were able to produce hepatocyte-like cells from mESCs after transfection with *Hnf3β* gene and differentiating with FGF2 [139]. In the case of human ESCs, the use of sodium butyrate induced hepatocyte

differentiation, shown by morphology, ALBUMIN, AAT, CK8, CK18 expression and inducible CYP450 expression and glycogen accumulation. [140]. Many studies have shown that ESCs-derived functional hepatocyte-like cells can be generated in sufficient quantity for experimental applications. However, more thorough and defined characterization of the derived hepatocyte-like cells is necessary to confirm and compare different states of hepatocyte-like cells. Table 1 shows a number of assays that can be performed to confirm the phenotype and functions of hepatocytes.

For clinical applications, hESCs have drawbacks; they cause immune responses, have potential to develop teratomas, and there are ethical concerns still remaining. In these aspects, iPSCs has an advantage for clinical use. As discussed in previous section, iPSCs can be induced from terminally differentiated adult somatic cells and have ESC-like properties. It has been shown that iPSCs can be differentiated into hepatic cells in several studies [141-143]. However, more confirmation of iPSCs differentiate successfully to hepatic lineage is needed. With translation of hESC differentiation models to the iPSCs technology, patient specific therapeutic cells may be produced in the future.

1.3.2.3. Applications of stem cell differentiated hepatocyte-like cells

Stem cell derived hepatocyte-like cells can be useful to many fields: cell transplantation therapies, extracorporeal devices, liver development and disease modeling, and drug screening [144]. While iPSC and adult stem cells which have hepatic differentiation potential, which make their use as a cell therapy promising, but more immediate employment is likely to be *in vitro* cell-based assays that model disease and drug

toxicology. This would provide a greater understanding of the disease mechanisms and pathogenesis, thereby enabling an improved opportunity ultimately for cell therapies. Also, these cells can be used as a human cell based experimental platform, avoiding the need for an animal model in toxicology studies for novel human drug development. Human cell type use in toxicology increases the efficiency of novel human drug development. In addition, hepatocytes generated from different cell lines or individuals, can be used to study drug metabolism, adverse drug reactions, or drug dosage requirements in individuals and ethnic populations.

Table 1. Recommended *in vitro* characterization of stem/ progenitor-derived hepatocyte-like cells (modified from [141])

RT-qPCR analysis of transcripts
(a) Demonstration of commitment to definitive endoderm for pluripotent cells An epiblast-like phase (*Brachyury, Nodal, Fgf8, Cripto*; not *Sox7*) A mesendoderm phase (*Eomes, Brachyury, Gsc, E-cadherin,* and *Foxa2*) A definitive endoderm phase (*Hex, Mixl1, Cxcr4, Tm4sf2, Gsc, Sox17, E-cadherin;* not *Sox7*)
(b) From definitive endoderm to hepatic cells Early hepatoblast genes (*Afp, Ttr, Krt19, Albumin*) Late fetal, postnatal hepatocyte genes: 1. Initial screen with Albumin, *Krt8, Krt18, Aat, Tat, G6p* 2. Extended screen with *Adh1C, ApoF, Hnf1α, Mrp2, C/EBPα, CPSase I, Pepck, HepPar1, To, Hnf4α, Cyp2B6, Cyp3A4, Cyp7A1, Bsep, Glycogen synthase* Liver-specific transcription factors (*Hnf4α, Hnf1α, Hnf6α, Prox1, Hex, C/EBPα, C/EBPβ*)
Protein expression
(a) Immunothistochemistry for SOX17, and FOXA2 (early), TTR, AFP, ALBUMIN (mid), HNF4α, AAT, MRP2, CX32, BSEP (late) endoderm stages
(b) Western blot for the same proteins
Ultrastructural evaluation
(a) Large polygonal polarized cells, large cytoplasm to nuclear ratio, canaliculus formation (apical pole), presence of gap and tight junctions (lateral pole)
(b) Presence of glycogen granules, high number of mitochondria, well organized rough endoplasmic reticulum
Functional analysis
(a) Albumin secretion
(b) Glycogen storage
(c) Ureagenesis
(d) Bilirubin metabolism
(e) Steroid metabolism
(f) CYP function
(g) Lidocaine clearance
(h) Ability to secrete bile

1.4. Bioreactor systems for stem cell expansion and differentiation

1.4.1. Bioreactor technologies for stem cells

Stem cells, with their ability to self-renew or differentiate into multiple cell types, are an attractive cell source for cell therapies, tissue engineering and drug screening. With the potential of stem cells for these applications, there is an increasing need for the design of robust bioprocesses for their scalable expansion and differentiation. Successful implementation of stem cell-based technologies requires large numbers of cells with carefully defined characteristics. However, cultivation of cells in tissue culture plates does not even approach the scale required to produce large number of cells, or controlled culture conditions required to obtain well-defined outcomes. Bioreactor cultivation of stem cells allows generation of larger quantity cells, continuous monitoring and control of the physical and chemical environment, and establishment of more spatially homogeneous culture environment. In addition, if necessary, gradients of cultivation conditions can be created in a single culture to study different cell responses to spatially distributed environment. Bioreactors are well established for the cultivation of microbes and mammalian cells under environment-controlled and operational conditions. Bioreactor culture technologies obtained from these previously established cells or organisms have been used as the basis for developing stem cell cultivation in various bioreactor systems.

Bioreactor systems typically include static or stirred vessels, rotating vessels and perfused vessels. The selection of bioreactor system for primary and stem cells largely depends on

whether the cells are adherent or grown in suspension as single cells or aggregates. The stirred culture system is widely employed for stem cell cultivation. Stirred vessels usually employ a magnetic stir bar to mix the culture. Medium is exchanged batch-wise, and continuous gas exchange is dependent on surface aeration of culture medium. Compared to static culture which mass transfer is only dependent on diffusion of molecules, mass transfer is by convection in mixed flasks, and fluid flow is turbulent. Shear stress should be carefully controlled to avoid cell damage caused when the turbulent Kolmogorov eddy size has the same order of magnitude as the diameter of a single cell, aggregate, or microcarrier [145]. Simple stirred vessels are easy to operate and provide access to samples for quality assessments. Especially in stem cell expansion and differentiation, frequent structural and functional assessments of the cells are mandatory in order to characterize different cell populations changing in response to temporal and spatial environment. Stirred reactor system provides the most accessible culture system among others. It also can be readily linked to on-line monitoring system for more controlled cultivation.

Cells which can be grown as single cells or aggregates are typically grown in stirred reactors. For non-adherent cells, especially those cultured as aggregates in a large scale are more likely to be cultivated in stirred vessels to prevent the agglomeration which causes restriction in oxygen and nutrient transport and necrosis. A sufficiently high agitation rate should be established to compromise the hydrodynamic shear stress created by agitation since the eddy size decreases with increasing agitation speed. For adherent

cells, carriers such as microcarriers or small size ECM templates may be required to provide attachment surface while in suspension.

Solid microcarriers are made of cross-linked dextran, cellulose or polystyrene and support cell growth on the surface. Only a few microcarrier types have been used for stem cell cultivation. Machanical agitation may cause subtle effect on cellular membrane further affecting cell properties. Since cells are directly exposed to the bulk medium, local microenvironment that is created inside the 3D cell construct or cells on stationary surface can be minimized by the extensive mixing. Macroporous microcarriers, typically made of soft materials such as gelatin and collagen, have open pores in their interior to provide larger growth surface area [146].

Cell seeding on the microcarriers is the first and critical step for reactor cultivation. Efficient seeding of cells include (1) high yield of cells after seeding, (2) high kinetic rate, minimial time in suspension for adherent and shear-sensitive cells, and (3) high and spatially uniform distribution of attached cells [147]. Stem cells are usually seeded onto microcarriers in static culture environment with no or lower stirring speed to optimize the cell-microcarrier collisions or interactions, and then transferred to the reactors.

Rotating reactors largely include two types: the slow-turning lateral vessel (STLV) and the high-aspect-ratio vessel (HARV) [148, 149]. The STLV is configured as the annular space between two concentric cylinders, the inner of which is a silicone-gas-exchange membrane, whereas the HARV is a cylindrical vessel with a gas exchange membrane at

its base. Rotational speed is adjusted such that cells remain suspended close to a stationary point within the reactor, due to a dynamic equilibrium between the acting gravitational, centrifugal, and drag forces. Medium is changed batch-wise and continuous gas exchange is achived by the internal membrane.

Fixed bed and fluidized bed bioreactors use perfusion system. Cells are immobilized in non-degradable cell culture substrates, and the substrates are arranged in column either packed (fixed bed) or floating (fluidized bed) and separated from the medium chamber [150]. Perfused columns were designed to balance culture conditions by replacing depleted nutrients and removing metabolic byproducts. The columns have an inlet at the one end and an outlet at the other end. Medium is continuously re-circulated between the columns, and an external membrane gas exchanger a slow rate. The perfusion system is often employed to study anchorage-dependent stem cells such as MSCs and epithelial stem cells.

1.4.2. Reactor systems for stem cell expansion

The first objective of stem cell expansion is to obtain sufficient cell numbers while maintaining the self-renewal capability and pluripotency or multipotency of cells as they are. The resulting cells after expansion are harvested for another run of expansion or differentiation. Characteristics of cells such as the proliferation rate and need of ECM should be carefully considered in selection and operation of a reactor system. Stem cells with the relatively long doubling time (e.g hESCs) require a larger quantity of

undifferentiated cells to start with in order to produce a sufficient number of cells for differentiation or clinical applications [151]. For faster-growing and/or low-density stem cells such as MAPCs can be started with a low density but may require frequent passages during the cultivation. Many studies have evaluated the expansion ESCs and adult stem cells using a variety of bioreactors (Table 2).

Cells are cultured either as aggregates themselves or on/in a carrier in suspension culture system. Hematopoietic stem and progenitor cells were among the first stem cells to be culture in bioreactors. They have been extensively cultured in stirred culture systems [152-154]. NSCs are also cultured in stirred culture systems [155-157]. Mouse NSCs were expanded in spinner flasks up to 44 days with subculturing every four days still retaining consistent growth rate and neural differentiation potential [156]. mNSC cultures were scaled up to 500 ml in an instrumented and controlled bioreactor [155]. Mouse mammary epithelial stem cells and breast cancer stem cells were also cultured as aggregates in suspension culture [158, 159]. MSCs embedded in a 3D scaffold were found to be uniformly distributed within the scaffolds, and the potency was not lost during their expansion [136, 160-163]. Human bone marrow stromal stem cells expanded and differentiated in the perfused 3D scaffolds were more effective in forming bone after implantation in mice than in 2D tissue culture plates [164].

Expansion of mESCs is more conducive to reactor culture than hESCs because many mESCs do not require a feeder layer to maintain their potency if LIF is provided.

Efficient expansion of mESCs as aggregates has been demonstrated in several studies [165, 166]. Expanded mESCs maintained expression of ESC surface markers and the ability to form EBs. Zur Nieden et al. showed that mESCs could be maintained as aggregates in suspension for at least 28 days (seven passages) [167]. Cell-cell interactions between mESCs in aggregates and on microcarriers appear to be mediated in large part by the cell adhesion molecule E-cadherin. mESCs have also expanded on microcarriers [166, 168].

Expansion of undifferentiated hESCs is more difficult than mESCs. hESCs cannot be passaged efficiently as single cells. A feeder layer or conditioned medium (CM) is typically required to maintain undifferentiated hESCs. Few studies have successfully cultivated undifferentiated hESCs in a stirred culture system. Feeder-free hESC expansion in defined, serum free media on surfaces coated with laminin [169] or fibronectin [170] improve the prospects for hESC expansion in stirred reactors. hESCs have been expanded on Matrigel coated microcarriers in the CM for short term or with frequent passages. Although this is a step forward to grow hESCs without a feeder layer in a reactor culture, use of CM should be replaced with a more defiend medium for a large scale culture. Since the CM is another type of cell product, production of the conditioned medium then becomes another cell process by itself, and quality control of the CM will be an additional concern. Studies on indirect or direct ESC-feeder layer interaction will help to develop defined culture medium [171] and to design reactor

systems for surface cultivation on a feeder layer or an engineered ECM or for compartmentalized cultivation only allowing indirect influence of the feeder layer.

1.4.3. Reactor systems for stem cell differentiation

The differentiation of stem cells is typically performed by expanding them as an adherent monolayer at high cell densities or by growing them as EBs in the case of ESCs. EBs were formed directly from dissociated mESCs in stirred reactor [172]. These EBs grew in size and retained cells with cardiomyocyte potential.

The initial stages of EB formation pose some challenges. Spontaneous EB formation does not produce aggregates with uniform sizes. This could pose an issue later in the differentiation by creating different gradients inside the EBs resulting in inhomogeneous environment. Large aggregates should also be avoided because of necrosis in the core. Use of methylcellulose in the medium, limiting the number of cells by hanging drop formation, and alginate encapsulation have been used to prevent the formation of excessively large EBs [173, 174].

Further EB agglomeration should be controlled during differentiation. Less extensive mouse EB aggregation can also be obtained by forming the EBs on tantalum scaffolds suspended in a spinner flask [175]. Encapsulation of mEBs in agarose beads was employed to prevent EB aggregation during culture [176]. Rotating vessels can be used to form EBs. Human ESCs were formed into EBs in a STLV and HARV reactors. Few large

necrotic aggregates were observed in HARV, and STLV allowed cell expansion and spontaneous differentiation into the three germ layers [177].

Determination of optimal shear stress range will also help EB based culture or differentiation since there is extensive clumping at very low shear stress and cell death at high shear stress [158, 159, 165, 166, 172]. Surface active anti-foams can be used to minimize cell damage by shear stress. mESC viability was shown to be not affected by low concentrations of Antifoam C. mEBs with antifoam C were successfully scaled up for expansion and differentiation [172].

Table 2. Stem cell culture in bioreactors (modified from [178]).

Stem cell type	Species	Bioreactor	Purpose	Reference
ESC	Human	Spinner flask	Differentiation	[166, 179]
		Spinner flask	Expansion and differentiation	[180]
		Spinner flask	Expansion	[181, 182]
	Mouse	Spinner flask	Expansion	[165-168]
		Stirred vessel	Differentiation	[172, 175]
		Rotary vessel	Differentiation	[183]
HSPC	Human	Spinner	Expansion	[184]
		Rotating wall vessel	Expansion	[185]
MSC	Human	Perfusion	Expansion	[161, 162, 183]
		Rotary vessel	Expansion	[136, 186]
		Spinner flask	Expansion	[186-188]
	Sheep	Perfusion	Expansion	[160]
NSC	Mouse	Spinner	Expansion	[155, 156]
Epithelial stem cells	Mouse	Stirred vessel	Expansion	[158]
Breast cancer stem cells	Mouse	Stirred vessel	Expansion	[159]

CHAPTER 2. EFFECT OF CELL DENSITY AND OXYGEN LEVEL ON MAINTENANCE OF RODENT MULTIPOTENT ADULT PROGENITOR CELLS

2.1. Introduction

As discussed in Chapter 1.2, MAPCs are isolated from the bone marrow of adult humans, rodents, and swine as rare cells that can be expanded *in vitro* without obvious senescence and differentiated into cells of the three germ layers including endoderm, mesoderm and ectoderm [51, 57, 189-192]. Therefore, MAPCs have a great potential for use in tissue engineering and regenerative medicine applications. Other groups have also isolated cells that may also have broader differentiation potential from bone marrow and other tissues including hBMSCs, MIAMI cells, MRPCs, VSEL cells, USSCs, and pre-MSC like cells as described in I.2.3. The culture conditions and phenotype varies among these cells, but all of them appear to have the ability to differentiate into a wide range of cell lineages. Whether these cells exist *in vivo* or arise as a culture phenomenon during isolation is yet to be determined.

Whether they exist *in vivo* or are strictly a culture induced cell phenotype, all these cells are a useful resource for exploration in tissue engineering applications and regenerative medicine. An optimized culture environment, which facilitates expansion of undifferentiated cells in sufficient quantities, will be important for such applications. To that end, it is important to understand parameters in the culture environment that might affect the cell expansion and cell potency, and to use an appropriate set of markers to assess cell potency.

Rodent MAPCs are routinely cultured at low densities of 150-300 cells/cm^2 as it was believed that this was required for maintenance of their broader potency. The cell density effect on cell proliferation was also demonstrated for MSC, that are commonly passaged at 70-90% confluence as contact inhibition reduces MSC proliferation and potency [193]. Compared to MSC culture, rodent MAPC culture was until now done at much lower cell densities. The large culture surface needed to produce sufficient quantities of cells and the associated media and labor cost could pose a road block for many potential applications.

In addition to cell density, oxygen tension affects stem cell proliferation and differentiation. Low oxygen tension is thought to more closely resemble the oxygen environment of the early embryo and the hematopoietic stem cell (HSC) niche within the bone marrow. Some studies have shown that hypoxia promotes stem cell proliferation and decreases the rate of differentiation. Human as well as mouse embryonic stem cells (ESC) expand more rapidly under low oxygen tension (2-5% O_2) than under normoxic conditions (20% O_2) [194, 195]. Moreover, the frequency of spontaneous chromosomal aberrations was reduced when hESC were cultured at 2% versus 20% O_2 [194], and hESC also showed a decrease in spontaneous differentiation rate when cultured under low oxygen conditions [196]. Mouse ESC cultured at 5% O_2 proliferated three times faster compared with cells maintained at 20% O_2 [195]. The effect of O_2 tension has also been evaluated on adult stem cells, especially hematopoietic stem cells (HSCs) [197, 198] as well as MSCs. rMSCs proliferated better and had greater osteogenic potency in 2D

culture under low oxygen tension [199]. hMSC cultured in 3D scaffolds and MIAMI cells also demonstrate a greater degree of cell expansion under 2% and 3% O_2 respectively[197, 198].

As described in 2006 by Breyer et al. [52], we currently isolated rMAPC under hypoxic condition (5% O_2). The resulting cell populations express the ESC specific transcription factor *Oct4* at levels 10-20% of those found in mESC, which is almost 100-fold higher than cells described in 2002 by Jiang et al. [189]. Compared to clonal cell populations that are cultured under MAPC conditions but that do not express Oct4 mRNA or protein, high Oct4 expressing mouse and rat MAPCs have greater potency [52, 54, 200]. These mouse and rat MAPC lines are currently maintained at 5% O_2, even though we have not yet tested whether hypoxic conditions remain a critical factor in maintaining potency of rodent MAPC. Likewise, although subcloning and maintenance of the cells at very low densities during isolation appear imperative, the necessity of low density culture for the long term maintenance of potency subsequent to rodent MAPC isolation has not yet been investigated.

In this chapter, we evaluated whether low cell density and hypoxic culture conditions are required to maintain long-term potency of two lines of rat MAPC expressing high levels of Oct4.

2.2. Materials and Methods

2.2.1. Cell lines

rMAPC-1 was previously described [54, 200]. rMAPC-2 was isolated subsequently using methods similar to those described for rMAPC-1[53]. Like rMAPC-1, rMAPC-2 express *Oct4* at a deltaCT compared with *Gapdh* of 4-5, and express high levels of *Epas1*. rMAPC-2 differentiates into cells expressing hepatic, endothelial and neuronal progenitor transcripts and functions.

2.2.2. MAPC maintenance culture

rMAPC-1 and rMAPC-2 were cultured on tissue culture plates (Nunc) coated with 100 ng/ml rat fibronectin (FN) (Sigma). The medium used was a mixture of 60% Dulbecco's Modified Eagle medium (DMEM) low glucose (Gibco) and 40% MCDB-201 (Sigma) supplemented with 1x Insulin-transferrin-selenium (ITS) (Sigma), 1x linoleic acid-bovine serum albumin (LA-BSA) (Sigma), 100 IU/ml penicillin and 100 μg/ml streptomycin (Cellgro), 100 μM L-ascorbic acid (Sigma), 2% qualified fetal bovine serum, 10 ng/ml human platelet derived growth factor (PDGF) (R&D systems), 5 ng/ml mouse epidermal growth factor (EGF) (R&D Systems), 0.05 μM dexamethasone (Sigma), 1000 Units/ml mouse leukemia inhibitory factor (LIF) (Chemicon), and 55 μM 2-mecaptoethanol (Gibco) (referred to as MAPC medium). Cells were seeded at 300 cells/cm^2 or 1000 cells/cm^2 and passaged every second day. 0.05% Trypsin-EDTA (Cellgro) was used to detach the cells. Plates were incubated at 37°C with 5% or 21% O_2 and 5.5-6.0% CO_2.

Cells were collected on day 48 of maintenance culture for differentiation assays. For each data point, two dishes were used for cell counting. Three independent experiments were performed using a freshly thawed vial of cells.

2.2.3. *In vitro* differentiation

Endothelial differentiation. Cells were plated at 45,000 cells/cm^2 in a FN coated 24-well-tissue culture plate (Corning) in MAPC medium. The plates were incubated overnight to reach 70-80% confluence before the medium was changed to endothelial differentiation media consisting of 60% DMEM low glucose, 40% MCDB-201, 1x ITS, 1x LA-BSA, 100 units of penicillin,1000 units of streptomycin (Pen/Strep), 100 μM L-ascorbic acid, 2% FBS, 0.5 μM dexamethasone, and 10 ng/ml VEGF (R&D Systems). 65% of the medium was changed every two days for 18 days.

Hepatocyte differentiation. Cells were plated at 55,000 cells/cm^2 in a 2% Matrigel (Becton, Dickenson and company) coated 24 well Corning tissue culture plate. The plates were incubated overnight in the MAPC medium to allow the cells to reach over 90%-95% confluence. After the overnight culture, the culture medium was changed to differentiation medium. Differentiation medium I (DMI), used from differentiation day 0 to day 12, contains 60% (by volume) DMEM low glucose, 40% MCDB-201 at pH 7.2, 100 units of penicillin/ 1000 units of streptomycin (Pen/Strep), 100 μM L-ascorbic acid, 1 μM dexamethasone, 2% FBS, 0.25x ITS, 0.5x LA-BSA. DM II which was used from day 12 to day 18 contains same ingredients as DMI but lacks FBS and LA-BSA. In

addition to DM, the following cytokines and growth factors were used at different stages: 10 ng/ml bFGF and 50 ng/ml BMP4 (day0-6), 20 ng/ml HGF and 25 ng/ml FGF8b (day 6-9), 20 ng/ml HGF and 10 ng/ml Oncostatin M (day 9-12), 20 ng/ml HGF, 10 ng/ml Oncostatin M and 2% FBS (day 12-15), 20 ng/ml HGF and 10 ng/ml Oncostatin M (day 15-18). Full media changes were performed on day 6 and day 9. 65% media changes were performed on day 3, 12 and 15.

Neuroectodermal differentiation. MAPCs were plated in 0.1% gelatin coated T75 flasks at 1500 cells/ cm^2 in 1:1 (v/v) mixture of DMEM/F12 and Neurobasal A medium supplemented with 0.5x N2 plus supplement, 0.5x B27 supplement, Pen/Strep, 0.1mM β-mercaptoethanol, and 200 µM L-glutamine. After 2 days, the medium was changed to Euromed medium with 1x N2 plus, 2mM L-glutamine, 10ng/ml bFGF, and 10ng/ml EGF. 10 ng/ml bFGF and 10ng/ml EGF was added on day 4. On day 6 cells were replated in 0.1% gelatine coated T25 flasks in 1:1 mixture of DMEM/F12 and Neurobasal A medium supplemented with 0.5x N2 plus supplement, 0.5x B27 supplement, Pen/Strep, 0.1mM β-mercaptoethanol, and 200 µM L-glutamine. EGF and bFGF (both 10ng/ml) were added every 2 days until day14.

2.2.4. OCT4 immunocytochemical staining

Cells were plated at 200-500 cells/cm^2 in a 24-well plate and stained with goat anti OCT3A/4 polyclonal IgG (Santa Cruz, goat polyclonal N19, 1:200) or incubated with goat gamma globulin (Jason ImmunoResearch, 1:11100) as negative control. Biotin-SP-

conjugated anti-goat IgG (Jackson ImmunoResearch, 1:1500) was used as the secondary antibody. Cells were treated 30 minutes with ABComplex-HRP (DakoCytomation) and developed with DAB+ (DacoCytomation) for 5 minutes.

2.2.5. Flow cytometry

Intracellular OCT4 staining. Cells collected from culture dishes were washed twice with PBS and fixed for 15 minutes at room temperature with 4% paraformaldehyde (PFA). After two additional washes with PBS, the cells were permeabilized for 10 minutes in PBS containing 0.1% (w/v) saponin and 0.05% (w/v) sodium azide (SAP buffer). Blocking was done with one hour with SAP buffer supplemented with 10% donkey serum for 10 minutes. The cells were then incubated for one hour at room temperature in SAP buffer with anti OCT3/4 antibody (Santa Cruz, 1:200) or goat IgG isotype control (Jackson Immunoresearch, 1:11100). After washing twice with SAP buffer, cells were incubated with Cy-5 labeled antigoat IgG (Jackson Immunoresearch, 1:1500) and washed twice with SAP buffer. The cells were then resuspended in PBS for flow cytometry analysis using FACScalibur (Becton Dickinson).

Cell surface phenotype. Cells were washed and resuspended in staining buffer of PBS and 2% FBS. Labeling was done by incubating the cells with conjugated antibodies anti-rat CD31 and CD45 (BD Pharminogen) at 4°C for 30 minutes.

2.2.6. RNA isolation and Real Time quantitative Polymerase Chain Reaction (RT-qPCR)

Total RNA was isolated from the cells with the RNAeasy microkit (Qiagen). The samples were treated with Turbo DNAse free kit (Ambion) for 30 minutes at 37°C. Superscript III reverse transcriptase (Invitrogen) was used for cDNA synthesis. cDNA samples were run for 40 cycles of two step amplification (95°C for 15 min and 60°C for 60 min) on Realplex mastercycler (Eppendorf) after initial denaturation (95°C for 19 minutes) and incubation with 1µl of DNA solution, 1x SYBR Green Mix PCR reaction buffer (Applied Biosystems). The primer sequences used are listed in table 1. mRNA levels were normalized using *Gapdh* as housekeeping gene.

2.2.7. Statistical analysis

Cell count data at each passage were checked for normality by residuals vs. fitted values and normal Q-Q plots. The data was transformed to have normality if necessary. Then, two factorial treatment analysis (2-way ANOVA) was run on the data set to check statistical significance.

Table 3. Primer sequences used in Chapter 2.

Primers	Forward	Reverse
Gapdh	TGCACCACCAACTGCTTAG	GATGCAGGGATGATGTTC
Oct4	CTGTAACCGGCGCCAGAA	TGCATGGGAGAGCCCAGA
Epas1	CAGTCCTCCAGGAGCTCAAA	CTCCCCTGCAGGAGTGTAGA
Flk1	CCAAGCTCAGCACACAAAAA	CCAACCACTCTGGGAACTGT
vWF	CCCACCGGATGGCTAGGTATT	GAGGCGGATCTGTTTGAGGTT
Afp	ACCTGACAGGGAAGATGGTG	GCAGTGGTTGATACCGGAGT
Albumin	CTGGGAGTGTGCAGATATCAGAGT	GAGAAGGTCACCAAGTGCTGTAGT
Sox2	AACCCCAAGATGCACAACTC	CCGGGAAGCGTGTACTTATC
Pax6	GTCCATCTTTGCTTGGGAAA	TAGCCAGGTTGCGAAGAACT

2.3. Results

rMAPC-1 cells were seeded at 300 or 1000 cells/cm^2 and passaged every two days for a period of 48 days either at 5% or 21% O_2. The number of cells recovered at each passage was enumerated. The cumulative expansion curves for the 48 day experiment are shown in Figure 6. rMAPC-1 plated at 1000 cells/cm^2 at each passage exhibited a statistically significant increase in cell expansion (Two-way ANOVA, $p < 2.2 \times 10^{-16}$). Normoxic conditions resulted in a decrease in the cell expansion of rMAPC-1, and the decrease was more pronounced in low cell density cultures than in higher cell density cultures. At 5% O_2, the average doubling time of the cells plated at the 300 cells/cm^2 was 11.5±0.3 h, while that of the cells plated at 1000 cells/cm^2 was 11.2±0.1 h (average of triplicates). Oxygen level also has an effect on the proliferation rates and compounded the effect of cell density. Cell proliferation was consistently slower at 21% O_2 condition and this was more profound for higher cell density. The doubling time of rMAPC-1 was 14.5±0.3 h, and 13.9±0.8 h for MAPC cultured at 21% O_2 and at seeding densities of 300 cells/cm^2 and 1000 cells/cm^2 respectively.

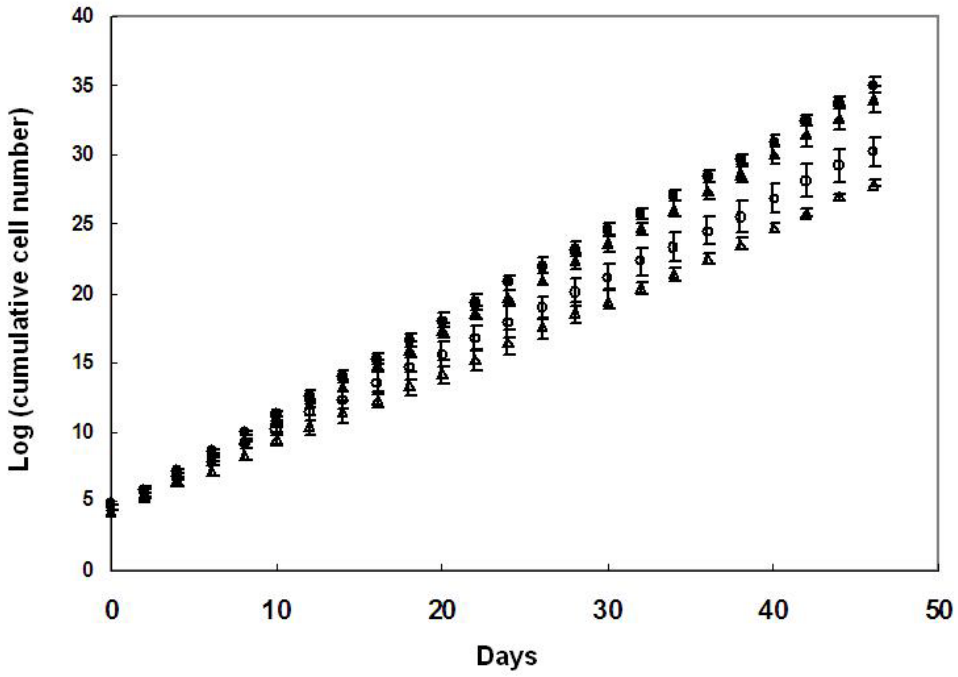

Figure 6. Effect of cell density and oxygen level on cell proliferation. (●) 5% oxygen, 1000 cells/cm^2; (▲) 5% oxygen, 300 cells/cm^2; (○) 21% oxygen, 1000 cells/cm^2; (△) 21% oxygen, 300 cells/cm^2. Error bars represent standard deviations (n=3).

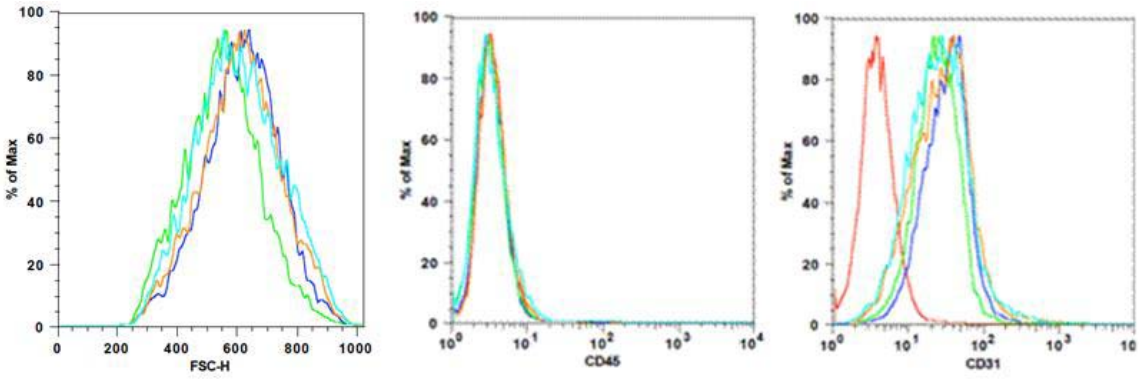

Figure 7. Effect of cell density and oxygen level on cell size and phenotype of CD45 and CD31. Isotype; 5% oxygen and 300 cells/cm^2; 5% oxygen and 1000 cells/cm^2; 21% oxygen and 300 cells/cm^2; 21% oxygen and 1000 cells/cm^2.

The cell surface characteristic of rMAPC-1 were described in Ulloa et al. as $CD45^{neg}$, $THY\text{-}1^{neg}$, $MHC\text{-}II^{neg}$, $MHC\text{-}I^{dim}$, $CD44^{dim}$, and $CD31^{pos}$ [54]. Among these, the CD31 and CD45 antigens are two markers that are routinely used to define rat MAPC phenotype. FACS analysis showed that neither higher cell density nor normoxia changed CD31 or CD45 expression of rMAPC-1 after 48 days of culture (Figure 7). Furthermore, there was no change in cell size over 48 days.

Oct4 is known to be essential to the self-renewal of undifferentiated ES cells [8, 201]. Undifferentiated rat MAPC also expresses *Oct4* near ESC levels. As Ulloa et al. showed that the potency of rat and mouse MAPC is correlated to the level of *Oct4* expression [54], we routinely follow Oct4 mRNA and protein levels as a surrogate marker of rat MAPC potency. *Oct4* mRNA levels, measured every 12 days, fluctuated by 1-3 CTs, but we found no statistically significant changes in *Oct4* expression levels over the 48 days of culture (Figure 8a). FACS and immunohistochemistry results confirmed that intracellular OCT4 protein expression was similar under all conditions for the duration of the expansion culture (Figure 8b,c).

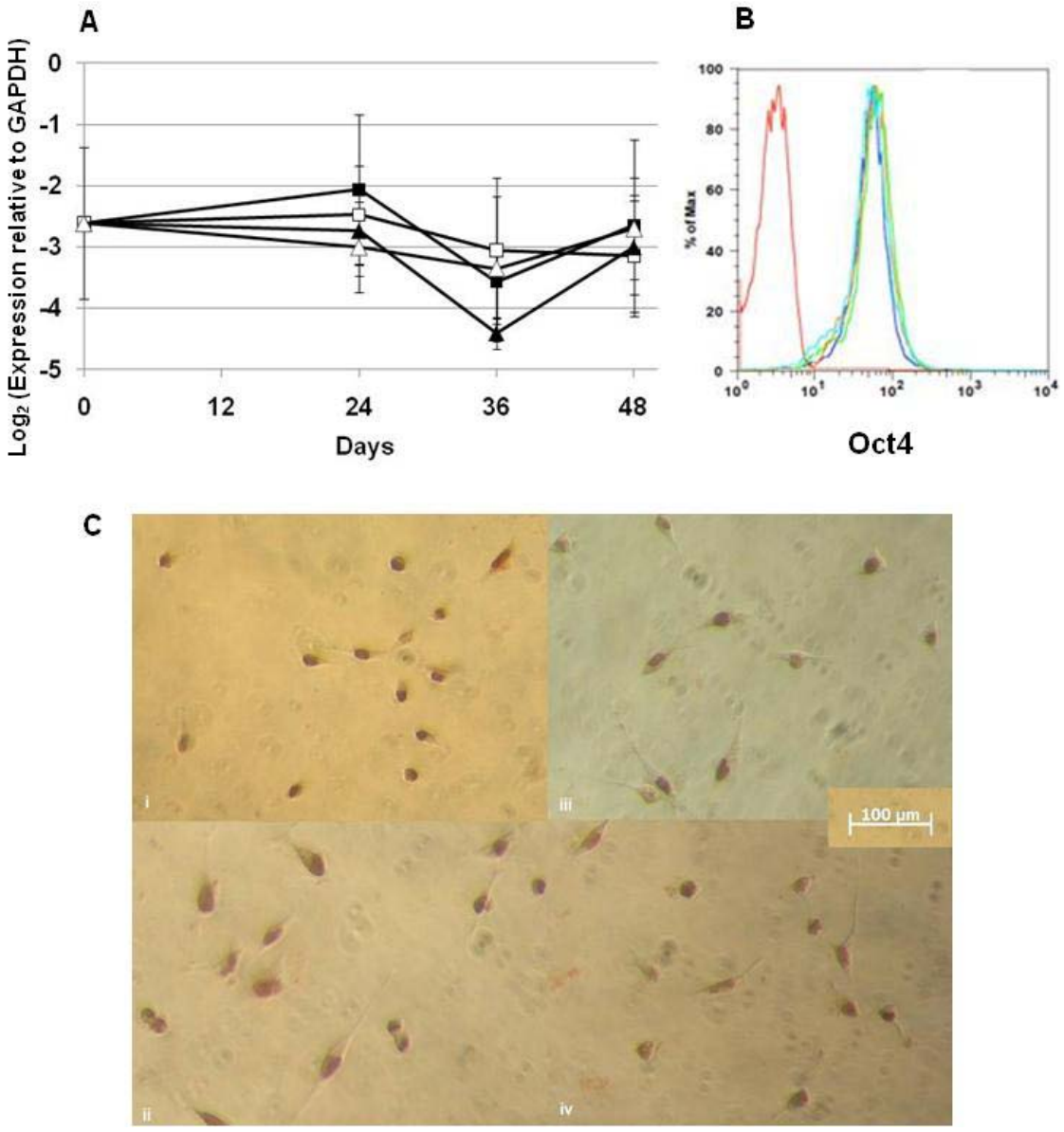

Figure 8. Effect of cell density and oxygen level on Oct4 expression level (a) mRNA expression of *Oct4* (n=3). ■5% O_2, 300 cells/cm^2; □5% O_2, 1000 cells/cm^2; ▲ 21% O_2, 300 cells/cm^2 ;△ 21% O_2, 1000 cells/cm^2 (b) Intracellular OCT4 staining by FACS at day 48 (p24). Isotype; 5% oxygen and 300 cells/cm^2; 5% oxygen and 1000 cells/cm^2; 21% oxygen and 300 cells/cm^2; 21% oxygen and 1000 cells/cm^2 (c) Immunohistochemistry of OCT4 protein at day 48 (p24). (i) 5% 300; (ii) 21% 300; (iii) 5% 1000; (iv) 21% 1000.

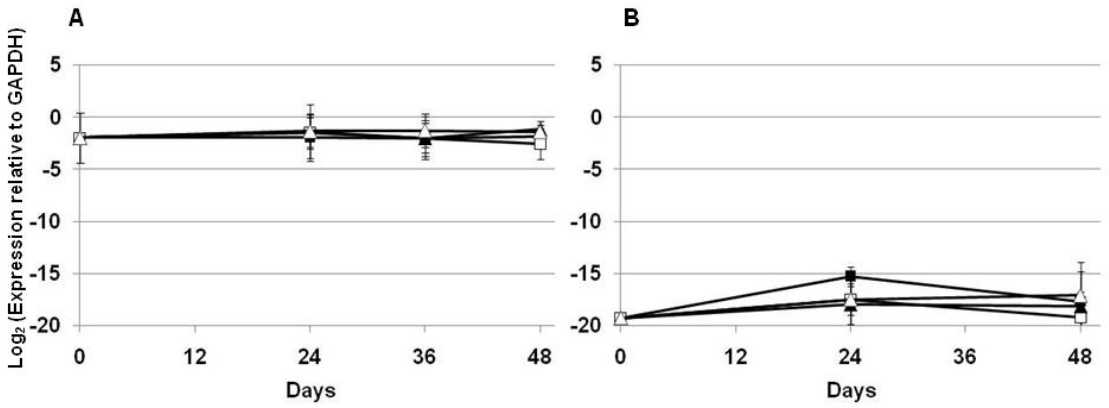

Figure 9. Effect of different oxygen level on (a) *Epas1* and (b) *Afp* transcript expression (n=3). ■5% O_2, 300 cells/cm^2; □5% O_2, 1000 cells/cm^2; ▲ 21% O_2, 300 cells/cm^2 ;Δ 21% O_2, 1000 cells/cm^2 .

In addition to *Oct4* mRNA expression, we examined the transcript level of *endothelial PAS domain protein 1* (*Epas1*) over the 48 day period. *Epas1* or *HIF2α* (Hypoxia inducible factor-2-alpha), like *HIF1α*, is stimulated by hypoxic conditions. While *HIF1α* is ubiquitously expressed, *Epas1* transcripts are restricted to particular cell types including highly vascularized tissues of adult humans and in endothelial cells of the mouse adult and embryo [202]. *Epas1* is also a direct upstream activator of *Oct4* in primordial germ cells [203]. As shown in Figure 9a, the expression level of *Epas1* relative to day 0 varied by 1-2 CTs over 48 days, but none of these changes were statistically significant. Thus, neither higher cell density nor normoxia affected *Epas1* mRNA expression levels in rMAPC-1. The fluctuations in *Epas1* expression were also not accompanied by similar fluctuations in *Oct4* expression. An early endoderm differentiation gene, *Alpha fetoprotein* (*Afp*), which is usually up-regulated quickly when rMAPC starts to differentiate, also remained undetectable (Figure 9b).

We also assessed the differentiation capability of rMAPC-1 after 48 days of culture under each of the four conditions. Directed differentiation towards endothelium-(mesoderm), hepatocyte-(endoderm), and neuroectoderm (ectoderm)-like cells were evaluated by RT-qPCR for lineage specific markers. Figure 10a and b shows the change of *Flk1* and *vWF* expression over 18 days of differentiation to endothelium lineage. Expression of *Flk1*, an early marker of endothelium, increased by 30,000 fold compared to undifferentiated cells in all conditions. Expression of *vWF*, a later marker of endothelial differentiation, increased to 4-16 fold on day 18, irrespective of the MAPC maintenance culture conditions. Under hepatocyte differentiation conditions (Figure 10c,d), levels of *Afp* increase by 10^6 fold on day 18 and *Albumin* by 4,000-30,000 fold, again independent of conditions used to expand the rMAPC-1 population before differentiation. A neural differentiation protocol previously described in Ulloa et al. was also tested. Although increases in expression levels of *Sox2* and *Pax6* were less pronounced compared with *Flk1*, *Afp* or *Albumin*, there was again no difference between cells cultured for 48 days under the four different maintenance conditions (Figure 10e,f).

To confirm the effect of cell density and O_2 level on rMAPC proliferation and potency, the experiment was replicated using a second MAPC line, rMAPC-2. The proliferation rate of rMAPC-2 was comparable to that of rMAPC-1 (Figure 6 and Figure 11a). rMAPC-2 expresses similar levels of Oct4 mRNA and protein, *Epas1*, and *Afp* transcripts as rMAPC-1 (Figure 11b). Expression of *Oct4* and *Epas1* transcripts was not significantly affected by any change in culture condition. Likewise, OCT4 protein levels,

determined by FACS, as well as the cell surface phenotype of rMAPC-2 were not affected by changing culture conditions (data not shown). Directed differentiation towards endothelium-, hepatocyte-, and neuroectoderm-like cells also showed that differentiation capability was comparable to the other rMAPC cell line (Figure 12).

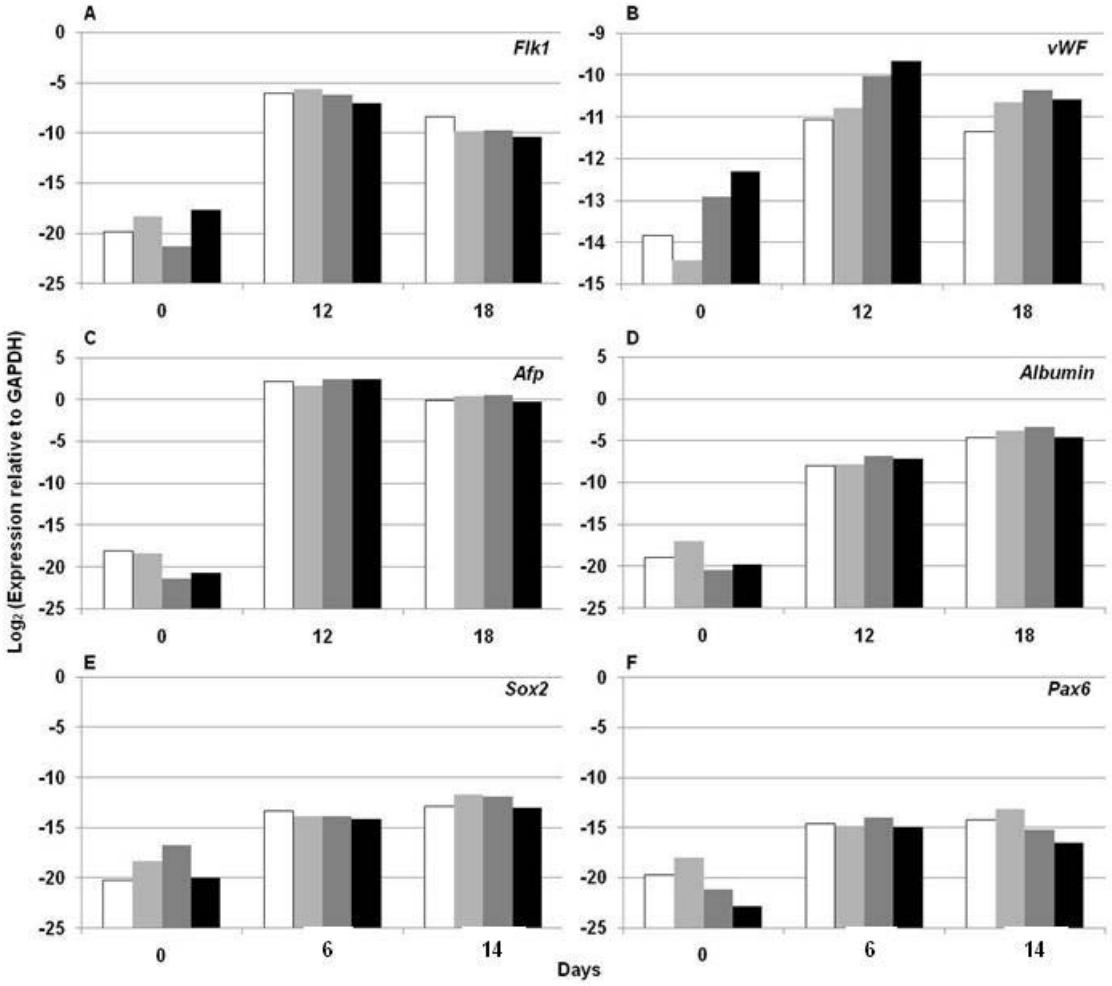

Figure 10. Effect of cell density and oxygen level on lineage expansion of cultured rMAPC-1 into endothelium-, hepatocyte-, neuroectoderm-like cells (N3). Endothelial markers (a) *Flk1*, (b) *vWF* , hepatocyte markers (c) *Afp*, (d) *Albumin*, neuroectodermal markers (e) *Sox2*, (f) *Pax6*; □ 5% O_2, 300 cells/cm^2; ■ 5% O_2, 1000 cells/cm^2; ■ 21% O_2, 300 cells/cm^2 ; ■ 21% O_2, 1000 cells/cm^2.

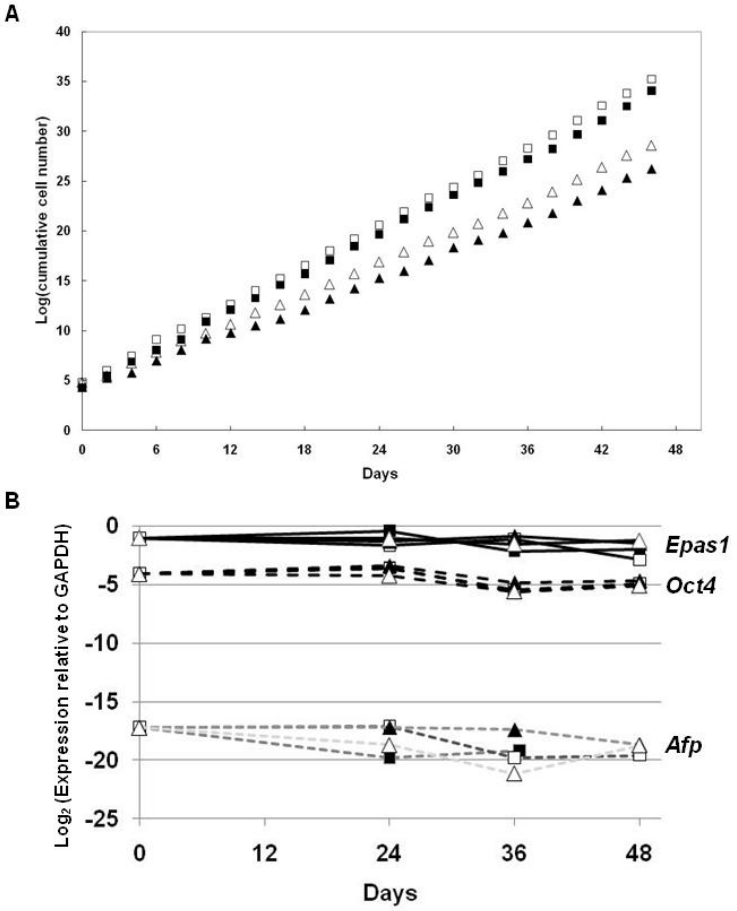

Figure 11. Effect of cell density and oxygen level on rMAPC-2 cell line (n=1). (a) cell proliferation (b) mRNA expression of *Oct4*(--) , *Epas1*(-), and *Afp* (--); ■ 5% O_2, 300 cells/cm^2; □5% O_2, 1000 cells/cm^2; ▲ 21% O_2, 300 cells/cm^2 ;Δ 21% O_2, 1000 cells/cm^2 .

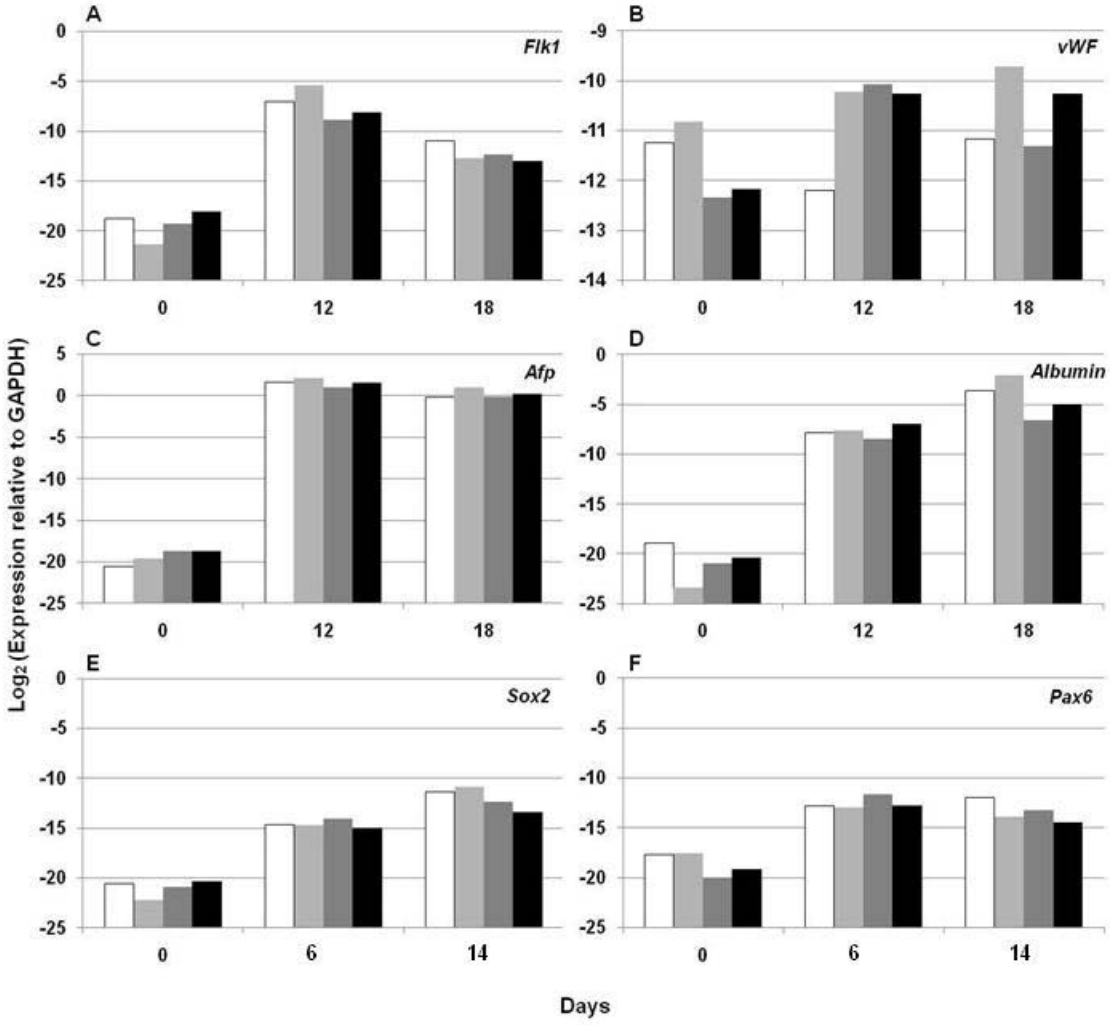

Figure 12. Effect of cell density and oxygen level on lineage expansion of cultured rMAPC-2 into endothelium-, hepatocyte-, neuroectoderm-like cells. Endothelial markers (a) *Flk1*, (b) *vWF* , hepatocyte markers (c) *Afp*, (d) *Albumin*, neuroectodermal markers (e) *Sox2*, (f) *Pax6*; □ 5% O_2, 300 cells/cm^2; ■ 5% O_2, 1000 cells/cm^2; ■ 21% O_2, 300 cells/cm^2 ; ■ 21% O_2, 1000 cells/cm^2.

2.4. Discussion

Rodent MAPC have been isolated as well as maintained long-term at very low cell densities as we believed that cell-cell contact would affect their differentiation potential. As the cell lines used (rMAPC-1 and rMAPC-2) was isolated under hypoxic conditions, it was also assumed that their maintenance would require hypoxic conditions. However, no studies were as yet performed to carefully examine the effect of cell density, and ambient O_2 levels on maintenance of rodent MAPC. In this chapter, it was demonstrated that maintenance of rMAPC-1 and newly isolated rMAPC-2 at higher cell densities and under higher oxygen tension do not significantly influence Oct4 expression of undifferentiated MAPC or their differentiation capability, even though these culture parameters may affect cell proliferation.

Oct4 is highly expressed in the rat and mouse MAPC isolated over the last 4-5 years in our laboratories [41]. The expression level of Oct4 in mouse MAPC is about 5-20% of that found in mESCs, and we have shown that compared with cells isolated and cultured under similar conditions, mouse and rat MAPC expressing high levels of Oct4 have greater potency. We therefore monitor levels of *Oct4* as a surrogate marker for rat and mouse MAPC potency. Throughout the 48 days of culture, *Oct4* transcript levels fluctuated by 1-3 CTs, or 2-8 fold. However, at the end of 48 days of culture no significant differences in differentiation ability between any of the culture conditions were found. Niwa et al demonstrated that the levels of *Oct4* are regulated in a very

narrow range in mESC, and that a two fold increase or decrease in *Oct4* expression provokes differentiation [8]. However, mESC also express the other pluripotency transcription factors, *Nanog* and *Sox2*, and it is clear that the relative expression of these three are responsible for the differentiation state of mESC [204]. By contrast, rat MAPC do not express *Nanog* or *Sox2*. It is possible that the precise level of *Oct4* in the absence of *Nanog* and *Sox2* may not be as crucial for the potency of MAPC[204].

Although the upstream regulators of *Oct4* are not fully elucidated, *Epas1* is known to be a direct upstream activator of Oct4 in primordial germ cells, but not ESC [203]. Like *Hif1a*, *Hif2a* is activated by hypoxic conditions, and the fact that *Hif2a* expression is restricted to highly vascularized tissues and endothelium [205] led us to hypothesize that the high levels of *Epas1* expression in rMAPC might be due to the hypoxic culture conditions, and these high levels of *Epas1* may further correlate with *Oct4* expression in rMAPC. However, this hypothesis was disproven. *Epas1* expression did not significantly change whether cells were maintained in normoxic conditions at either cell density for 48 days. In addition, no apparent correlation was seen between *Epas1* and *Oct4* transcript levels in rMAPC. Obviously the small changes in either transcription factors (1-3 CTs) may not allow us to determine whether changes in *Epas1* levels affect levels of *Oct4*. Specific knockdown studies will be needed to address this question.

Ulloa et al. have previously shown that high Oct4 expressing rat and mouse MAPCs have significantly broader differentiation potential than MSC-like cells isolated under MAPC

conditions that do not express *Oct4*, although the relationship may not be casual. The ability of rMAPC to differentiate into endothelial-, hepatocyte-, or neural progenitor-like cells was not critically affected by maintaining the cells at higher cell densities and higher ambient oxygen. An increase in expression of differentiation marker genes was seen (*Flk1*, *vWF*, *Afp*, *Albumin*, *Sox2*, *Pax6*), although not all triplicates showed the same state of maturity. This is more evident in later differentiation markers such as *vWF* and *Albumin*. These late markers are more difficult to induce to high expression levels. Therefore, the levels seem to differ more among different replicate runs. Since the completion of the experiments which not fully optimized hepatocyte-like-cell differentiation protocol was used, we have developed an improved hepatic lineage differentiation protocol for rMAPC, hESC and mouse iPS (induced pluripotent stem cells) [206]. The improved protocol was used for the hepatic differentiation in other chapters. However, the protocol is yet to be tested in rMAPC from high cell density culture. In contrast to our findings that O_2 concentrations during MAPC expansion do not appear to affect MAPC potency, there is evidence from HSC, ESC, MSC, and MIAMI cells that hypoxic culture conditions improve the undifferentiated phenotype and the potency of stem cells [196, 207, 208]. As some of these studies used even lower O_2 concentrations, the possibility remains that maintenance of rMAPC at 2-3% O_2 may affect their potency further.

Continued MAPC expansion under higher cell densities as well as high oxygen level does not change the potency of rMAPC over 48 days even though cell proliferation rate was

affected. Higher cell density increased cell proliferation rates, but the effect was more profound under low oxygen level. Low oxygen tension is thought to be more physiologic than ambient oxygen tension; indeed oxygen concentration ranges from 1% to 13% *in vivo*. Our result that rMAPC expanded significantly faster at low oxygen tension (5%) is consistent with several studies which have shown that hypoxia promotes stem cell proliferation including ESC, MSC, and HSC [194, 199, 209, 210]. Why hypoxia improves stem cell expansion, and in particular MAPC expansion, is not known. Low oxygen tension may affect proliferation and maintenance of stem cells by reducing the frequency of chromosomal aberrations, thus providing more stable growth in culture [194]. It may reduce oxidative stress, as oxygen radicals, nitrogen oxide, and hydrogen peroxide inhibit cell proliferation possibly by toxic effects of oxidizing adjacent molecules, and these radicals may be less prevalent at low oxygen than at high oxygen concentrations [211, 212]. Oxygen tension is also known to modulate the expression of cytokine receptors, transcription factors and lineage-specific markers [213].

In summary, in this chapter, it was demonstrated that even though hypoxia and low density culture is required for isolation of high Oct4 rMAPC, once the culture has been established rat MAPC can be cultured at a higher cell density and under normoxic level with maintaining their potency. Hypoxia promotes the MAPC proliferation, but is not a critical factor in maintaining Oct4 expression and potency of rodent MAPC. This study provides evidences that rMAPC can be readily cultured at a higher cell density and under low oxygen level for growing more cells efficiently. These findings open the possibility

for easy scale up of rodent MAPC cultures that will allow testing their usefulness in preclinical models of tissue repair or bioengineering applications.

CHAPTER 3. REACTOR CULTURE SYSTEM OF RAT MAPC AS AGGREGATES FOR EXPANSION

.

3.1. Introduction

MAPC have traditionally been cultured at low density (200-300 cells/cm^2) on tissue culture dishes, as it was believed that the higher-density may result in differentiation and loss of potency, as has been suggested for MSC [193]. In Chapter 2, we have shown that rMAPC can be grown at higher cell densities while maintaining potency. This finding encouraged us to employ a reactor culture system with very high cell densities.

With the growing potential of stem cells for applications in cellular therapy and drug toxicity screening, there is an increasing need for the design of robust bioprocesses for their scalable expansion and differentiation. The widespread use and extensive experience with stirred suspension culture systems for microbial and mammalian cell culture makes them an attractive option as a large scale culture system for stem cell technologies. By adapting the culture system that has been commonly used in the conventional cell culture industry, development of stem cell related bioprocesses would be straightforward and thus minimize design costs.

Stirred suspension cultures provide a more homogenous culture environment than static cultures along with the capability for online monitoring and control of physicochemical parameters such as nutrient and cytokine concentrations, oxygen and pH. Moreover, cell concentrations of 10^6-10^7 cells/ml can be attained in conventional suspension bioreactors, which is within the range to meet the clinical need of ~10^9-10^{10} cells per treatment. High cell density culture in the bioreactors and minimal need of manual intervention results in

a more cost-effective bioprocess. Suspension culture has been widely used in the expansion and differentiation of many types of stem cells including murine and human embryonic stem cells (ESC), adult stem cells such as HSPCs, NSCs, and MSCs as discussed in Chapter 1.4. The stem cells were cultivated as aggregates, embedded in 3D polymeric scaffolds, or on microcarriers.

Aside from the obvious advantage of large-scale cell production in a spinner culture system, there is also increasing evidence of a significantly better recapitulation of the *in-vivo* phenotype and biological response in 3D aggregates than in traditional two-dimensional (2D) monolayer culture methods. This is thought to be due to differences in cell-cell and cell-matrix interactions, cell shape, and spatial gradients, leading to differences in gene and protein expression. Thus, the potential applications of these 3D systems also extend to developing 'biomemtic' 3D tissues/organoids and as a *in vitro* model for studying differentiation, organogenesis, migration, tumor biology, and in high-throughput drug screening [214-219].

In Chapter 3, we explored culturing rMAPC as 3D cell aggregates amenable to suspension culture and scalable expansion in bioreactors. MAPCs self-assemble into 3D cell aggregates while maintaining differentiation potency over culture period and their scalable expansion in the suspension culture system retain the potential for liver differentiation application. The principles developed in this study may also be applicable for the scalable growth and differentiation of MSCs and other stem and progenitor cells.

This chapter describes the results of a close collaboration with Kartik Subramanian. Figures with * were from results of experiments conducted by KS

3.2. Materials and Methods

3.2.1. Establishment and Maintenance of Rat MAPC lines

The rMAPC-1 line was used in this study. The isolation of rat MAPC lines has been previously described [52, 54]. Briefly, rat MAPC lines were isolated from the tibia and femur of 4 week old female rat (Fischer). Cells were plated on 6 well tissue culture plates in MAPC medium at $6x10^6$/well and cultured in a humidified incubator at 37°C with 5% oxygen and 5.5% CO_2. After 4 weeks of culture, hematopoeitic cells were removed using magnetic microbeads against CD45 and TER119 (Miltenyi Biotec) and the remaining cells were seeded into 96 well plates at 5 cells/well. Cells with small size and spindle shaped morphology that appear in the wells were subsequently picked, expanded and screened for MAPC phenotype (expression of *Oct4, Rex1* and *CD31*) and tri-lineage differentiation potential [52]. The established MAPC cell lines were maintained in MAPC medium at 37°C in a 5% oxygen and 5-6% CO_2 incubator at a starting cell density of 300 cells/cm^2 and passaged using 0.05% (w/v) Trypsin-EDTA (5 mg/l Cellgro) every two days [52].

3.2.2. MAPC media

MAPC medium consisted of a basal medium that was a 60/40 (v/v) mixture of low glucose Dulbecco's Modified Eagle media (DMEM) (Gibco, USA) and MCDB-201

(Sigma) supplemented with 0.026 μg/ml ascorbic acid 3-phosphate (Sigma), linoleic acid bovine serum albumin (LA-BSA, Sigma)) (final concentrations of 10^3 μg/ml BSA and 8.13 μg/ml linoleic acid), insulin-transferrin-selenium (ITS, Sigma) (final concentration 10 μg/ml insulin, 5.5 μg/ml transferrin, 0.005 μg/ml sodium selenite), 0.02 μg/ml dexamethasone (Sigma), 4.3 μg/ml β-mercaptoethanol and 2% (v/v) qualified fetal bovine serum (Hyclone). Complete MAPC medium also contained three growth factors: human platelet derived growth factor (PDGF-BB, R&D) (10 ng/ml), mouse epidermal growth factor (EGF, Sigma) (10 ng/ml) and mouse leukemia inhibitory factor (LIF) (10^3 Units/ml) (Chemicon, ESGRO). All media used were also supplemented with 100 IU/ml penicillin and 100 μg/ml streptomycin (Gibco).

3.2.3. Static plate Culture of MAPC aggregates

MAPC aggregates were formed from single cell suspensions of MAPCs using the forced aggregation method [220]. Briefly, cells in suspension were placed in a well of an ultra-low attachment round bottomed 96 well plate (Corning) and centrifugal force (1500 rpm, 4 min) was applied to settle them to the bottom of the well thus forcing them to agglomerate. The plates were subsequently incubated in a 37°C incubator at 5% or 21% oxygen and MAPC aggregates formed with time.

For static plate culture, aggregates were formed and usually cultured for four days in 96 well plates. If the aggregates were cultured more than four days, MAPC medium and 5% oxygen conditions were used with 50% medium changes every two days. MAPC

aggregates were also plated in differentiation conditions (MAPC medium without LIF, PDGF and EGF and 21% oxygen) for the same time period as maintenance cultures.

3.2.4. Suspension flask culture of MAPC aggregates

Prior to suspension culture, MAPC aggregates were formed using the forced aggregation method in static culture for two days. Aggregates were then transferred to a 250 ml spinner flask at an initial cell concentration of 50,000 cells/ml in 100ml medium and the culture was stirred at 70 rpm. MAPCs aggregates were expanded for four days in a spinner flask. After two days of culture in a spinner flask, the culture was either half-diluted (fresh medium of 50ml added upon 50 ml removel of the culture) or re-inoculated into a new spinner flask at the initial cell concentration of 50,000 cells/ml. For 8 day spinner culture, MAPC aggregates were inoculated into a new spinner flask at the initial cell concentration every two days.

3.2.5. RNA Isolation and RT-qPCR

Total RNA was isolated from rMAPC cell lysates using RNAeasy microkit (Qiagen) according to instructions provided in the kit. cDNA was synthesized from the extracted RNA using the Superscript III reverse transcriptase (Invitrogen) method. The PCR reaction mix consisted of cDNA samples, SYBR Green Mix PCR reaction buffer (Applied Biosystems) and primers (5 μM stocks, sequences listed in table 1). The RT-qPCR reaction was run on a Realplex mastercycler (Eppendorf) using the following program: 50°C for 2 min, 95°C for 10 min, and 40 cycles at 95°C for 15 sec and 60°C for 1 min followed by a dissociation protocol to obtain a melting curve. Transcript abundance relative to *Gapdh* was expressed as $\log_2$(Transcript expression relative to

Gapdh) and calculated as ΔCt which is Ct(gene of interest)-Ct(*Gapdh*) and Transcript abundance in sample relative to day 0 was expressed as the $\log_2$(Transcript expression level relative to day 0) and calculated as ΔCt (day 0)- ΔCt(day of sample).

3.2.6. Intracellular staining for OCT4 by flow cytometry

Cells harvested by trypsinization were washed with and suspended in PBS with 3% (v/v) serum at 100,000 cells per FACS tube. After fixing with 4% paraformaldehyde for 15-20 min, and blocking for 1 hr in SAP buffer (PBS with 0.1% (w/v) saponin and 0.05% (w/v) sodium azide) supplemented with 10% donkey serum, cells were incubated for 1 hr with 1 μg/ml Oct3/4 antibody (Santa-Cruz, N19) or Goat IgG isotype control (Jackson Immunoresearch) diluted in SAP buffer before incubating with Cy5 labeled anti-goat IgG (Jackson Immunoresearch, 1:500 in SAP buffer) for 30 min. Finally, cells were washed, filtered and re-suspended in 500 μl PBS for flow cytometric analysis using FACS Calibur (Becton Dickinson).

3.2.7. *In vitro* differentiation for evaluating maintenance of differentiation potency of MAPC

In order to evaluate the maintenance of the differentiation capacity of rMAPC cultured as aggregates in the stirred culture system, spontaneous differentiation into multiple lineages and directed differentiation to the hepatic cell lineage were performed and the results of differentiations were evaluated by the expression of several lineage-specific markers.

rMAPC aggregates were removed from the spinner culture and washed twice with PBS by centrifugation at 1000 rpm for 3 minutes. Aggregates were transferred to wells of an

ultra-low attachment flat bottomed 24 well plate (Corning) (total 1-2 million cells/ 0.5ml differentiation medium/well).

Spontaneous differentiation

Spontaneous differentiation medium consisted of 60% (v/v) low glucose Dulbecco's modified eagle medium (DMEM), 40% MCDB-201 at pH 7.2, 1x Insulin-transferrin-selenium (ITS), 1x linoleic acid-bovine serum (LA-BSA), 100 IU/ml penicillin and 100 µg/ml streptomycin, 100 µM L-ascorbic acid, 1 µM dexamethasone (Sigma), 55 µM ß-mercaptoethanol supplemented with 2% fetal bovine serum (Hyclone). Differentiation was continued for 21 days with half media changes every two days.

Directed hepatic differentiation

The composition of the differentiation basal medium was the same as MAPC medium except that ITS and LA-BSA were at 25% of the amount in MAPC medium, dexamethasone was at 0.4 µg/ml and the three protein factors and serum were absent. Furthermore, additional protein factors were added as described below. The cytokines and growth factor supplements were added as follows: (i) Day 0: Activin A at 100 ng/ml and Wnt3a at 50 ng/ml (ii) Day 6: bFGF at 10 ng/ml and BMP4 at 50 ng/ml (iii) Day 10: FGF8b at 25 ng/ml, aFGF at 50 ng/ml and FGF4 at 10 ng/ml (iv) Day 14: HGF at 20 ng/ml and Follistatin at 100 ng/ml. Differentiations were carried out for twenty days in 21% oxygen conditions with 50% media change, corresponding to the differentiation stage, every two days. On days 0, 6, 10, and 14, complete medium was replaced with fresh medium with supplements for the ensuing differentiation stage.

3.2.8. Time lapse microscopy

MAPCs were seeded at 1000 cells/well in ultra-low attachment round bottom 96 well plates (Corning). The initial aggregation of the cells was observed by microscope (Leica) located in an incubation system of 37°C, 5% CO_2, and 5% or 21% O_2 for 48 hours. Pictures taken every four minutes over a period of 48 hr were arranged to make an animated video clip. From the pictures, the size of the aggregates was also estimated.

3.2.9. Transmission Electron Microscopy

Cell aggregates were washed thrice with 0.1 M cacodylate buffer and fixed in 2.5% glutaraldehyde and 0.1 M sodium cacodylate buffer (pH 7.2) for 40 min. After post-fixation in 1% osmium tetroxide and 0.1 M of cacodylate buffer, the samples were dehydrated in graded series of ethanol folloed by propylene oxide treatment, and embedded in epoxy resin. Ultrathin sections were cut, stained with uranyl acetate and lead citrate, and examined using a JEOL 1200 EXII electron microscope at the Characterization facility at University of Minnesota.

3.2.10. E-CADHERIN Staining

Cells aggregates were fixed in 4% paraformaldehyde for 30 min and washed with PBS. The samples were incubated in 5% sucrose in PBS overnight and supercooled with isopentane before freezing in OCT and obtaining sections. H_2O_2 was used to inhibit endogenous peroxidase and incubated with fetal bovine serum (FBS) to reduce non-specific binding. Cells were then incubated with anti-E-CADHERIN (BD) antibody or

with isotype-matched negative control antibodies (mouse IgG2a) and then subsequently visualized using EnVision-Peroxidase with DAB substrate (Dako).

3.2.11. DNA statining for cell cycle analysis

Aggregates were dissociated into single cells with 0.25% Trypsin EDTA, washed and resuspended in staining buffer of PBS and 2% FBS, and fixed in 80% ethanol at -20°C. Cells were vortexed and stored below 4°C. Cells were washed twice in the staining buffer, then labeled by incubating overnight at 4°C in PBS with 50μg/ml propidium idodide and 0.1mg/ml RNAse. Cells were resuspended in PBS for flow cytometric analysis using FACScalibur (Becton Dickinson).

3.2.12. Cell viability staining

The “live/dead viability/cytotoxicity kit” (Invitrogen) was used to stain cell aggregates with calcein and ethidium. Component B was added first to DPBS (1:1000) and then component A was added to DPBS with component B (1:2000). Aggregates were incubated with the staining solution for 30 min at 37°C. Cells were washed once with PBS and observed under inverted fluorescent microscope (Axiovert 200, Zeiss). Live and dead cells appear as green and red respectively.

Table 4. List of primers used in Chapter 3.

Cell Lineage	Gene	Forward Primer	Reverse Primer
Housekeeping	*Gapdh*	AAGGGCTCATGACCACAGTC	GGATGCAGGCATGATGTTCT
Pluripotency /MAPC	*Oct4*	CTGTAACCGGCGCCAGAA	TGCATGGGAGAGCCCAGA
	Rex1	AAAGCTTTTACAGAGAGCTCGAAA CTA	GTGCGCAAGTTGAAATCCAGT
	Sall4	AGAACTTCTCGTCTGCCAGTG	CTCTATGGCCAGCTTCCTTC
	CD31	GGACTGGCCCTGTCACGTT	TTGTTCATGGTGCCAAAACAC T
Endoderm	*Hnf3b*	GCAGAACTCCATCCGTCATT	TCGAACATGTTGCCAGAGTC
	Gata4	CTGTGCCAACTGCCAGACTA	AGATTCTTGGGCTTCCGTTT
	Gata6	GTCTGGATGGAGCCACAGTT	ATCATCACCACCCGACCTAC
	Sox7	CAAGGATGAGAGGAAACGTC	CTCTGCCTCATCCACATAGG
	Sox17	GCCAAAGACGAACGCAAGCGG	TCATGCGCTTCACCTGCTTG
	Hnf1α	CAGCCACAACCATTCACATC	GCCATCTGGGTGGAGATAAA
	Hnf4α	AAATGTGCAGGTGTTGACCA	CACGCTCCTGAAGAATC
Hepatic lineage	*Afp*	ACCTGACAGGGAAGATGGTG	GCAGTGGTTGATACCGGAGT
	Albumin	TCTGCACACTCCCAGACAAG	AGTCACCCATCACCGTCTTC
	Aat	CAAACAAGGTCAGCCATTCTC	CAGCATCATTGTTGAAGACCC
	Tat	GGAAGCTAAGGATGTCATTCTG	GACCTCAATTCCCATAGACTC
Endothelium	*Flk1*	CCAAGCTCAGCACACAAAAA	CCAACCACTCTGGGAACTGT
	Ve-Cadherin	GGCCAACGAATTGGATTCTA	GTTTACTGGCACCACGTCCT
	vWF	CCCACCGGATGGCTAGGTATT	GAGGCGGATCTGTTTGAGGTT
	Enos	TCCAGTAACACAGACAGTGCA	CAGGAAGTAAGTGAGAGC
	VEGFa	CAATGATGAAGCCCTGGAGT	TTTCTTGCGCTTTCGTTTTT
Neuroectoderm	*Sox2*	GGCCAACGAATTGGATTCTA	GTTTACTGGCACCACGTCCT
	Pax6	GTCCATCTTTGCTTGGGAAA	TAGCCAGGTTGCGAAGAACT
	Nestin	CCCCAGAAACAGAAGAAGATGAG	CATGGGCATCTGTCAGGATTG

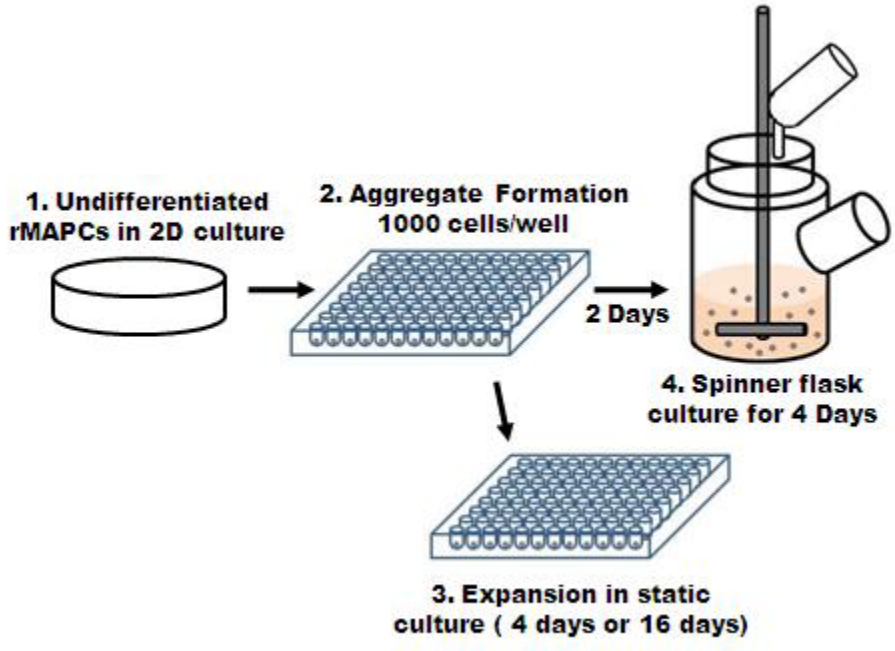

Figure 13. Experimental strategy for formation, expansion and maintenance of undifferentiated MAPC aggregates

3.3. Results

3.3.1. Characterization of the MAPC aggregates and their formation

We evaluated aggregate formation from single cell suspensions of MAPCs using the forced aggregation method described in 2.2.3. rMAPCs were inoculated at a starting cell concentration of 10,000 cells/ml (1000 cells per well), and single aggregate from each well was readily formed (Figure 13). Aggregates were formed in complete MAPC medium or MAPC medium without LIF, PDGF and EGF (differentiation medium) in 5% or 21% oxygen.

Time-lapse microscopy was used to visualize the process of aggregate formation over a period of 48 hr. After the centrifugal settling to the bottom of a well, single cells clustered together at an average size of 540 μm. Subsequent compaction led to the cell aggregates of about 250 μm in size. The aggregates then increased in size to about 460 μm by 48 hr after the initial agglomeration (Figure 14a). 10 aggregates were dissociated by trypsinization every day for cell counting. The average number of cells in each aggregate increased from 1000 to 17,758 cells per aggregate (668 ± 19 μm) in four days (Figure 14b). The size of an aggregate also increased from 300 μm to about 650 μm in diameter during four day culture (Figure 14c).

The population doubling time during the four days of formation was about 23 hr, slower than that seen when cultivated on a 2D surface (12-14 hr) (Chapter 2). Cell cycle analysis

done by flow cytometry indicated that a larger fraction (60%) of MAPC in aggregates were in G0/G1, in comparison to 2D surface culture (40%) (Figure 14d).

Oxygen levels had a minimal effect during initial aggregation phase (<48 hours); aggregates grew smaller under the normoxic condition than under the hypoxic condition. Over four day culture, different oxygen levels did not show any differential effect on the cell proliferation, aggregate size increase and cell cycle of the cells (Figure 14).

Four days after cell seeding, the MAPC aggregates had barely distinguishable cell-cell boundaries (Figure 15a) with necrotic core inside (Figure 15b). TEM analysis of the aggregates showed tightly packed cells with high nucleus to cytoplasm ratio, a characteristic of MAPCs. Tight junctions were seen at cell-cell boundaries (Figure 15d). Immunohistochemistry demonstrated that MAPC in aggregates expressed the cell membrane associated adhesion protein E-CADHERIN (Figure 15c). MAPC aggregates formed in differentiation basal medium did not grow as big as the aggregates in MAPC culture medium. Also, the boundaries were irregular with some cells spreading out on the bottom of the well (data not shown).

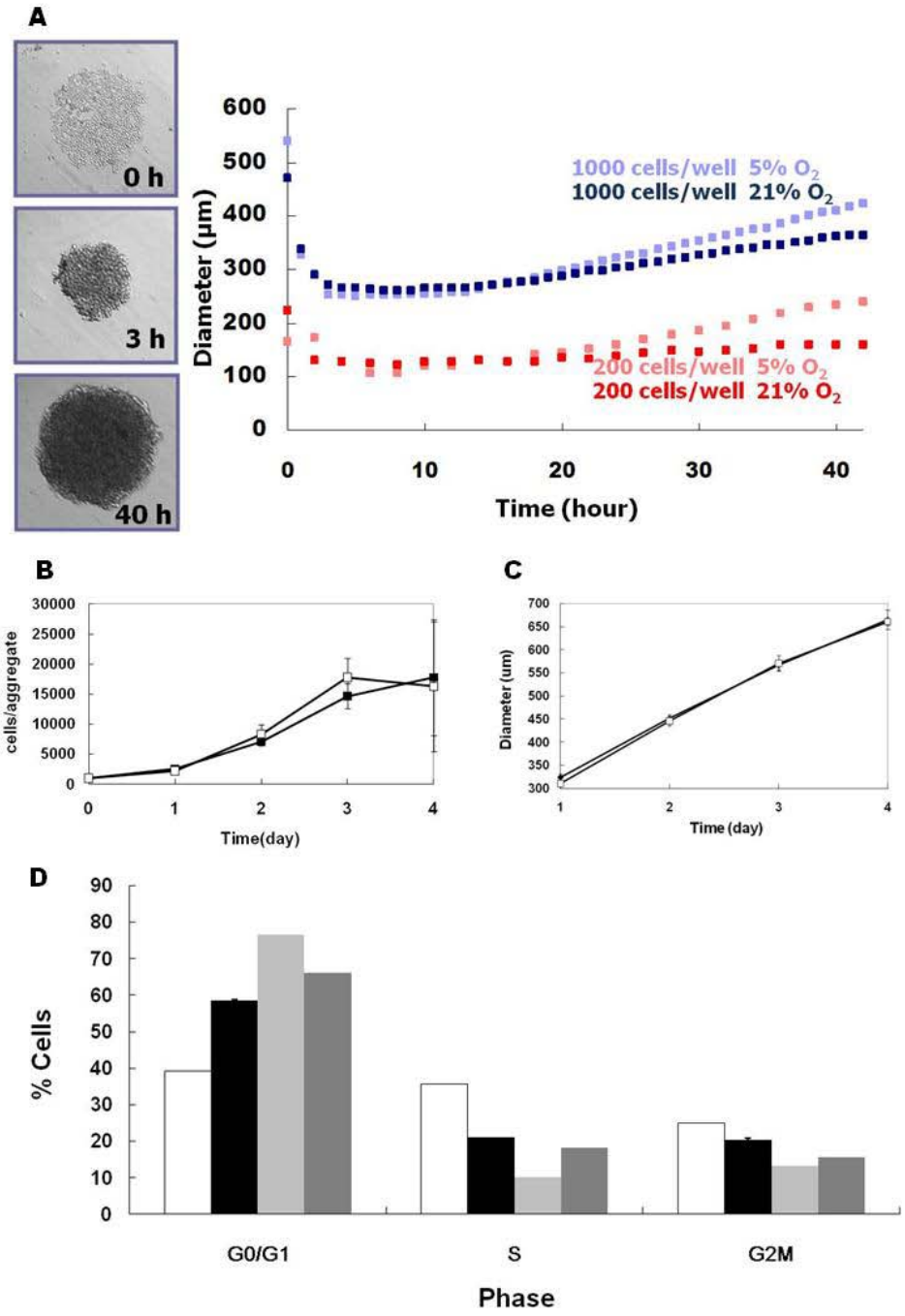

Figure 14. Characterization of MAPC aggregates and effect of different ambient oxygen. (a) Change in cell size during initial aggregate formation. (b) Cell proliferation during aggregate formation (■ 5% O_2; □ 21% O_2). (c) Diameter change with time (■ 5% O_2; □ 21% O_2). (d) Cell cycle on day 4 (□ 2D 5% O_2 in MAPC culture medium; ■ 3D 5% O_2 in MAPC culture medium; ■ 3D 21% O_2 in MAPC culture medium; ■ 2D 5% O_2 in differentiation basal medium).

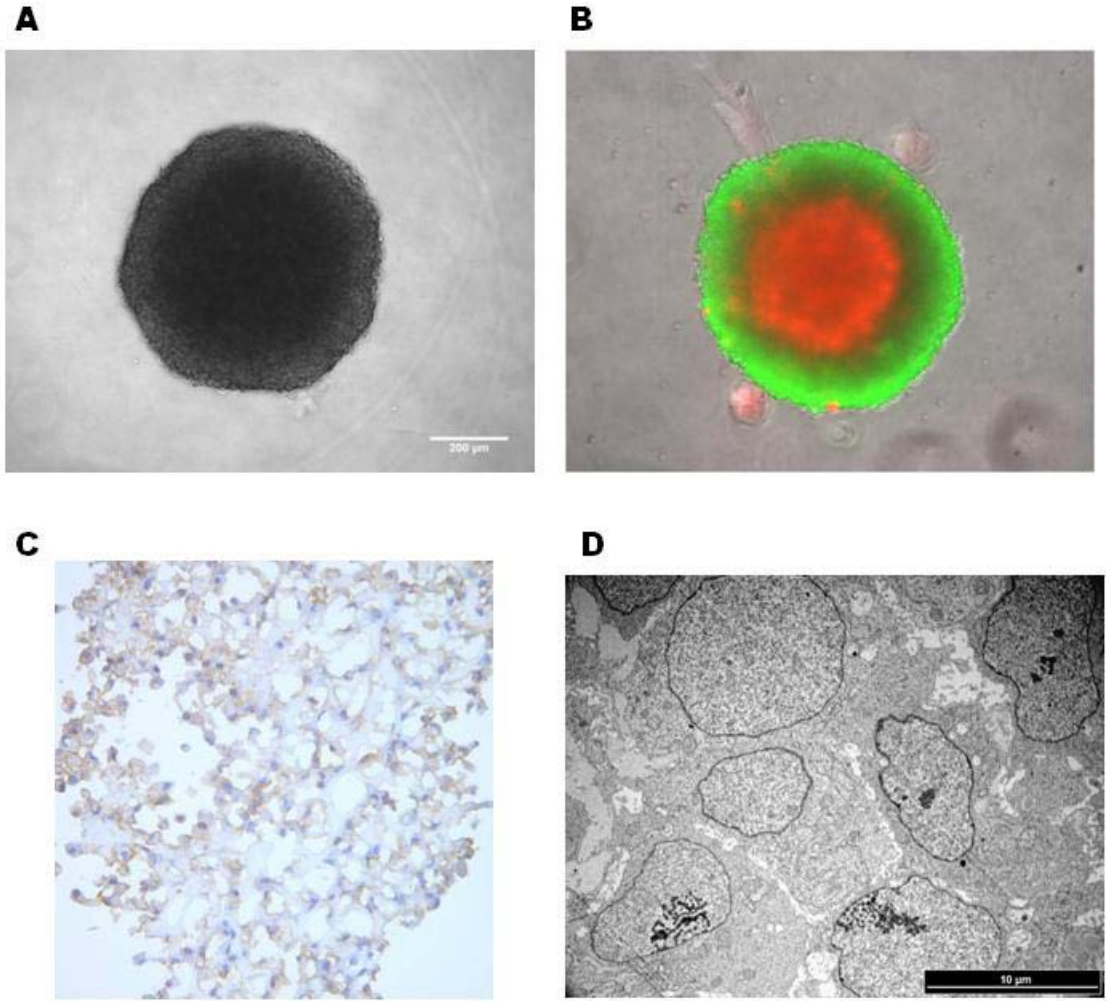

Figure 15. Morphology of aggregates at culture day 4 (in 5% O_2). (a) Phase contrast. (b) Viability staining; live (green) and dead (red) merged. (c) E-CADHERIN staining. (d) TEM section of MAPC aggregate.*

*Figure 15 (c) and (d) were from results of experiments conducted by KS.

3.3.2. MAPC aggregates retain MAPC phenotype in culture

Aggregates formed in complete MAPC medium with 5% oxygen, on day 4, expressed MAPC pluropotency-related transcripts (*Oct4, Rex1, Sall4 and CD31*) and primitive endoderm transcripts (*Gata4, Gata6, Sox7, Sox17,* and *Hnf3β*) at levels comparable to the parent MAPC-line cultured on 2D surface (Figure 16ab). Lineage specific transcripts (*Sox2, Pax6, Flk1,* and *Afp*) were chosen to show whether there was an onset of differentiation. Differentiation was not detected. *Pax6* and especially *Afp,* a gene which is rapidly up-regulated when MAPCs differentiate spontaneously, remained undetectable (Figure 16c). *Sox2* and *Flk1* transcript levels increased by more than 5 CTs, but this may be more indicative of the hypoxic condition inside the aggregates than differentiation. In addition, OCT4 protein expression was maintained in these aggregates as shown by flow cytometry (Figure 16d).

In contrast, aggregates formed in MAPC medium at 21% oxygen differentiated as they expressed a 32 fold more *Afp* transcript (Figure 17a) and the fraction of cells expressing OCT4 protein decreased by about 50% (Figure 17b). Formation of aggregates in MAPC medium without LIF, PDGF and EGF, even in 5% oxygen resulted in a 21 fold decrease in *Oct4* transcripts (Figure 17a) with only about 4% of the cells expressing OCT4 protein (Figure 17b). Thus, both high ambient oxygen concentrations and removal of LIF, PDGF and EGF negatively affected the *Oct4* expression during aggregate formation, and resulted in differentiation.

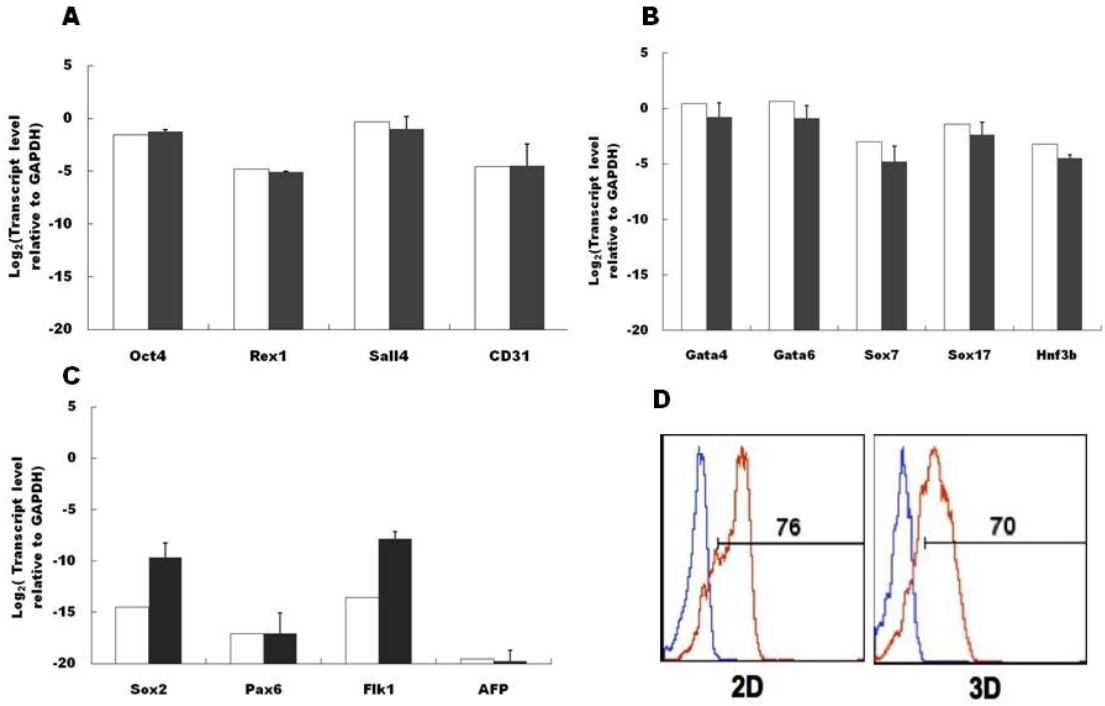

Figure 16. Transcript expression of MAPC aggregates in static culture (day 4) in 5% O_2. RT-qPCR for (a) pluripotency-related genes (b) primitive endoderm genes (c) lineage specific genes (□ 2D; ■ 3D). (d) *OCT4 protein staining on 2D culture and 3D aggregate culture.

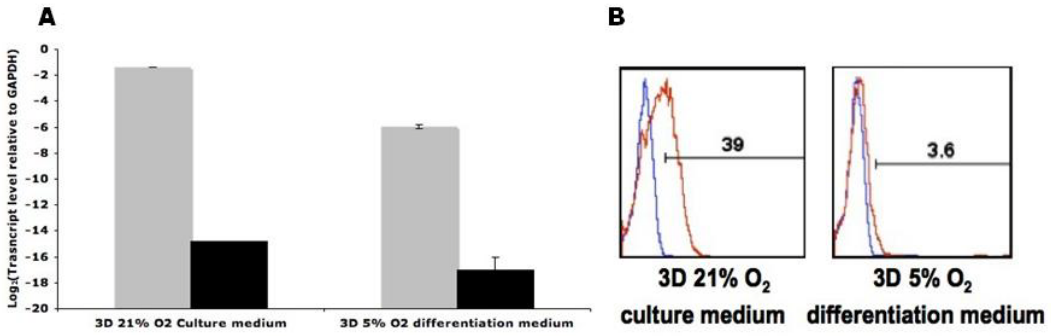

Figure 17. Effect of different culture conditions. (a) *Oct4* (■) and *Afp* (■) level change in 21% oxygen and in differentiation conditions. (b) OCT4 protein staining measured by FACS.*

* Figure 16(d) and Figure 17(b) were produced by KS.

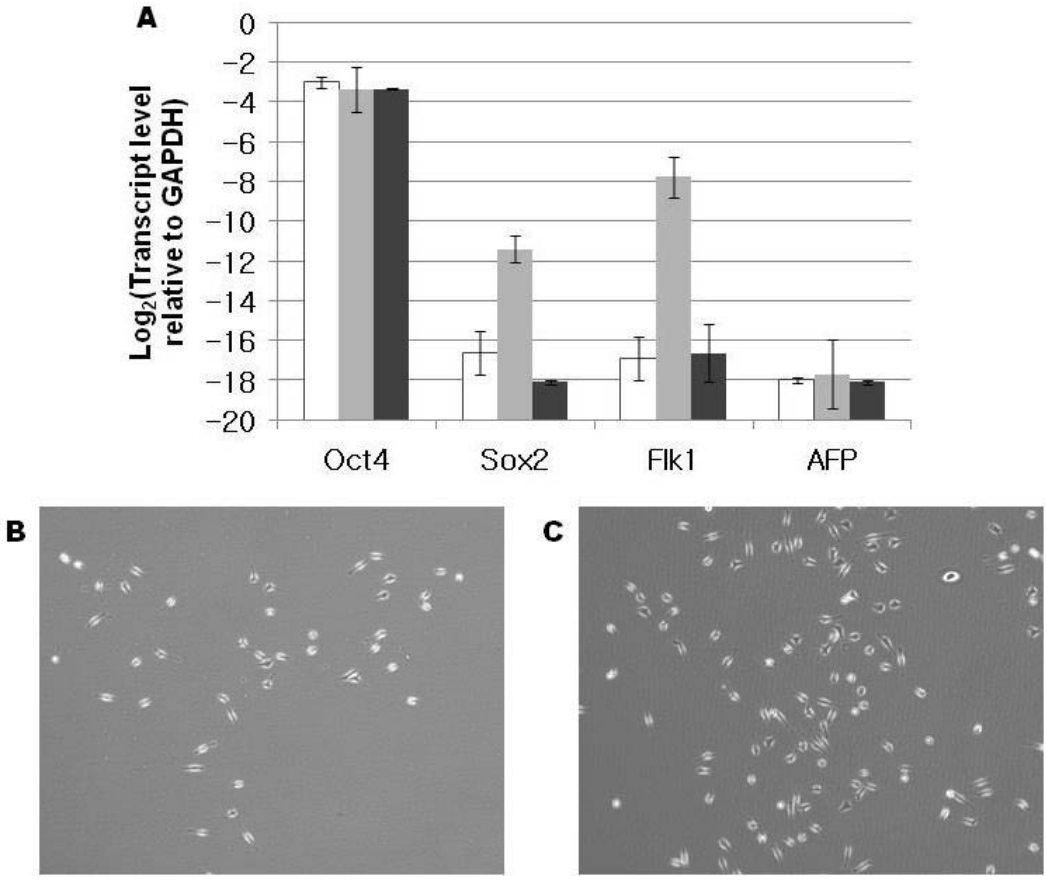

Figure 18. Recovery of rMAPC from 3D aggregate culture (4 days) to 2D culture (4 days). (a) RT-qPCR (□ 2D day 0; ■ 3D day 4; ■ 3D to 2D day 8). (b) Morphology of MAPC in 2D culture. (c) Morphology of MAPC in 3D culture for 4 days followed by 2D culture for 4 days.

Cells in MAPC aggregates formed under 5% O_2 in complete MAPC medium could also be trypsinized to single cell suspensions and re-cultivated on 2D surface exhibiting typical MAPC proliferation profiles and phenotype (Figure 18). Transcript levels of *Sox2* and *Flk1* recovered to the level of those in typical MAPC culture in 2D. *Oct4* levels were maintained, and *Afp* remained undetected during 3D and 2D culture.

MAPCs expanded as aggregates in the static culture condition also did not lose the capability of differentiating into different types of cells: neuroectoderm, hepatocyte-like cells, endothelial cells. After static culture as aggregates, MAPCs were dissociated and plated onto regular tissue culture plates for directed differentiation into aforementioned three lineages. The lineage specific markers were all expressed at similar levels compared with conventional 2D differentiation methods (data not shown, Subramanian and Park et al. manuscript submitted).

3.3.3. Expansion of MAPC as aggregates in suspension culture

We also explored whether MAPCs can be expanded as aggregates in suspension culture. MAPC aggregates were formed under static culture conditions for two days and then inoculated into a 250 ml spinner flask with a 100 ml working volume (Figure 13). During the spinner flask culture, inoculated aggregates continue to grow as they did in static culture but interestingly give rise to small clumps of cells (Figure 19 and Figure 20.). Initially 2-3 cell clumps were observed and the clumps grew in their sizes to become in the range of 30-200 μm after four days (Figure 20. b). During the first two days of static culture (day -2 to day 0) cell concentration increased from 10^4 to $5x10^4$ cells/ml. From day 0 to day 2 of suspension culture, an additional six-fold increase in cell number was seen. On day 2 of suspension culture, cell aggregates and clumps were harvested and the cell concentration in the flask was either reduced to 50% and 50 ml of fresh medium was added (half dilution) or reduced to the initial inoculation concentration (~50,000 cells/ml) in 100 ml of fresh medium (full dilution). At the end of six days of

culture, a final cell concentration of $7x10^5$ cells/ml, equivalent to 70 fold expansion, was obtained from the half-diluted flask culture (Figure 21a), and a cell concentration of $2.7x10^5$ cells/ml was obtained from the full-diluted flask culture. Staining with the LIVE/DEAD cytotoxicty kit (Molecluar Probes) demonstrated that the cells within the aggregates (day 4) retained high viability (Figure 19f). MAPCs were detached well with light trypsin treatment, and the detached cells were highly viable (Figure 19g).

To monitor cell metabolism, glucose consumption and lactate production were determined to calculate lactate production/glucose consumption ratio. The results suggest that medium replacement allowed the supply of the nutrients and the removal of waste products inhibiting cell growth, leading to the maintenance of the cultures in relatively steady state for four days. MAPCs are usually grown in low glucose medium; therefore glucose is not an important limiting factor. Lactate production rate is used to characterize the viability status of the culture. In the MAPC spinner culture, the yield ratio of $\Delta L/\Delta G$ was relatively maintained under 2.0 (except day 1 with a very low starting cell concentration), which is in accordance with the low cell death observed in the culture (Figure 21b).

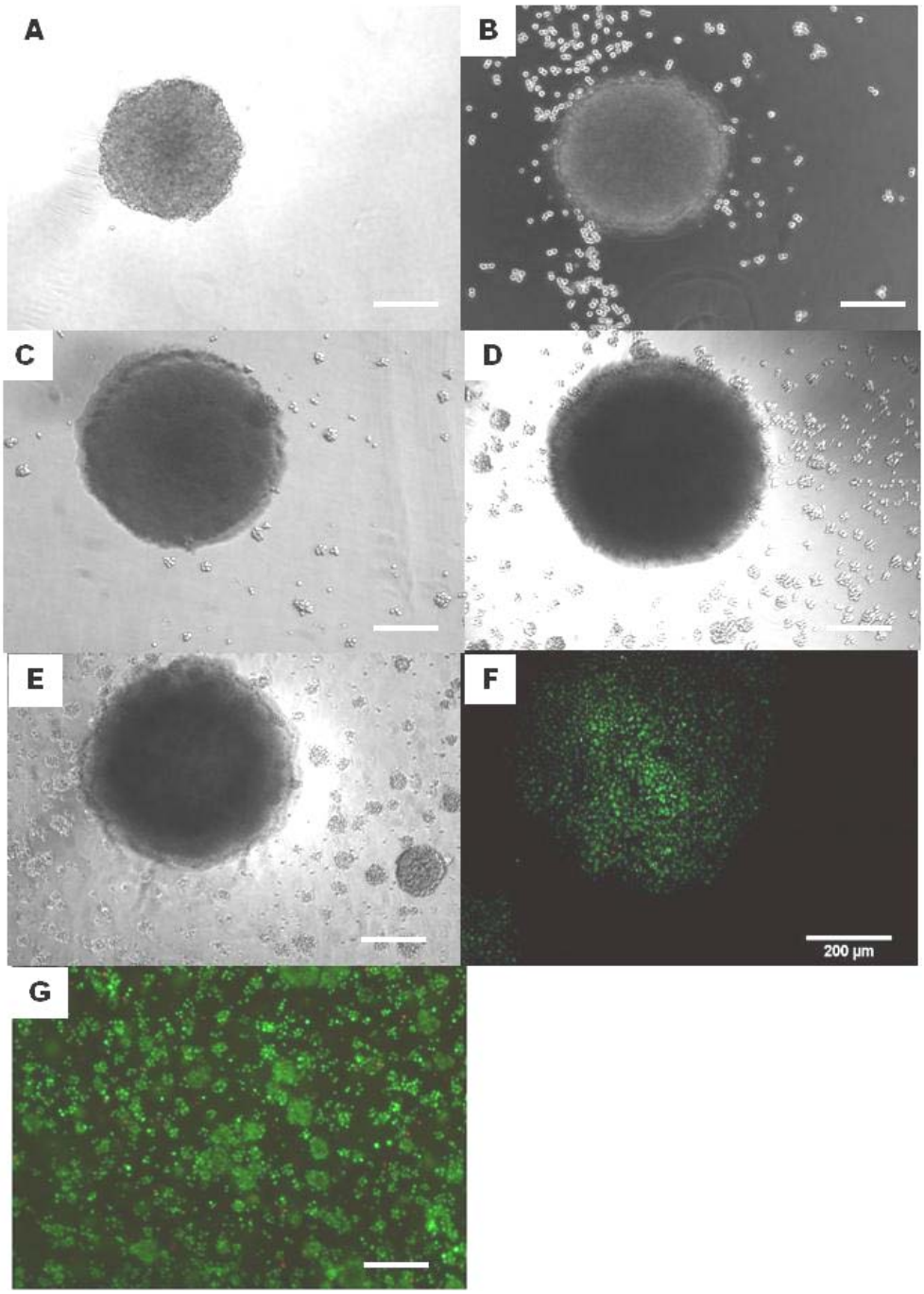

Figure 19. Morphology of MAPC aggregates during four day spinner culture. (a) Day 0 (b) Day 1 (c) Day2 (d) Day 3 (e) Day 4. (f)(g) Viability staining on day 4 (merged green (live) and red (dead)); (f) confocal image of an aggregate section (g) clumps. (Scale bar: 200 µm).

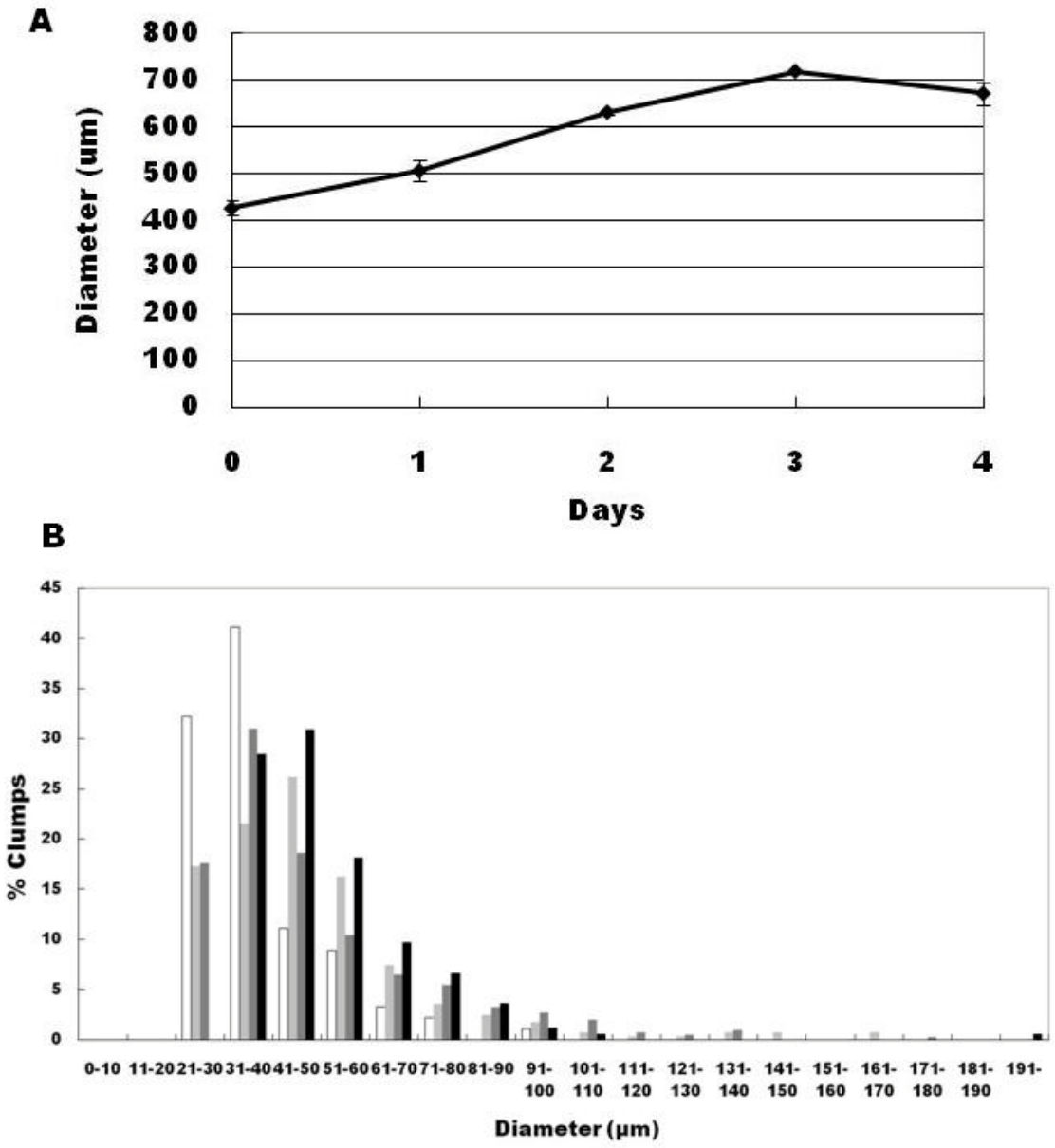

Figure 20. Size measurement of aggregates and small clumps. (a) Increase in diameter. (b) Size distribution of small clumps over four days (□ day 1; ■ day 2; ■ day 3; ■ day 4).

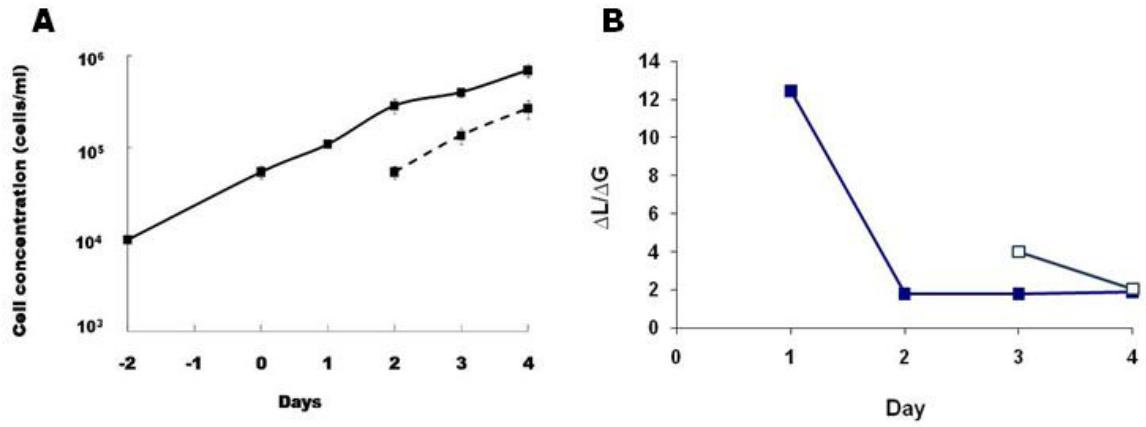

Figure 21. (a) MAPCs expanded by 70 fold in four days of spinner culture. Solid line (half dilution on day 2); dotted line (full dilution on day 2). (b) Ratio of the lactate production to glucose consumption during spinner culture (■ half dilution; □ full dilution).

The transcript levels of key MAPC genes (*Oct4*, *Rex1*, *CD31*, *Sall4)*, primitive endoderm genes (*Gata4*, *Gata6, Sox7, Sox17, and Hnf3b*), and lineage specific genes (*Hnf1a*, *Hnf4a*, *Flk1*, *Afp, VEGF*) of Day -2 (cells from 2D maintenance culture), Day 0 (cells after 48 h aggregation in wells) and Day 2 and 4 (aggregates in spinner cultures) were assessed by RT-qPCR. No differences in *Oct4*, *Rex1*, *CD31 and Sall4* transcripts could be detected, and no increase in *Afp* expression was observed (Figure 22). Maintained levels of *Hnf1a* and *VEGF* ruled out the possibility that cell may have differentiated to visceral endoderm or endothelial cells as suggested by the increased level of *Flk1* transcript; the increase of *Flk1* was thought to be related to the aggregate structure, not to the result of differentiation. Thus, the cells in stirred suspension culture could be expanded without obvious signs of differentiation.

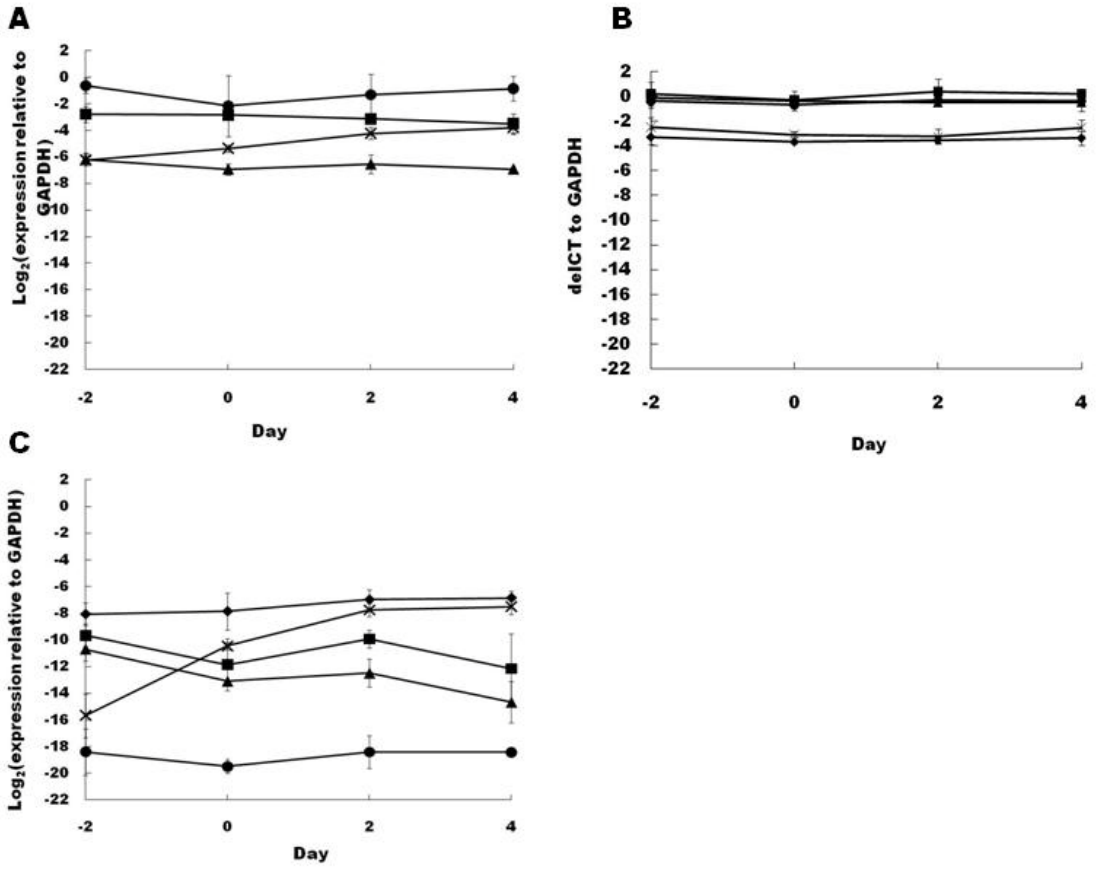

Figure 22. RT-qPCR of (a) pluripotency-related markers maintained during spinner culture (■*Oct4;* ▲*Rex1;* X *CD31;* ●*Sall4*), (b) primitive endoderm markers (■*Gata4;* ▲*Gata6;* x *Sox7;* ●*Sox17;* ◆*Hnf3b*), and (c) lineage specific markers (■*Hnf1a*; ▲*Hnf4a*; x *Flk1*; ●*Afp*; ◆*VEGF*).

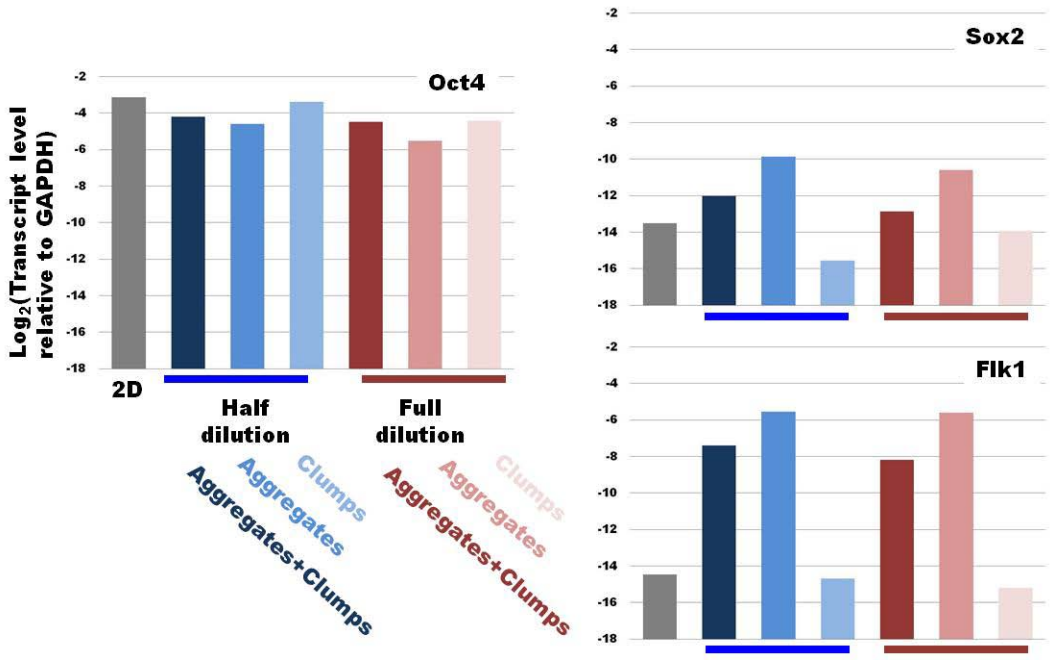

Figure 23. Comparison of stem cell marker expression in aggregates and clumps. *Oct4* was expressed at a similar level in all samples. Expression level of *Sox2* and *Flk1* differ between aggregates and clumps.

At day 4 of spinner flask culture, aggregates and small clumps were segregated and assessed by RT-qPCR to see if there is any differential gene expression between aggregates and small clumps. *Oct4* transcript level and other MAPC characteristic transcripts were expressed at similar levels in both aggregates and small clumps except *Sox2* and *Flk1*. The transcript level comparison between aggregates and small clumps also supported that the increase of *Flk1* level was unlikely the sign of differentiation. Aggregates, which were 4-20 times larger than clumps, expressed higher level of both *Sox2* and *Flk1* (Figure 23).

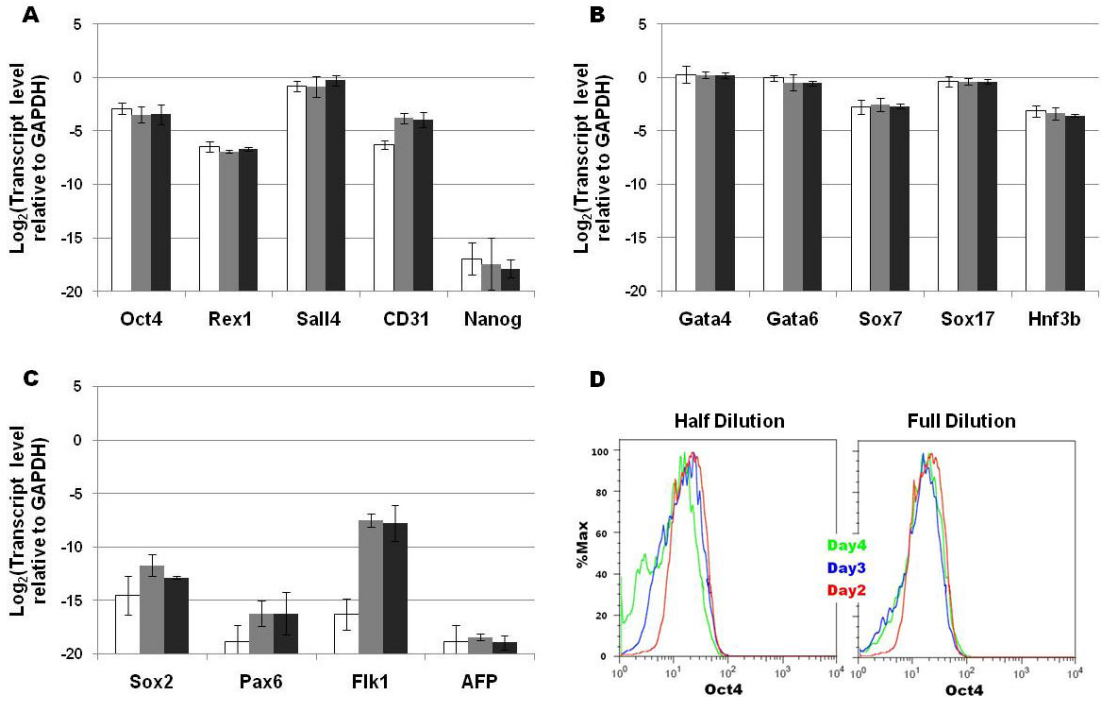

Figure 24. Comparison of cell phenotype at day 4 from full dilution and half dilution medium change on culture day 2. RT-qPCR for (a) pluripotency-related genes, (b) primitive endoderm genes, and (c) lineage-specific genes (□ 2D; ■ Half dilution; ■ Full dilution). (d) OCT4 protein staining by FACS.*

Replacement of half or the entire medium on day 2, did not influence maintaining MAPC as undifferentiated for four days in the spinner culture (Figure 24). As MAPCs express pluripotency related genes (*Oct4, Rex1, Sall4, CD31*) and primitive endoderm genes (*Gata4, Gata6, Sox7, Sox17, Hnf3β*), these genes were expressed similarly in half dilution and in full dilution cultures. *Nanog* and lineage specific genes (*Pax6, Afp*) were undetectable in both culture conditions. OCT4 positive cells were observed at similar

* Figure 24 (d) was produced by KS.

levels in both cultures although there was a small population of OCT4 negative cells observed in the half-diluted culture (Figure 24d).

To evaluate whether MAPC aggregates cultivated in spinner flasks maintained similar differentiation potential, Day 0, 2 and 4 aggregates and clumps were subjected to either spontaneous differentiation or directed hepatic differentiation as aggregates in static culture on 24 well ultra-low attachment plates using a protocol previously developed in our lab (Pauwelyn et al. manuscript submitted). As spontaneous differentiation proceeded, cells expressed decreased level of *Oct4* and increased levels of *Flk1* and *Afp*. The levels were similar among cells from different expansion days, (Figure 25a).

Differentiation towards the hepatocyte lineage was chosen because *in vitro* drug testing applications require large quantities of hepatocytes. The extent of up-regulation of hepatocyte-specific transcripts was evaluated by RT-qPCR at the end of twenty days of differentiation for cell aggregates collected at different points of spinner culture expansion. Expression levels were compared with the levels in the starting cell aggregates in each case. MAPC aggregates (from Day 0, 2 and 4 of spinner culture) were differentiated to 'hepatocyte-like' cells as shown by the up-regulation of hepatocyte specific transcripts *Afp*, *Albumin*, *Aat* and *Tat* (Figure 25b). The level of up-regulation of these genes was similar for all starting cell populations. In addition, differentiated cells from each of the differentiations also secreted albumin at 0.7-0.8 pg/cell/day or about 10% of the level secreted by adult rat hepatocytes, and urea was secreted at 4-7 μg/day.

Thus, the cells expanded in the spinner culture can also be used for generating large numbers of ‘hepatocyte-like’ cells.

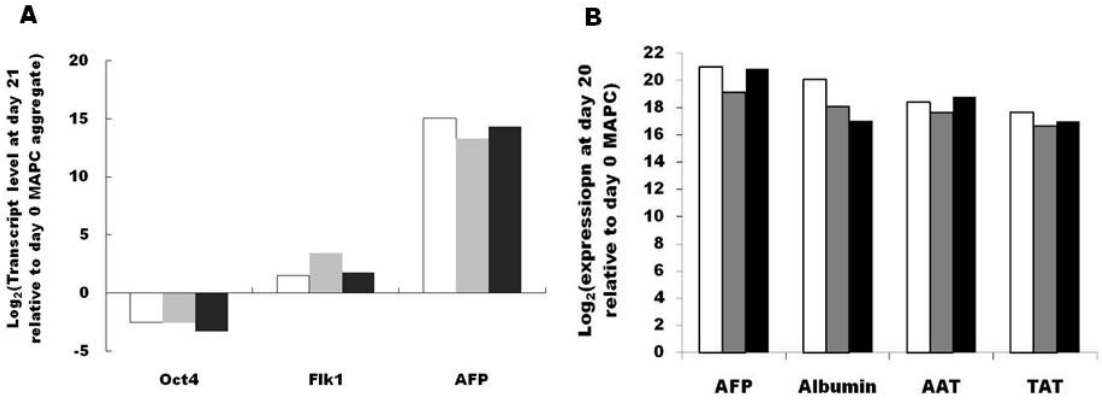

Figure 25. Differentiation potential of cells expanded in spinner culture (n-=1). (a) Spontaneous differentiation for 21 days. (b) Directed hepatic differentiation for 20 days. (□ from spinner culture day 2; ■ from spinner culture day 4 with half dilution; ■ from spinner culture day 4 with full dilution).

3.3.4. Expansion of MAPC as aggregates in longer-term spinner culture

MAPCs were further cultivated as aggregates for longer time (8 days) in the spinner culture system. First, RT-qPCR results showed that MAPCs started to differentiate in a continuous culture without any medium change after 4 day culture (data not shown). Since LIF is known as a major component of maintaining cell potency in MAPC culture medium as it is in mouse ESC culture, the effect of LIF supplementation was studied. Clumps and/or aggregates were collected on day 4, transferred, and centrifuged down in

wells of an ultra low attachment 96 well plate with three different media: fresh MAPC medium, cultured medium from day 4 spinner culture, and cultured medium supplemented with LIF (Figure 26). Only cells with the fresh medium formed compact aggregates with clear boundaries. Cells in the conditioned medium, even with LIF supplementation, clearly showed a sign of differentiation with spreading of cells and irregular surface boundaries of small-size aggregation. This morphology is similar to the aggregate formation in differentiation basal medium which resulted in the upregualtion of lineage specific genes and down-regulation of *Oct4* (Figure 17). These observations suggest that nutrient depletion in the MAPC medium, production of lactic acid or other toxins in addition to LIF depletion play a role in maintaining aggregates in the spinner culture.

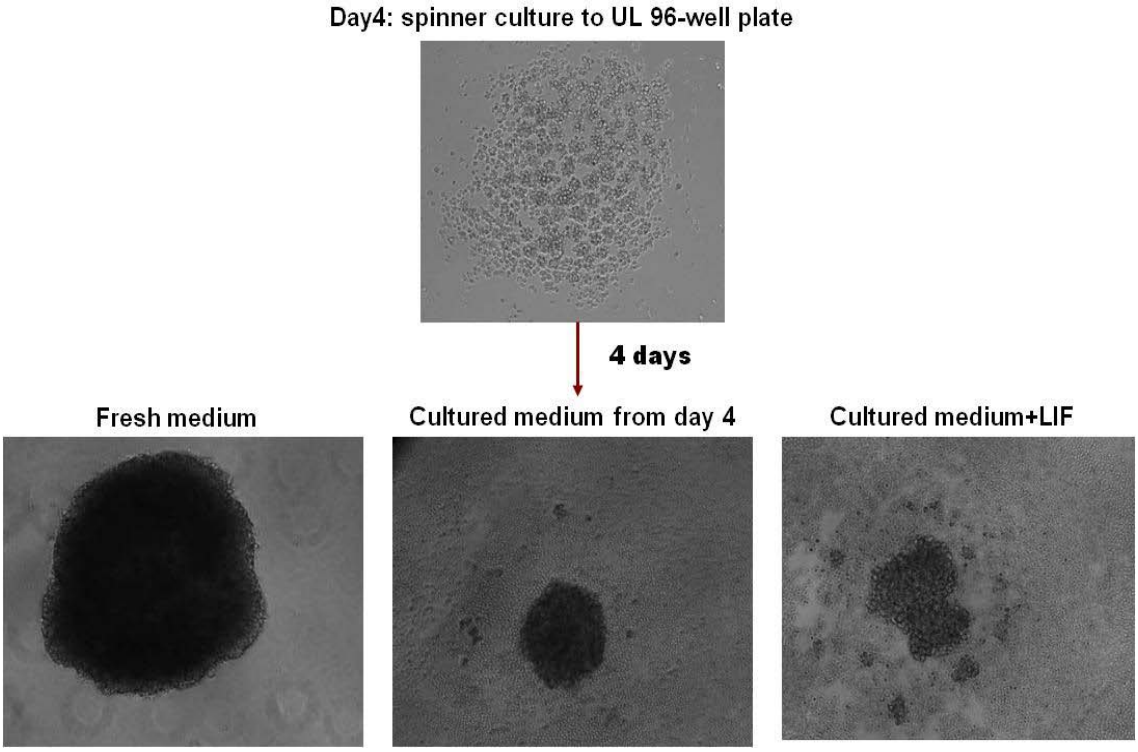

Figure 26. Effect of different media change on day 4 culture seen by morphology of aggregate formation.

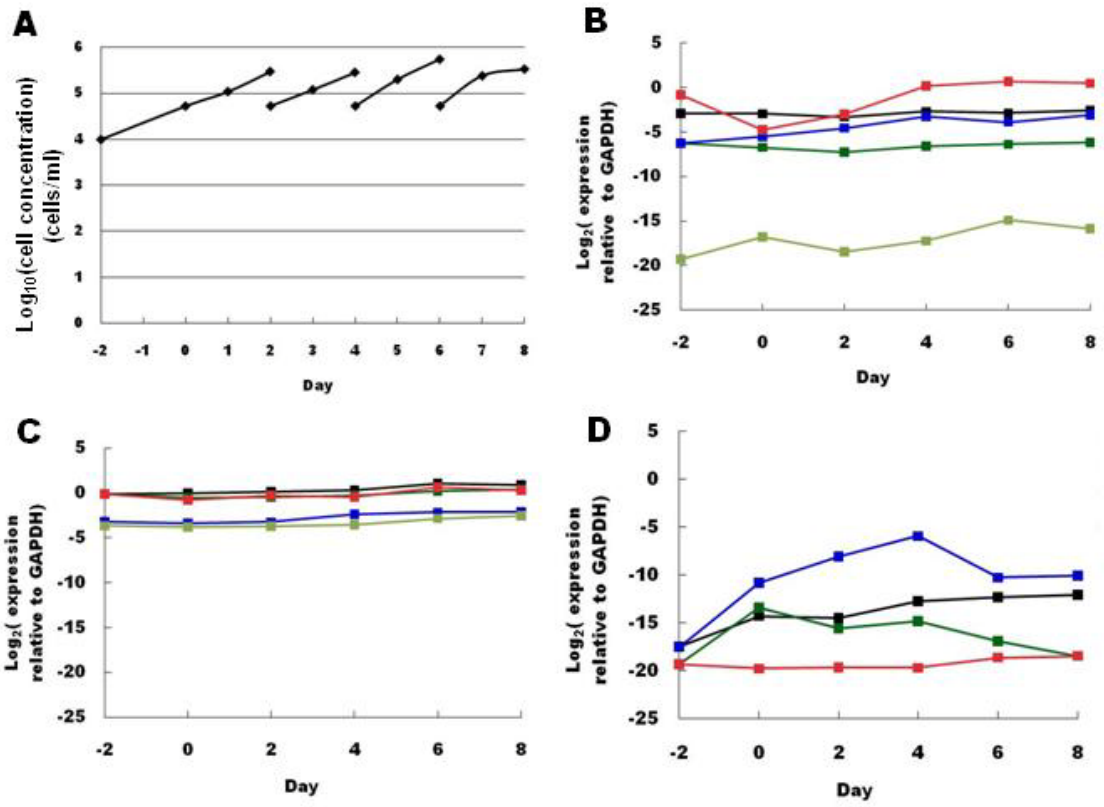

Figure 27. Aggregate culture for 8 days with a full medium change every two days. (a) Growth kinetics. RT-qPCR for (b) pluripotency related genes (*Oct4; Sall4; CD31; Rex1; Nanog*), (c) primitive endoderm genes (*Gata4; Gata6; Sox7; Sox17; Hnf3b*), (d) lineage specific genes (*Sox2; Pax6; Flk1; Afp*).

Knowing the culture requires an appropriate medium change, we cultured MAPC aggregates with full medium changes (into initial inoculation cell concentration in fresh medium) every two days. Cells proliferated at similar rates to those seen in 4 day cultures. The cell concentration reached ~3.0x10^5 cells/ml every two days (Figure 27a). Transcript levels of MAPC expressing potency related genes (*Oct4, Sall4, Rex1, CD31*) and primitive endoderm genes (*Gata4, Gata6, Sox7, Sox17, Hnf3β*) were maintained (Figure 27bc). *Nanog, Pax6* and *Afp* were maintained at undetectable level for 8 days (Figure

27bd). As observed in all 3D cultures, whether static or suspension, *Sox2* and *Flk1* expressions increased compared to 2D MAPC culture. While *Sox2* levels continued to increase over 8 days, a decrease of *Flk1* levels after day 4 was observed due to the dilution of big aggregates (Figure 27d).

3.4. Discussion

Stem cells offer great potential for regenerating and replacing dysfunctional tissues, and as tools for research on normal differentiation processes, models of disease, and for drug toxicity testing. Because of their importance in regenerative medicine and research, there is an increasing interest in the development of robust bioprocesses for generating large quantities of stem cells and their differentiated derivatives. Several bioreactor designs have been tested for cultivation of different stem cell types as reviewed in the Chapter 1. Among the different bioreactors, stirred tank based designs have been most widely used for the cultivation of mammalian cells because of the ease in maintaining homogenous environment with online process monitoring and control. Furthermore, extensive experience and knowledge on their design and operation has accumulated in the past that will be useful in the scale up of stem cell bioprocesses.

MAPCs posess extensive self-renewal and multi-lineage differentiation capacities. This makes them an excellent model among different stem cells for studying developmental

processes. As discussed in previous chapters, we have optimized a robust isolation procedure to obtain rat MAPC lines subsequent to the first isolation of a rat MAPC-1 line, with very similar phenotype and differentiation capabilities (Chapter 1, Subramanian et al. Methods in Molecular Biology, in press). MAPCs can be cultured at higher cell densities (1000 cells/cm^2) without change in multi-lineage differentiation capability when cultivated in 2D under 5% oxygen (Chapter 2). This prompted us to evaluate the possibility of growing MAPC as aggregates for suspension culture in a stirred tank. We adopted a forced aggregation method [220] because of their ease of use and the high-efficiency of aggregate formation. The forced aggregation method gave relatively uniform sizes of aggregates and allowed cells to continue to proliferate during aggregate formation [221, 222] (Figure 14). The aggregates appeared tightly packed, expressing cell membrane associated E-CADHERIN. This enhanced cell-cell and cell-matrix interactions seen in 3D aggregates may also help in better recapitulating the native microenvironment for applications in the study of development and morphogenesis, drug screening, stem cell differentiation, tissue engineering and tumor biology, in addition to their applicability in scalable suspension cultures. As an illustration, improved efficiency and maturation of hepatocyte differentiation from 3D MAPC aggregates was observed as compared to 2D MAPC surface culture (Subramanian et al. manuscript in preparation).

MAPCs express OCT4 protein in their nuclei [52]. *Oct4* is a transcription factor expressed in morula, inner cell mass (ICM), epiblast and hypoblast of mammalian embryos as well as in embryonic stem cells (ESC) and male germline stem cells [3, 223,

224]. As discussed in Chapter 1.1, maintaining Oct4 expression is crucial to maintain the pluripotent nature of cells in the ICM, epiblast and ESC. In addition to MAPC, other bone marrow derived stem and progenitor cells have been reported to express Oct4 mRNA/protein. When cultured without LIF, MAPC rapidly lose *Oct4* expression and begin to show signs of differentiation with rapid up-regulation of *Afp* expressed in the visceral and definitive endoderm (manuscript in preparation). In addition to *Oct4*, MAPC also express other ESC transcription factors including *Sall4* and *Rex1* as well as transcription factors of primitive endoderm/visceral endoderm/definitive endoderm such as *Hnf3b, Gata4, Gata6, Sox7, and Sox17* [54]. Aggregates formed in complete MAPC medium and 5% oxygen and maintained in either static or suspension culture expressed *Oct4, Sall4, Rex1, CD31, Gata6, Gata4, Sox7, Sox17* and *Hnf3b* transcripts at levels expressed in MAPC grown in 2D, but no *Afp* transcripts (Figure 16). MAPC aggregates also expressed similar levels of OCT4 protein that in 2D (Figure 16). Other pluripotent stem cells including mouse ESCs have been cultured in suspension as undifferentiated aggregates in a medium supplemented with LIF [165]. For mESC, withdrawal of LIF from the medium results in differentiation of ESC into embryoid bodies (EBs) [222, 225]. In addition to the requirement for LIF (and EGF, PDGF), we found 5% oxygen is favorable for maintaining and expanding undifferentiated MAPC as aggregates or in 2D surface culture (Figure 17). This is consistent with the findings that culturing hematopoietic stem and progenitor cells (HSCs) at low oxygen tension (1-5%) maintained the earliest progenitor cells, while increase in oxygen tension resulted in

differentiation into more mature cell types [226, 227]. Low oxygen tension facilitated the expansion and maintenance of stem cell assicoated genes in MSCs as well [207, 208].

While the phenotype of MAPC in aggregates was similar to that of MAPC in 2D surface culture, we noticed increased expression of *Flk1* and *Sox2* in the aggregates compared with MAPCs harvested from 2D adherent cultures. We speculate that up-regulation of *Flk1* may be due to hypoxic responsiveness of the cells within the aggregate, as has been observed in other systems [228]. It is interesting to see a modest up-regulation of *Sox2*, a transcription factor found in the ICM, epiblast and ESC as well as in NSC, in the MAPC aggregates[229]. In N2/B27 medium which induces neuroectodermal differentiation, MAPC express transcripts specific for neuroectoderm progenitors including *Sox2* and *Pax6* [230]. However, as no increase in expression of *Pax6* was observed in the aggregates, an early commitment to the neuroectoderm lineage is unlikely. Upon cell dissociation of the aggregates and replating in 2D surface culture, the expression of *Flk1* and *Sox2* transcripts returned to levels seen before 3D aggregate formation (Figure 18). In spinner culture, small clumps expressed lower levels of *Flk1* and *Sox2* than aggregates did. This also supports that increased expression of these genes is more related to the aggregate structure and degree of hypoxia created inside aggregates or clumps, than to the sign of differentiation.

Unlike in the static culture of aggregates, spinner cultures gave rise to small clumps, and these clumps proliferated over time. In the stirred culture system, aggregates and clumps

showed high viability; the necrotic core of cells inside, which was seen in the aggregates from the static culture, was not observed. Also, the clumps did not seem to grow during the culture in an unlimited manner. They do not grow larger than 300 μm in diameter. As MAPCs from the clumps have similar characteristic phenotype and differentiation potential compared to those from pre-formed aggregates (Figure 23), generation and control of the clumps seem to be an interesting phenomenon in scaled-up spinner culture of MAPCs. With more articulate control of shear stress and initial aggregate size, small clumps may have an advantage of maintaining MAPCs in aggregates for longer term and more robust bioprocessing.

In order to culture the aggregates for longer periods of time, proper medium replacement is necessary in order to maintain undifferentiated MAPCs. LIF supplement study in Figure 26 suggests that LIF is not the only limiting factor which is depleted during the spinner culture as the cells proliferate. Because of this, with the fresh medium replacement, the cell concentration should be tightly controlled during the spinner culture because MAPCs proliferate rapidly as clumps. Half medium replacement every two days gave inconsistent results in maintenance of undifferentiated MAPC related genes. Diluting the cell concentration into the initial inoculation concentration every two days worked best for 8-day suspension culture. However, further optimization is needed to improve the longer-term culture conditions.

Importantly, to demonstrate that MAPCs in aggregates retained their potency, cells cultured as aggregates were tested for their ability to spontaneously differentiate in differentiation basal medium and for directed differentiation to the hepatic lineage. If the cells derived from aggregates were expanded in 2D to obtain enough cells for differentiation, the possibility exists that the differentiation seen is the result of a subfraction of cells that retained this ability and outgrew other cells that had lost differentiation potential. We therefore assessed if differentiation results could be obtained from the MAPC aggregates themselves, without replating onto 2D surface cultures. Consistent with our finding that the phenotype of MAPC was unchanged when cultured in aggregates, the induction of lineage-specific transcripts was similar for cells as aggregates and the cells maintained in low-density 2D surface culture (Figure 25). Thus, we demonstrated that the cells in the aggregate cultures retained multi-lineage differentiation potential. For directed hepatic differentiation, the aggregates collected at different points of spinner culture (day 0, 2 and 4) could be differentiated to hepatocyte-like cells with similar levels of induction of hepatocyte specific transcripts as well as albumin and urea secretion rates. This strongly suggests that there was no progressive loss of potency of MAPCs during the four days of spinner culture as aggregates (Figure 25).

In conclusion, we have developed a suspension based culture platform with 70 fold cell expansion of rat MAPCs as aggregates to a final cell concentration of 10^6 cells/ml (8-10 x 10^7 cells). In addition, we demonstrated the differentiation of these spinner expanded

MAPCs into ‘hepatocyte-like’ cells that has applications in *in vitro* hepatoxicity screening and as a model for studies related to liver development and regeneration. The protocol developed for rat MAPC differentiation to hepatocytes can be readily applicable for human ESC differentiation, with minor modifications for clinical applications. Further, we have demonstrated that aggregates can be maintained undifferentiated in spinner culture for a longer term with appropriate medium replacements. Thus, this study lays the foundation for the development of a scalable culture platform for expansion of human MAPCs and ESCs, and their differentiation into human hepatocytes, in the future.

CHAPTER 4. EXPANSION AND DIRECTED HEPATIC DIFFERENTIATION OF MAPC IN MICROCARRIER SUSPENSION CULTURE

4.1. Introduction

Advances in stem cell research have opened the possibility that stem cells may be used as therapeutics. Among the many organs and tissues for which developing stem cell applications is being pursued, the liver is of particular importance because of the lack of effective therapies for liver failure. Existing treatments for liver failure are limited, and the only real cure is liver cell or organ transplantation. However, the shortage of donor cells and organs makes this option often unavailable for a large number of patients. Hepatocytes isolated from liver have limited proliferation potential in culture, and cultured hepatocytes very quickly lose their functional attributes. Therefore, there has been intensive research for a source of cells that can proliferate extensively and sustain liver functions in culture. Cultivation of hepatic progenitor cells, immortalization of hepatocytes, and derivation of functional hepatocytes from stem cells are among the more prevalent approaches [106, 108, 123, 133, 134, 231-233]. With the progress in stem cell science, hepatic cells derived from stem cells, which are capable of virtually unlimited self-renewal, have great potential to be such a steady cell source.

The liver is the largest internal organ in the adult body. Any therapeutic application will require a large quantity of cells in the order of ~10^9-10^{10} cells per treatment. Employing a scalable reactor system could facilitate production of a sufficient supply of differentiation-competent or differentiated cells to meet such a clinical need. Since the conventional method of expanding and differentiating stem cells in tissue culture plates is

labor intensive and difficult to scale up, several culture systems including rotary culture systems, perfusion culture systems, and stirred suspension systems for expansion and differentiation of stem cells have been investigated [155, 161, 166, 172, 176, 179, 184, 185]. Among those systems, the stirred suspension culture has the advantage of having been widely used in growing mammalian cells for decades. It also allows high density culture in a more homogeneous environment than other culture methods. Stirred reactor cultures have been used to expand or differentiate hematopoietic stem and progenitor cells (HSPCs), neural stem cells (NSCs), and human and mouse embryonic stem cells (ESCs) grown as embryoid bodies (EBs) [155, 166, 179, 184]. In Chapter 3, it was demonstrated that rMAPCs as aggregates can be expanded undifferentiated in a stirred suspension culure.

Although aggregate expansion in stirred reactors allows a high density culture, produces a large number of cells, may provide physiologically more relevant cell culture environment, it has some technical drawbacks. If the aggregates are formed spontaneously, variation in aggregate sizes may produce heterogeneity in the culture, and forced aggregation methods by centrifugation still requires a scaled-up system to produce large numbers of aggregates. Also as aggregates increase their size by cell proliferation, necrotic cores form inside the largest aggregates, which may negatively influence the culture.

For cells grown as monolayers like those on tissue culture plates, microcarriers have the advantage of providing a large surface area for a given reactor volume. Microcarriers are particles, typically made of cellulose, glass, plastic, or polyester, and usually with diameters of 100-250 μm. By providing a surface for attachment, they allow anchorage-dependent cells to be cultivated in stirred tank bioreactors for large scale operations. They have been used for cultivation of mouse and human ESCs, mesenchymal stem cells, and umbilical cord stem cells [180-182, 188, 234-237]. For differentiation applications, microcarriers have been used in a few studies wherein pluripotent stem cells were differentiated into cardiomyocyte-like cells, endoderm progenitor cells, and early three germ lineages [166, 176, 179, 180]. rMAPCs are lightly adherent cells that can be grown on the microcarrier surface.

In Chapter 4, using rMAPCs as a model system, we show that microcarrier culture has the potential of being a highly efficient scalable means of stem cell expansion and directed hepatocyte differentiation. This chapter describes the results of a close collaboration with Kartik Subramanian. Figures with * were from results of experiments conducted by KS

4.2. Materials and Methods

4.2.1. Establishment and maintenance of Rat MAPC line

One rat MAPC line (rMAPC-1) was used in this study. The isolation of rat MAPC lines has been previously described [52, 54]. To explain the procedure in short, rMAPC-1 were isolated from bone marrow of the tibia and femur of a four week old female rat (Fischer). Isolated bone marrow cells were plated on 6 well tissue culture plates in MAPC medium at $6x10^6$ cells/well and cultured in a 5% O_2 and 5-6% CO_2 incubator at 37°C. After four weeks of culture, hematopoeitic cells were removed using magnetic microbeads against CD45 and TER119 (Miltenyi Biotec) and the remaining cells are seeded into 96 well plates at 5-10 cells/well. Small and spindle shaped cells that appeared in the wells were subsequently expanded and screened for MAPC phenotype (expression of *Oct4, Rex1* and *CD31*) and tri-lineage (neuroectoderm, endoderm, mesoderm) differentiation potential [52]. The established MAPC cell line was maintained at 37°C in 5% oxygen and 5-6% CO_2 at a seeding cell density of 300 cells/cm^2 and passaged using 0.05% (w/v) Trypsin-EDTA (5 mg/l, Cellgro) every two days [52].

4.2.2. MAPC medium

Basal culture medium consisted of a 60/40 (v/v) mixture of low glucose Dulbecco's Modified Eagle medium (DMEM) (Gibco, USA) and MCDB-201(Sigma) supplemented with 0.026 μg/ml ascorbic acid 3-phosphate (Sigma), linoleic acid bovine serum albumin (LA-BSA, Sigma) (final concentrations of 10^3 μg/ml BSA and 8.13 μg/ml linoleic acid),

insulin-transferrin-selenium (ITS, Sigma) (final concentration 10 μg/ml insulin, 5.5 μg/ml transferring, 0.005 μg/ml sodium selenite), 0.02 μg/ml dexamethasone (Sigma), 4.3 μg/ml β-mercaptoethanol. For MAPC expansion, basal medium was supplemented with 2% (v/v) qualified fetal bovine serum (Hyclone). In addition, MAPC medium also contained three protein factors: human platelet derived growth factor (PDGF-BB, R&D) (10 ng/ml), mouse epidermal growth factor (EGF, Sigma) (10 ng/ml), and mouse leukemia inhibitory factor (LIF) (Chemicon, ESGRO) (10^3 units/ml). All media used were also supplemented with 100 IU/ml penicillin and 100 μg/ml streptomycin (Gibco).

4.2.3. Suspension flask culture of MAPC on microcarriers

Cytodex 1, a crosslinked dextran microbead with N, N-diethylamioethyl groups on the surface, was purchased from GE healthcare as dry powders. Cytodex 1 stock was prepared by washing 1g of microcarrier powder with PBS for 3-5 times. Swollen beads were sedimented in 100 ml fresh PBS and sterilized by autoclaving.

Prior to suspension culture, microcarriers were washed with low glucose DMEM (Gibco) twice and incubated in MAPC medium for two hours at 37°C. rMAPC from 10cm adherent tissue culture plates (NUNC) were washed with PBS. 1 ml 0.05% (w/v) Trypsin-EDTA (Cellgro) was added to each plate and the plates were lightly tapped several times. 5 ml of previously collected culture supernatant was added to each well to neutralize trypsin. The cells were collected, washed, and resuspended in MAPC expansion medium at a concentration of 1.2 $x10^6$ cells/ml. Cells were added to 12 mg/ml

Cytodex 1 microcarriers at the concentration of 0.6 $x10^6$ cells/ml. The mixture was incubated for 30 minutes at 37°C to allow initial cell attachment to the beads with occasional shaking of the tube. Then the mixture was transferred into a 98 ml of MAPC expansion medium in a 250 ml spinner flask (Wilbur). The culture was stirred at 70 rpm on a belt-driven magnetic stir plate (Bellco), and maintained at 37°C, 5% O_2 tension and 5% CO_2 for 4 days of expansion culture without any medium change.

4.2.4. *In vitro* directed hepatic differentiation

MAPC were differentiated into hepatocytes using a four step twenty days hepatic differentiation protocol with modifications. For static plate differentiation, cells were inoculated in an ultra-low attachment 24 well plate (Corning) at a starting cell concentration of $1.2x10^4$ cells/ml with 0.23 mg/ml Cytodex 1 microcarriers. For stirred suspension differentiation, cells were inoculated in a 250 ml spinner flask at $3.6x10^4$ cells/ml with 0.6 mg/ml of Cytodex 1 microcarriers in 100ml MAPC medium. The cells were expanded in a 5% O_2 and 5% CO_2 37°C incubator. After 2 days of expansion culture, when the cells were 80-90% confluent on the microcarrier surface, the cells with microcarriers were washed once with PBS and resuspended in 1ml of hepatic differentiation medium for static plate differentiation or 80 ml of hepatic differentiation medium in a 250 ml spinner flask for stirred suspension differentiation. The composition of differentiation basal medium was the same as basal MAPC medium except that ITS and LA-BSA were at 25% of the amount in MAPC medium, and the concentration of

dexamethasone was at 0.4 μg/ml and the three protein factors and serum were absent. Furthermore, additional protein factors were added as described below. The cytokines and growth factor supplements were added as follows: (i) Day 0:Activin A (100 ng/ml) and Wnt3a (50 ng/ml) (ii) Day 6:bFGF (10 ng/ml) and BMP4 (50 ng/ml) (iii) Day 10: FGF8b (25 ng/ml), aFGF (50 ng/ml) and FGF4 (10 ng/ml) (iv) Day 14: HGF (20 ng/ml) and Follistatin (100 ng/ml). Differentiations were carried out at 21% O_2 and 5% CO_2 37°C for twenty days with 50% media change, corresponding to the differentiation stage, every two days.

After 20 days of differentiation on microcarriers, cells were dissociated by 0.05% Trypsin with 2% chicken serum. Microcarriers were filtered out by a 40μm cell strainer. The single cell suspended cells were than seeded into a ultra low attachment 96-well plate at 8000 cells/well and cultured overnight to allow aggregation. The newly formed aggregates were transferred to a spinner flask and cultured for 15 days in step 4 hepatic differentiation medium.

4.2.5. RNA Isolation and RT-qPCR

Total RNA was isolated from rMAPC cell lysates using RNAeasy microkit (Qiagen) according to instructions provided in the kit. cDNA was synthesized from the extracted RNA using the Superscript III reverse transcriptase (Invitrogen) method. The PCR reaction mix consisted of cDNA samples, SYBR Green Mix PCR reaction buffer (Applied Biosystems) and primers (5 μM stocks, sequence in table 1). The RT-qPCR

reaction was run on a Realplex mastercycler (Eppendorf) using the following program: 50°C for 2 min, 95°C for 10 min, and 40 cycles at 95°C for 15 sec and 60°C for 1 min followed by a dissociation protocol to obtain a melting curve. Transcription abundance relative to *Gapdh* was calculated as $\triangle$Ct which is Ct(transcript of interest)-Ct(*Gapdh*) and transcript abundance in sample relative to day 0 was calculated as $\triangle$Ct (day0)-$\triangle$Ct(day of sample).

4.2.6. Intracellular staining for OCT4 by flow cytometry

Trypsinized cells were washed with and suspended in PBS with 3% (v/v) serum. After 15-20 min fixing with 4% paraformaldehyde (PFA), and 1 hr blocking in SAP buffer (PBS with 0.1% (w/v) saponin and 0.05% (w/v) sodium azide) supplemented with 10% donkey serum, cells were incubated for 1 hr with 1μg/ml OCT3/4 antibody (Santa-Cruz, N19) or Goat IgG isotype control (Jackson Immunoresearch) diluted in SAP buffer followed by incubating with Cy5 labeled anti-goat IgG (Jackson Immunoresearch, 1:500 in SAP buffer) for 30 min. Finally, cells were washed and resuspended in 500 μl PBS for flow cytometry analysis using a FACS Calibur (Becton Dickinson).

4.2.7. Asialoglycoprotein receptor-1 (ASGPR-1) immunostaining by flow cytometry

To determine functional maturation to hepatocytes, flow cytometric analysis was performed with an anti-asialoglycoprotein receptor 1 (ASGPR-1) antibody. Cells were harvested from the microcarriers by trypsinization. After fixing with 4% PFA for 20 min

and blocking for 1 hr in PBS with 3% (v/v) FBS, cells were incubated with anti-ASGPR-1 antibody (Thermoscientific, 1:10) for 30 min, followed by Alexa 488-conjugated goat anti-mouse IgG secondary antibody (Invitrogen, 1:500) for 30 min. Then cells were washed and resuspended in 500 μl PBS for flow cytometry analysis using a FACS Calibur (Becton Dickinson).

4.2.8. Phosphoinopyruvate carboxykinase (PEPCK) immunostaining

Cell-laden microcarriers were fixed with 4% PFA for 20 min and blocked in SAP serum buffer for 1 hr. Cells were stained with an anti-PEPCK antibody in SAP buffer (Santa cruz, 1:2000) at 4°C for overnight and stained with A488 anti-rabbit IgG (Invitrogen, 1:500) for 30 min. Then cells-microcarriers were washed, resuspended in PBS, and observed under inverted fluorescent microscope (Axiovert 200, Zeiss).

4.2.9. Cell viability staining

The “live/dead viability/cytotoxicity kit” (Invitrogen) was used to stain cells on microcarriers with calcein and ethidium. Component B was added first to DPBS (1:1000) and then component A was added to DPBS with component B (1:2000). Cells were incubated with the staining solution for 15-30 min at 37°C. Cells were washed once with PBS and observed under inverted fluorescent microscope (Axiovert 200, Zeiss). Live and dead cells appear as green and red respectively.

4.2.10. Cell enumaration by nuclei counting

Microcarriers from 1 ml culture were centrifuged at 500 rpm for 30 sec to remove supernatant. After adding 300-500 µl counting staining solution (0.1% (w/v) crystal violet (Sigma) in 0.1 M citric acid solution (Sigma)), the sample was incubated for 1 hr at 37°C. Nuclei were released by gentle shearing using a Pasteur pipette in a vertical position. The nuclei were counted with a hemacytometer.

For fixative staining, Cells-microcarriers in 1 ml culture were stained by adding a drop or two of fixative staining solution (0.5% (w/v) crystal violet in 40% ethanol and 60% PBS) for 1-2 min. Stained cells-microcarriers were washed with PBS twice to remove the staining solution from the supernatant.

4.2.11. Albumin and urea secretion assay

The albumin secretion rate was quantified using the rat albumin ELISA quantitation kit (Bethyl) according to instructions provided in the kit. Urea production rate was measured by using QuantiChrom urea assay kit (BioAssay Systems) following the instructions provided in the kit for low urea samples.

Table 5. List of primer sequences used in Chapter 4.

Tissue/Lineage	Gene	Forward Primer	Reverse Primer
Housekeeping	*Gapdh*	AAGGGCTCATGACCACAGTC	GGATGCAGGCATGATGTTCT
Pluripotency/ MAPC	*Oct4*	CTGTAACCGGCGCCAGAA	TGCATGGGAGAGCCCAGA
	CD31	GGACTGGCCCTGTCACGTT	TTGTTCATGGTGCCAAAACACT
	Rex1	AAAGCTTTTACAGAGAGCTCGAAACTA	GTGCGCAAGTTGAAATCCAGT
	Sall4	AGAACTTCTCGTCTGCCAGTG	CTCTATGGCCAGCTTCCTTC
Definitive endoderm	*Gsc*	CCCGGTTCTGTACTGGTGTC	CCCACGTCTGGGTACTTTTGT
	Mixl1	GGGAAGATTTCCTCCATCGT	CTGAGAACCAGATGTACAGAC
	Cxcr4	GGATGGTGGTGTTCCAGTTC	TCCCCACGTAATACGGTAGC
	Eomes	CCAGACCTTCACCTTCTCAG	GTGTACATGGAATCGTAGTTGTC
Hepatic lineage	*Afp*	ACCTGACAGGGAAGATGGTG	GCAGTGGTTGATACCGGAGT
	Ttr	CAGCAGTGGTGCTGTAGGAGTA	GGGTAGAACTGGACACCAAATC
	Albumin	TCTGCACACTCCCAGACAAG	AGTCACCCATCACCGTCTTC
	Aat	CAAACAAGGTCAGCCATTCTC	CAGCATCATTGTTGAAGACCC
	Tat	GGAAGCTAAGGATGTCATTCTG	GACCTCAATTCCCATAGACTC
	G6p	GATTCCGGTGCTTGAATGTC	AGGTGATGAGACAGTACCTC
	Mgst1	CAAGATTGAAAGCATGGCTG	AAACCTTGTTGGTTAGCCTC
	Factor V	CAATGCCAGATGTAACAGTC	TGTCAATATAAGCCTGCATCC
	Arginase1	TATCGGAGCGCCTTTCTCTA	ACATACCGTGGGTTCTTCAC
	Hnf4α	AAATGTGCAGGTGTTGACCA	CACGCTCCTCCTGAAGAATC
Differentiation markers	*Sox2*	GGCCAACGAATTGGATTCTA	GTTTACTGGCACCACGTCCT
	Pax6	GTCCATCTTTGCTTGGGAAA	TAGCCAGGTTGCGAAGAACT
	Flk1	CCAAGCTCAGCACACAAAAA	CCAACCACTCTGGGAACTGT
Mesoderm markers	*vWF*	CCCACCGGATGGCTAGGTATT	GAGGCGGATCTGTTTGAGGTT
	SM22	CCACAAACGACCAAGCCTTTT	CGGCTCATGCCATAGGATG
	αSMA	CGCCATCAGGAACCTCGAGA	CAAAGCCCGCCTTACAGA
	VE-cadherin	ATTGAGACAGACCCCAAACG	TTCTGGTTTTCTGGCAGCTT

4.3. Results

4.3.1. MAPC expansion on microcarriers

MAPCs were inoculated onto microcarriers at a seeding concentration of $6x10^5$ cells/ml in culture medium and incubated at 37°C for no more than 30 min with occasional shaking in order to increase the frequency of direct contact between microcarriers and cells. Immediately after inoculation, MAPCs attached to the bead surface readily. At the seeding density used, there were approximately 3-8 cells attached to each bead after 30 min incubation. The cell-laden microcarriers were then transferred into a 250 ml spinner flask with a 100 ml working volume of medium. During four days of suspension culture, MAPCs proliferated forming multiple layers of cells on most microcarriers (Figure 28). Calcein-ethidium stain of cells on microcarriers show that cells retained high viability for four days (Figure 28e,f,g). The cell concentration increased from 1.2 $x10^4$ cells/ml to 1.0 $x10^6$ cells/ml after four days of culture equivalent to more than 80-fold of cell expansion (Figure 29). The population doubling time was about 14 hr for the initial three days, which was comparable to that seen when MAPCs were cultivated on a regular tissue culture plates (12-14 hr). After day 3, MAPC began to form multiple layers, and the doubling time increased to more than 24 hr.

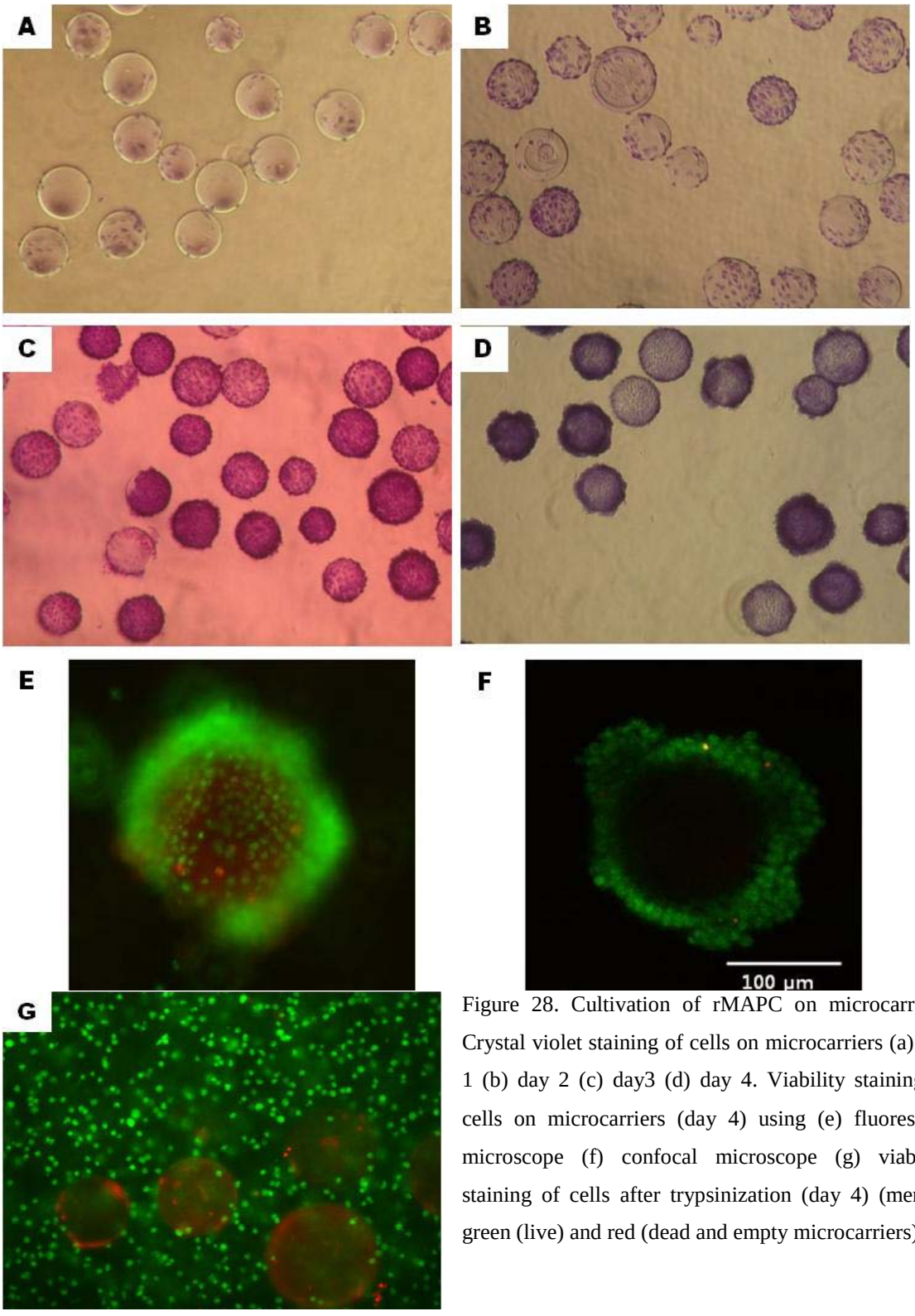

Figure 28. Cultivation of rMAPC on microcarriers. Crystal violet staining of cells on microcarriers (a) day 1 (b) day 2 (c) day3 (d) day 4. Viability staining of cells on microcarriers (day 4) using (e) fluorescent microscope (f) confocal microscope (g) viability staining of cells after trypsinization (day 4) (merged green (live) and red (dead and empty microcarriers)).

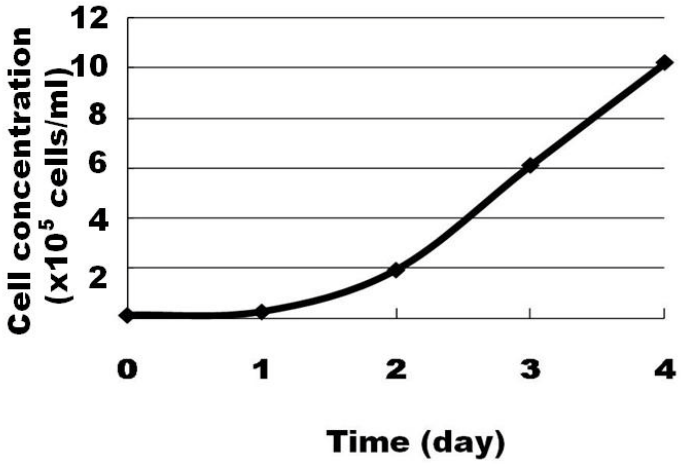

Figure 29. Growth kinetics of rMAPC expanded in microcarrier spinner culture.

4.3.2. Maintenance of undifferentiated MAPC on microcarriers in stirred suspension culture

We evaluated the retention of potency-related markers on MAPCs expanded on microcarriers for four days. The expression levels of key MAPC transcripts, *Oct4, Sall4, Rex1 and CD31*, and early differentiation transcripts, *Sox2, Pax6, Afp, and Flk1* were assessed by RT-qPCR on day 0, day 2, and day 4. Transcripts of *Oct4, Sall4, Rex1, and CD31* were sustained at high levels during MAPC proliferation in stirred reactor microcarrier culture (Figure 30a). Primitive endoderm gene expression was also maintained during that period (Figure 30b). Expression of genes which are indicative of early differentiation of MAPC into three different lineages (*Sox2, Pax6, Afp, and Flk1)* remained undetectable over the four days of expansion culture (Figure 30c).

Expression of the OCT4 protein, a critical pluripotency-related marker for MAPC, was also analyzed by intracellular OCT4 protein staining and quantified by flow cytometry.

Cells were detached from the microcarriers after the expansion culture and stained with an anti-OCT3/4 antibody. OCT4 protein levels were maintained during the microcarrier culture. Approximately 70% of the cells were $OCT4^{pos}$ after 4 days (Figure 30d). The percentage of $OCT4^{pos}$ cells from microcarrier culture was comparable to the percentage of $OCT4^{pos}$ cells (75%) from conventional static culture on tissue culture plates (Figure 30d). Our findings demonstrate that MAPC in microcarrier suspension culture can be expanded >80-fold without any medium change while maintaining stable pluripotency gene expression.

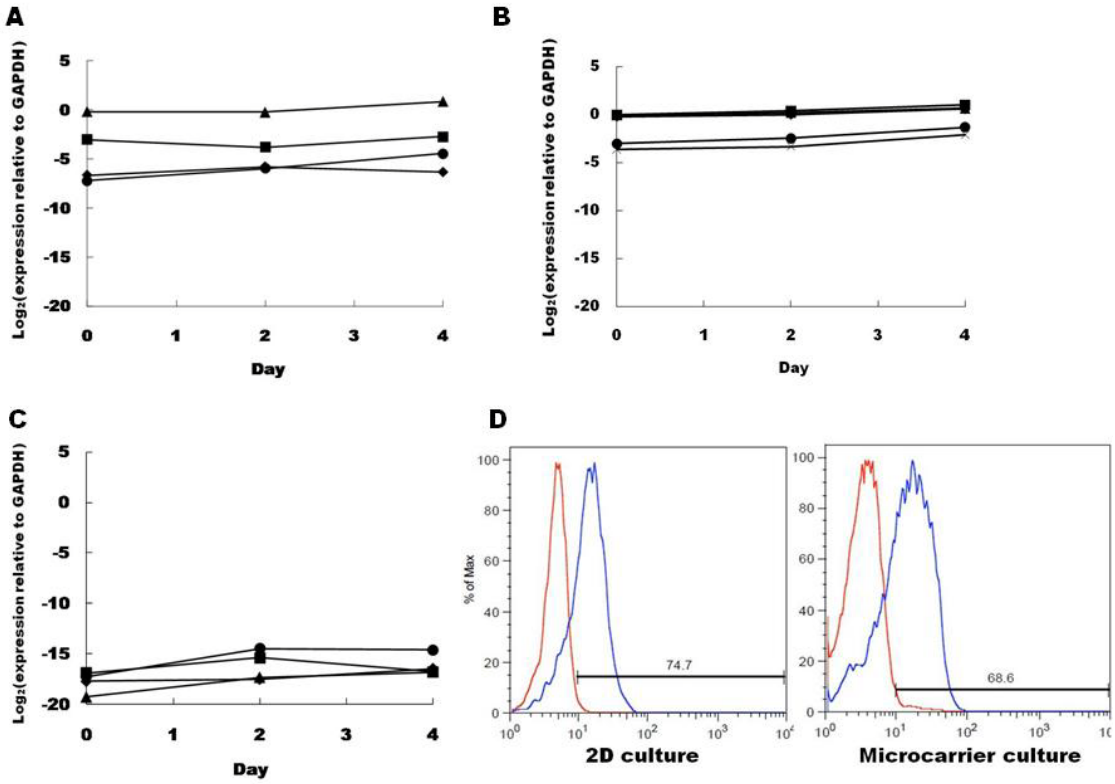

Figure 30. rMAPC were maintained undifferentiated in microcarrier. (a)Transcript levels of pluripotency markers *Oct4* (■), *Sall4* (▲), *CD31* (●), *Rex1* (◆). (b) Transcript levels of primitive endoderm markers *Gata4* (■), *Gata6* (▲), *Sox7* (●), *Sox17* (◆), *Hnf3b* (x). (c) Transcript levels of early differentiation markers *Sox2* (■), *Afp* (▲), *Flk1* (●), *Pax6* (◆) (d)*Intracellular Oct4 protein expression by flow cytometry.

4.3.3. Hepatocyte differentiation of MAPC on microcarriers

4.3.3.1. Differentiation in static culture

The feasibility of employing microcarrier in hepatic differentiation was first investigated in static culture. Cells were expanded on microcarriers for two days to reach confluent monolayer of cells. MAPC culture medium was then replaced with differentiation medium containing cytokines as described in 3.2. The cell concentration increased initially and then decreased until day 10. As the differentiation proceeded, cell morphology changes were similar to those seen in hepatic differentiation in 2D on tissue culture plates. As the cells proliferated on microcarriers, some started to form bulges, and the bulge size increased towards the end of the differentiation (Figure 31a). Immunostaining for PEPCK, for a gene involved in gluconeogenesis that becomes expressed near birth during development, identified small regions of positive cells (Figure 31b). The level of liver specific transcripts was evaluated at the end of hepatic differentiation in 2D and in 3D on microcarriers. Hepatic transcripts of *Afp, Ttr, Albumin, Aat, Tat, G6p, Mgst1, Factor V, Arginase1,* and *Hnf4α* were expressed at significant levels at the end of differentiation. The averaged expression level of hepatic markers observed from three replicate runs was comparable to that seen in differentiation carried out in 2D on culture plates (Figure 31c). By FACS, 18% of the cells expressed ASGPR-1, which is a type II transmembrane glycoprotein expressed on hepatocytes (Figure 31d). Albumin secretion rate was 0.06 pg/cell/day, and urea was produced at 18 pg/cell/day (Table 6). Thus, MAPC on microcarriers can be differentiated into hepatocyte-like cells as shown by the up-regulation of hepatic genes and the secretion of albumin and urea.

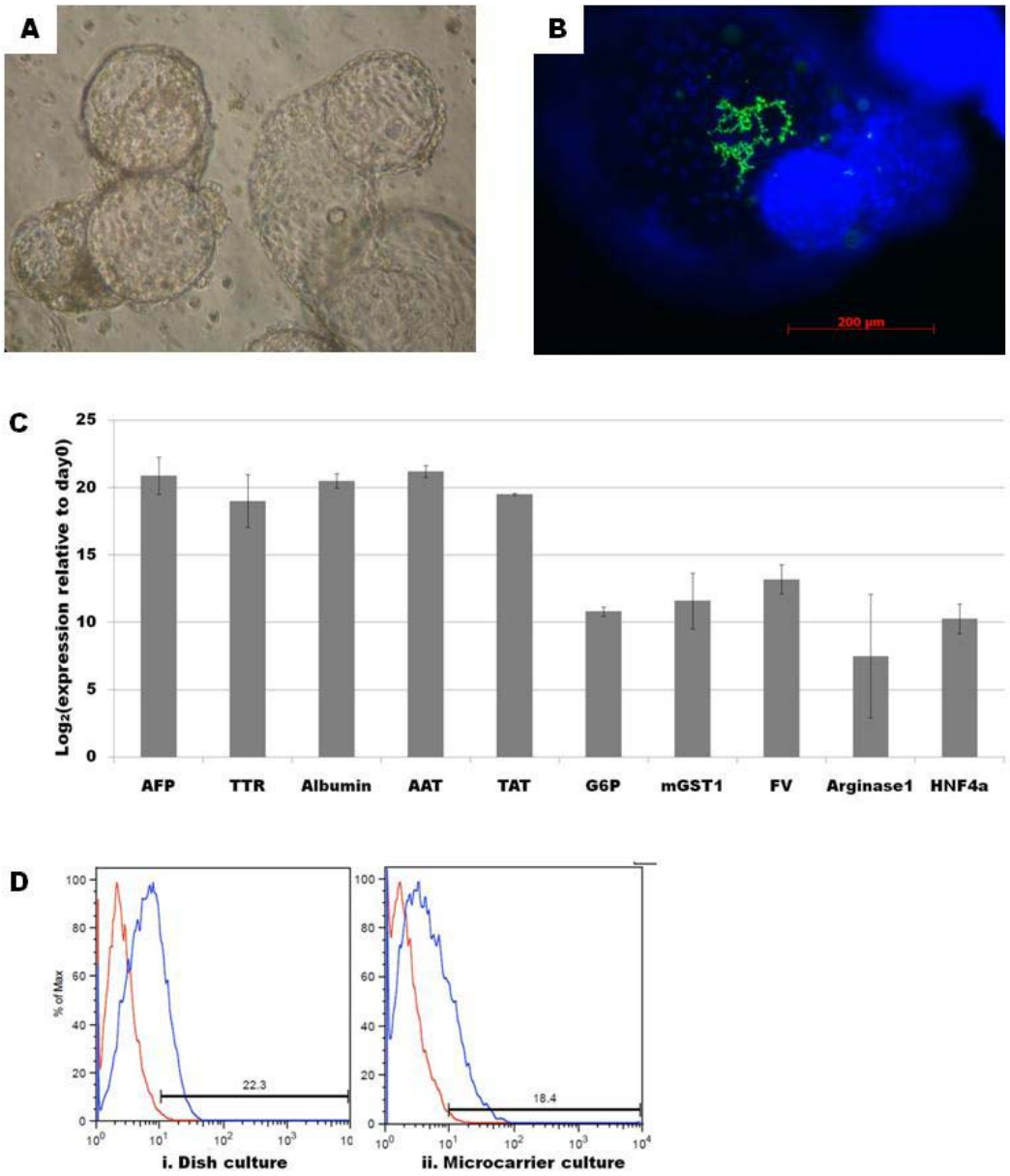

Figure 31. Hepatic differentiation in static microcarrier culture. (a) Morphology on day 20 (b) PEPCK (green) staining (c) Transcript levels of hepatic markers (n=3) (d) ASGPR-1 expression by flow cytometry on cells differentiated on (i) tissue culture plate and on (ii) microcarriers in static culture (blue: cells from differentiation day 20; red: isotype). *

* Figure 30(d) and Figure 31 was performed by KS.

4.3.3.2. Differentiation in stirred suspension culture

Next, MAPCs were expanded in microcarrier culture in a spinner flask, followed by directed differentiation to hepatic lineage. MAPCs were inoculated at $3.1x10^4$ cells/ml with 0.6 mg/ml of Cytodex 1 microcarriers. Upon reaching 80-90% confluence and a cell concentration of $3.0x10^5$ cells/ml, MAPC-laden-microcarriers were washed with PBS once and resuspended in differentiation medium as prescribed by differentiation protocol. The cell concentration increased to $6.7x10^5$ cells/ml after day 1 and then decreased to $4.2x10^5$ cells/ml after treatment in activin A and Wnt3a for six days. The concentration again increased up to $6.8x10^5$ cells/ml by day 10, then decreased again towards the end. Morphological changes of the cells seen in the bioreactor were similar to those seen in static culture. Bulges of cells on microcarriers were also seen and their size increased over the remaining time in culture (Figure 32). More microcarriers with bulges were observed in the spinner differentiation than in the static differentiation. After twenty days of hepatic differentiation, cells retained high viability (Figure 32d).

We also monitored gene expression involved in hepatic differentiation in the spinner flask cultures. Transcript levels of the definitive endoderm genes, *Gsc, Cxcr4, Mixl1,* and *Eomes* peaked on day 6 indicating the MAPCs were committed to the definitive endoderm lineage as expected during hepatic differentiation (Figure 33). Transcripts for hepatic endoderm genes, *Afp* and *Ttr,* increased from day 6 onwards and were maintained at a high level throughout the remaining differentiation process. Transcripts for the more mature hepatic genes *Albumin, Aat, Tat, G6p, Mgst1, Factor V, Arginase1,* and *Hnf4α*

up-regulated significantly by day 20 of the hepatic differentiation. The expression level of mature transcripts was comparable to that in conventional static differentiation and microcarrier static differentiation. In addition, differentiated cells at day 20 secreted albumin at 1.03 pg/cell/day, or about 12% of the level secreted by adult rat hepatocytes, and urea was secreted at 17.4 pg/cell/day (Table 6). These results suggest that hepatic differentiation on microcarriers in stirred suspension culture can provide hepatic cells in a larger scale.

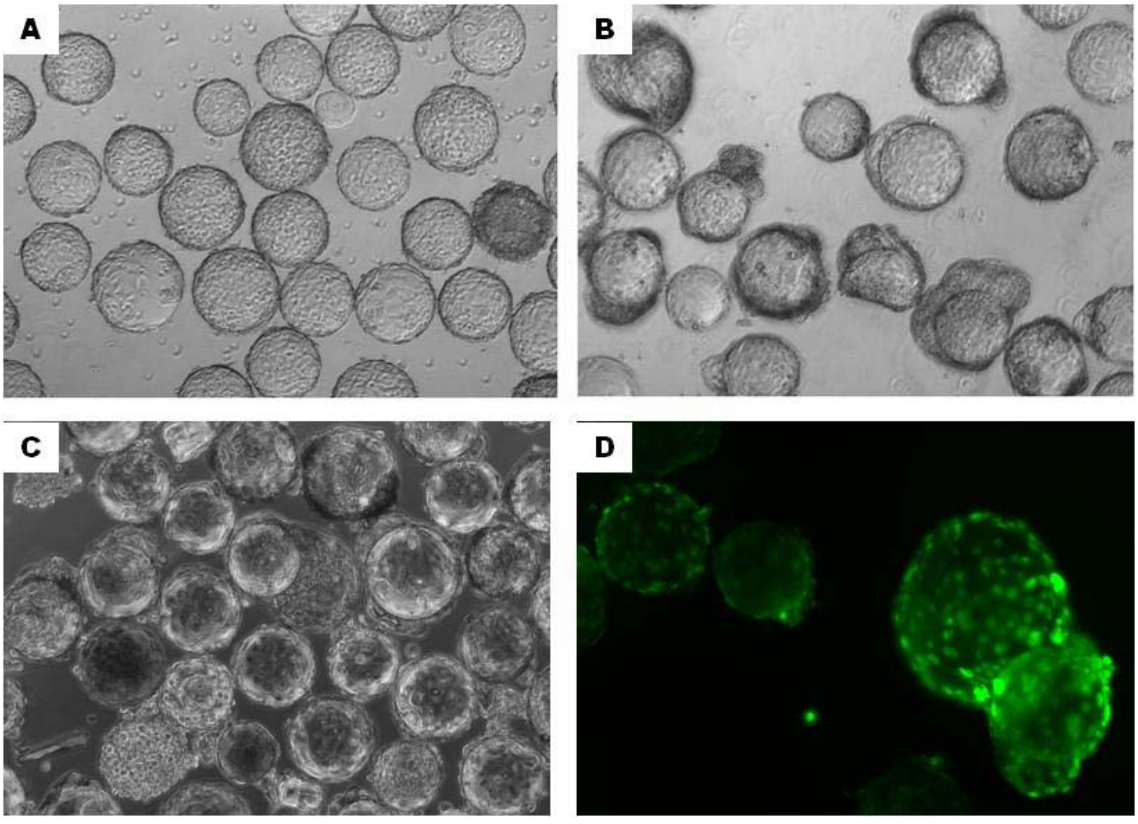

Figure 32. Morphology of cells during hepatic differentiation. (a) Day 0 (b) Day 14 (c) Day 20 (d) Vitality staining on day 20 cells.

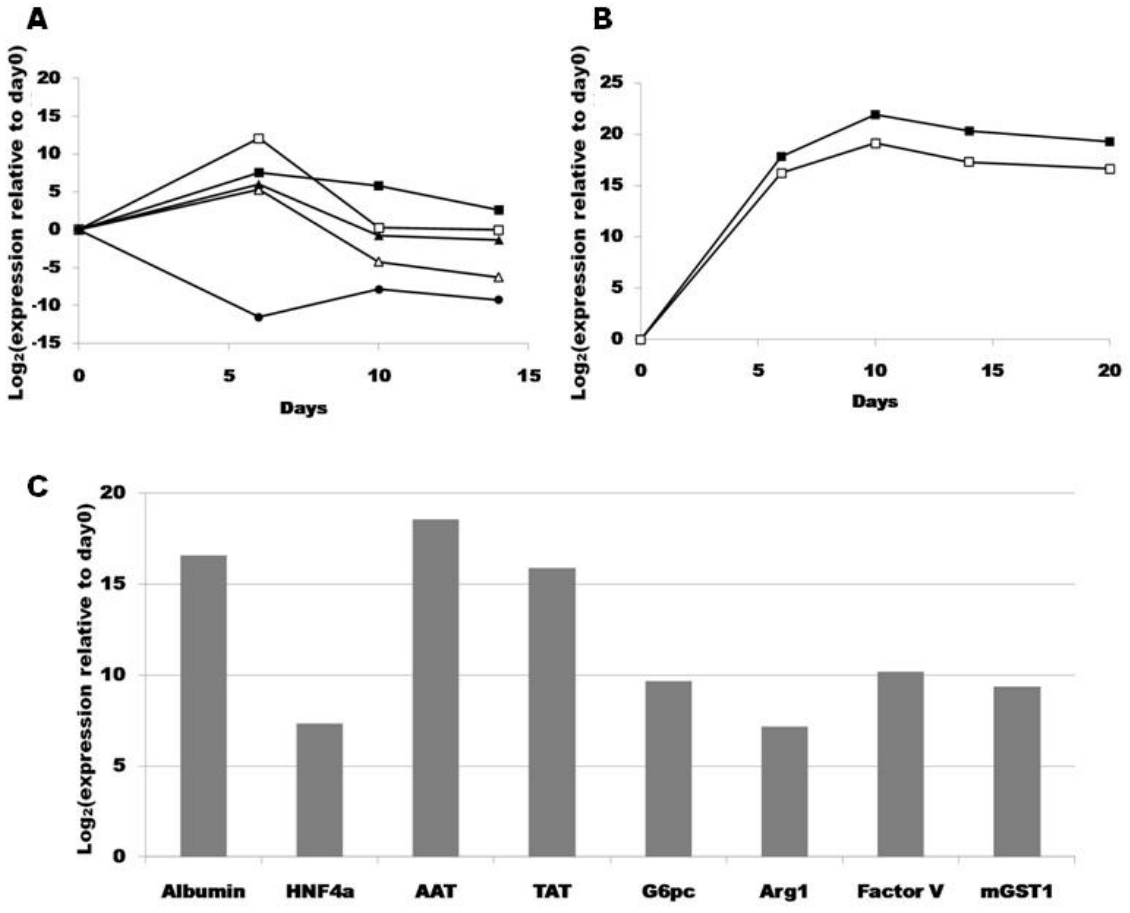

Figure 33. Hepatic differentiation in spinner microcarrier culture (n=1). Transcript levels of (a) *Oct4* (●) and definitive endoderm markers *Cxcr4* (■), *Mixl1* (□), *Eomes* (▲), *Gsc* (△) (b) Hepatic endoderm markers *Afp* (■), *Ttr* (□) (c) Mature hepatic markers at day 20.

To monitor cell metabolism, glucose consumption and lactate production was determined to calculate lactate production/glucose consumption ratio. The results suggested that medium replacement allowed the supply of the nutrients and the removal of waste products inhibiting cell growth, leading to the maintenance of the cultures in relatively

steady state for four days. Lactate production rate is used to characterize the viability status of the culture. Both in the MAPC spinner cultures for expansion and hepatic differentiation, the yield ratio (ΔL/ΔG) was maintained under 2.0 (except at day 1 of expansion with a very low cell concentration (Figure 34).

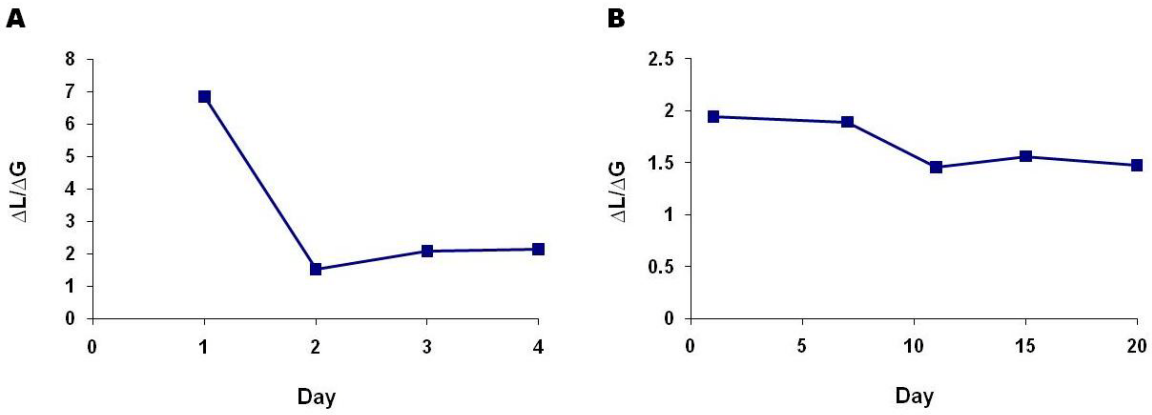

Figure 34. Ratio of lactate production to glucose consumption during microcarrier suspension culture. (a) Expansion culture. (b) Differentiation into hepatic lineage.

Table 6. Albumin secretion and urea production rates from hepatic differentiation

Rate (pg/cell/day)	Static culture	Spinner culture
Albumin	0.06	1.03
Urea	17.9	17.4

4.3.4. Combination of microcarrier and aggregate suspension culture system for directed hepatic differentiation

The microcarrier suspension culture system is known to provide homogenous culture environment. Furthermore, we have found that MAPC aggregates themselves in directed hepatic differentiation produced more mature hepatocyte-like cells expressing higher level of hepatocyte specific markers than surface adherent MAPCs (Subramanian et al. manuscript in preparation). Thus these two methods were combined in hepatic differentiation to further enhance the differentiation process in spinner culture. First, MAPCs were differentiated into the hepatic lineage in microcarrier suspension culture for 20 days. Then on day 20, the dissociated cells were formed into aggregates at 8000 cells/ aggregate using the forced aggregation method. The aggregates were resuspended in the spinner for another 15 days in the differentiation medium.

During the 3D culture, the size of aggregates increased to more than 1 mm in diameter at day 35 (Figure 35.). Cells were collected every three days to evaluate the hepatic gene expression by RT-qPCR. Additional 3D differentiation did not help to further mature the differentiated cells. The transcripts specific to hepatic cells (*Aat, Tat, G6pc, Arg1, FactorV, Mgst1, Afp, Ttr, Albumin, Hnf1α, and Hnf4α*) were down-regulated over 15 days. *Oct4* level increased suggesting the domination of early progenitor cells or dedifferentiation. However, up-regulation of mesoderm genes (*VE-cadherin, αSMA, vWF, and SM22*) was observed.

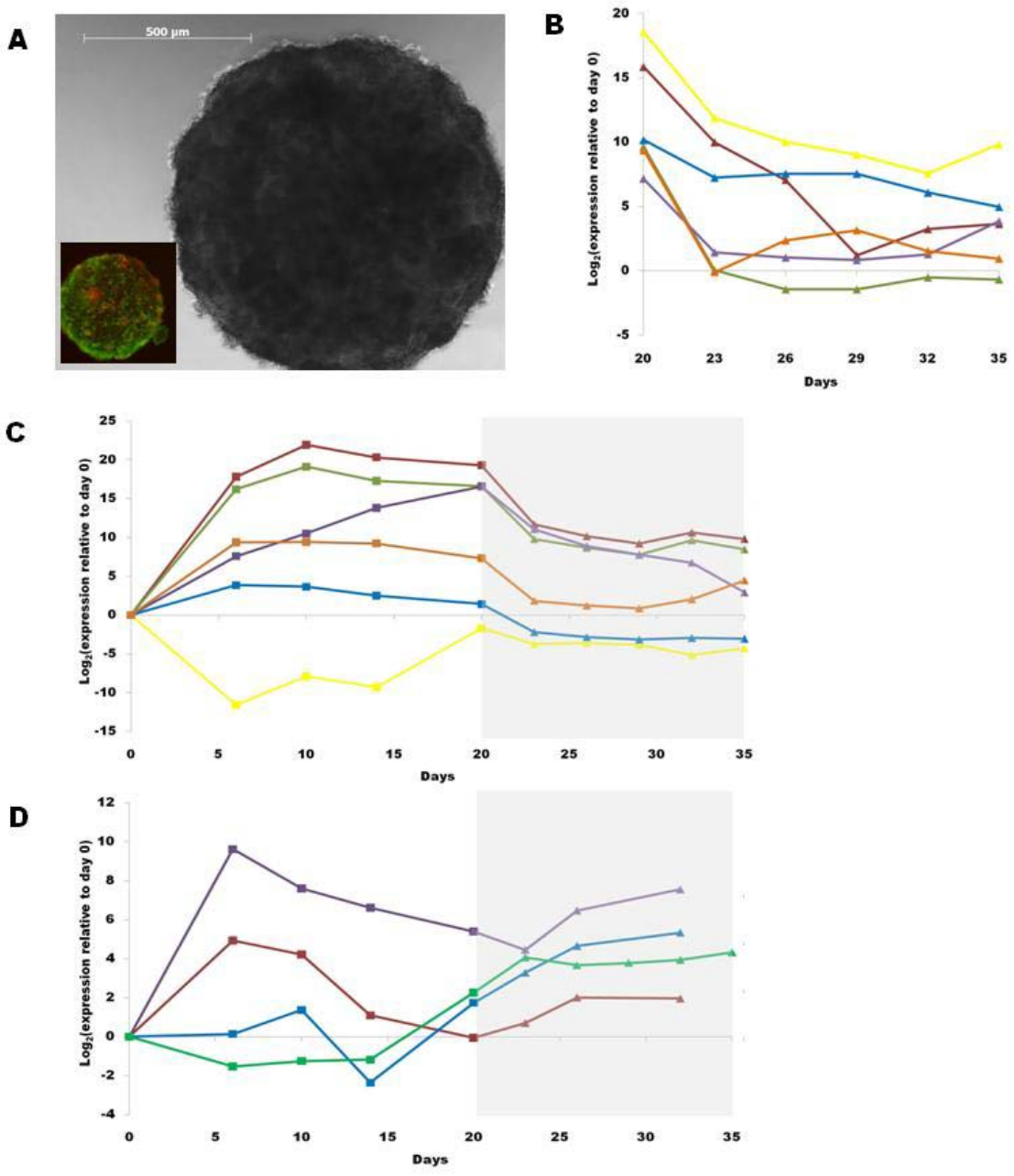

Figure 35. Combined microcarrier and aggregate culture systems for hepatic differentiation. (~20 days: on microcarriers; 20~35: as 3D aggregates) (a) Morphology. (b) RT-qPCR of mature hepatic markers (*Aat; Tat; G6pc; Arg1; FactorV; Mgst1*). (c) *Oct4* and hepatic markers (*Afp; Ttr; Albumin; Hnf1α; Hnf4α*) (d) mesoderm markers (*αSMA; SM22; vWF; VECadherin*).

SM22, a smooth muscle cell marker, was up-regulated by ~32 fold at day 6 and relatively maintained at that level during the differentiation. *αSMA* expression peaked on day 6 (16-fold increase in expression level), down-regulated during the microcarrier differentiation, and increased again when the differentiation scheme is switched from the microcarrier to the 3D. Endothelial cell-related genes, *VE-Cadherin* and *vWF*, were turned on after 14 days and continued to increase until day 32.

4.4. Discussion

Much progress has been made in directed hepatic differentiation of various stem cells, including human and mouse embryonic stem cells (ESCs) and induced pluripotent stem cells (iPS cells) in the past few years [141-143]. The achievements have renewed the hope that cell transplantation or bioartificial liver devices involving stem cell-derived hepatocytes may be getting closer to reality. The recent demonstration of iPSC differentiation to hepatocyte-like cells also raises the prospect that iPS cells derived from patients of different genetic background can be differentiated into hepatocytes and used for toxicity and metabolic studies. These advances heighten hopes as well as highlight the need for the development of robust bioprocesses, which are capable of producing large numbers of stem cells or their hepatic progenies appropriate for various applications.

The feasibility of cultivating different stem cells has been demonstrated for various types of bioreactors such as perfusion reactors, rotating vessels, spinner reactors, and others (Chapter 1.4). Ideally, a bioreactor should provide a homogeneous environment, for a

high concentration of cells, and allow easy access for sampling. In this regard, a stirred vessel based system is superior to recirculating flat-bed and rotating vessels. Some stem cells are capable of proliferation and/or differentiation when grown as aggregates, such as EBs from ESCs. Upon formation of such aggregates, they can be grown in a stirred bioreactor. However, not all cells can be cultivated efficiently as aggregates. Microcarrier culture combined with suspension culture systems allows the growth of adherent-dependent stem cells in high density.

The microcarrier concentration used in this study was relatively low, and the culture was initiated with a relatively low inoculation cell concentration compared with other types of mammalian cell culture. Hence, we inoculated cells onto microcarriers under stationary conditions with a reduced volume to increase the microcarrier and cell concentrations, thereby increasing the probability of successful contacts between cells and microcarriers. The initial cell distribution on microcarriers greatly affects subsequent growth kinetics. Occasional mixing resulted in a better distribution of cells on the microcarriers. We observed that MAPCs attached relatively fast to microcarriers, comparable to the attachment of fibroblastic cells [238].

Rat MAPCs are typically cultured on fibronectin-coated dishes at a low initial density of 300 cells/cm^2 as it was thought that maintenance at a high density may result in differentiation and a corresponding loss of potency, as is observed for MSC culture [52, 54, 193]. Upon inoculating into a Cytodex 1 microcarrier culture, even without

fibronectin coating, MAPC readily attach to microcarriers and proliferate at a growth rates similar to that seen on tissue culture plates (Figure 28). Eventually MAPC form multiple layers on microcarriers and, their doubling time increased from 14 hr to 24 hr. This result agrees with previous studies involving MAPC and mESC aggregate cultures; the doubling time of MAPC grown as aggregates is about 23 hr (Chapter3), and a similar increase in doubling time was also noted when mESCs were cultured as aggregates [166]. It is possible that cells grown as multiple layers on microcarriers actually resemble cells in aggregates in terms of morphology, structure, and physiological characteristics.

The high cell density seen on microcarriers did not affect the potency of MAPC over the short reactor culture period. The cells continued to express high levels of Oct4-transcripts and protein, a transcription factor expressed in early embryonic development and which is in ESCs essential for the maintenance of pluripotency in ESC. We have also shown that the level of Oct4 transcripts and protein in MAPC is correlated with the potency of the cells [54]. Other pluripotency-related markers of MAPC, namely *Rex1*, *Sall4*, and *CD31*, were expressed in MAPC in microcarrier stirred bioreactor culture at levels comparable to cells maintained at low density in 2D cultures. We also did not detect increased expression of genes associated with differentiation such as *Sox2, Pax6, Flk1*, and *Afp* (Figure 30).

Along with maintenance of MAPC potency during expansion, we used microcarrier culture systems for hepatocyte differentiation. This culture system allows large-scale

hepatic differentiation; about $4x10^7$ cells with hepatic phenotype and functions were obtained from 80ml culture. The extent of differentiation into hepatocyte-like cells on microcarriers, as measured by expression of various hepatocyte-specific genes, was similar to that seen in differentiation in 2D or in 3D in culture dishes. Furthermore, the dynamics of liver-specific gene expression profiles were similar in both microcarrier and dish cultures. Definitive endoderm transcripts (*Gsc, Cxcr4, Mixl1,* and *Eomes*) peaked during the earlier phase (day 6) of the differentiation, followed by expression of hepatic endoderm genes (*Afp, Ttr*) from day 6 onwards. Transcripts for mature hepatic-genes such as *Albumin, Aat, Tat, G6p, Mgst1, Factor V, Arginase1,* and *Hnf4α* were significantly up-regulated towards the end of hepatic differentiation (Figure 33). This gene expression profile confirms that MAPC differentiate according to the known hepatic developmental stages, progressing from foregut endoderm, to fetal liver stem cells (hepatoblasts) and finally hepatocytes. The observation that cell number increased at day 10 also supports the notion that this stage of differentiation corresponds to the hepatoblast stage.

ASGPR-1, a surface molecule characteristic of the mature hepatocytes phenotype, was used to quantify more mature hepatocyte-like cells. ASGPR-1 is known to be expressed in a smaller population of cells (18-22%) than is ALBUMIN in hESC hepatic differentiation [129]. In MAPC microcarrier differentiation, about 20% of the cells were positive for ASGPR-1, a level similar to conventional two-dimensional differentiation (Figure 31d).

The cells also displayed hepatic functions; albumin and urea were secreted at the end of differentiation. The differentiated MAPC not only expressed albumin transcripts, but also secreted albumin at a rate of 1.03 pg/cell/day, a level that was higher than that from culture dish differentiation (0.06 pg/cell/day). Measured rates for both albumin and urea secretion are still lower than that of adult rat hepatocytes (Table 6) (Pauwelyn et al. manuscript submitted).

The microcarrier suspension culture system may enhance differentiation by providing a more homogeneous environment than a dish culture system. It is, however, conceivable that the chemical environment in tightly packed aggregates, commonly used in stem cell differentiation in stirred bioreactors, is not homogeneous. Whereas in microcarrier systems, gradients of environmental cues for differentiation are less likely to form given that cells are only a few layers thick. In our experiment, albumin secretion rate of cells from spinner culture (1.03 pg/cell/day) was significantly higher than that from adherent culture differentiation (0.06 pg/cell/day). Also, more cells on microcarriers in bioreactor culture formed bulges than those in static culture (Figure 32); although it is not clear whether the formation of bulges is a definitive sign of more improved hepatic differentiation, we detected PEPCK, a mature marker suggestive of gluconeogenesis, on cells inside the bulges during differentiation. We speculate that, as cells differentiate into hepatocyte-like cells, they become larger and change to an octagonal or oval shape leading to a lack of space on the surface of microcarriers, and detachment of the cells from the beads. These hepatocyte-like cell clusters exhibit increased cell-cell adhesion

which may result in the tightly-bound cells detaching from microcarriers in the center, where space is limited, while maintaining attachment at the edges.

Having found that 3D differentiation produces more mature hepatocyte-like cells than 2D cultures (Subramanian et al. manuscript in preparation), first we expanded the number of cells on microcarriers during hepatic differentiation for more homogeneous differentiation such that major fraction of cells adopt hepatic phenotype with higher viability, and then further matured these cells by additional 3D differentiation. However, our results did not show improvement in maturation. By gene expression, cells appeared to de-differentiate during subsequent 3D differentiation. Cells proliferated as aggregates as shown by the size increase. It is likely that mesodermal cells, more specifically endothelial cells, dominate the cell population inside the aggregates. *vWF* and *VE-cadherin* expressions were turned on day 14 in the microcarrier differentiation and continued to increase through 3D differentiation.

Endothelial cells interact with endodermal cells and contribute to their progression towards a hepatic phenotype in the later stages of the fetal liver development. *In vitro*, co-culture with endothelial cell lines changed the protein expression pattern of the hepatic progenitor cells; it resulted in differentiated cells with $CK19^{neg}$ (a cholangiocyte marker) [239]. However, the change in expression pattern varied depending on the different endothelial cell lines used [239]. Although there was an increased expression of endothelium-related genes during the microcarrier hepatic differentiation, it is not clear

that we had the right type of endothelium-like-cells for further hepatocyte differentiation. Sets of markers such as *Gata4, Lmo3, Tcfec, Maf*, and *Leda1*[240] will be useful to define liver-sinusoidal-endothelium-like cells from the differentiation.

The other possible explanation for this phenomenon is the presence of hepatic progenitor cells that can differentiate into non-endodermal cell types. Mouse fetal liver progenitor cells can differentiate into not only hepatocytes and cholangiocytes, but also intestinal and pancreatic epithelial cells [241]. Multipotent progenitor cells isolated from human fetal liver are capable of differentiating into liver and mesenchymal cell lineages [242]. It is possible that these hepatic progenitor cells may have generated during the microcarrier differentiation, later to trans-differentiate into mesodermal cells upon the unknown cues from 3D formation and differentiation.

Regardless of whether they support right hepatic commitment, endothelial cell signaling may need to be turned off at some point to prevent fibroblast cells from proliferating and overtaking the hepatic cell populations. The control of different cell populations and time of aggregation in the later phase of differentiation process seem to play an important role in utilizing 3D culture system for stem cell differentiation in spinner culture.

To further improve the microcarrier differentiation system, additional technical issues must be addressed. In our multi-step differentiation protocol, the differentiation medium with different cytokines is replaced periodically to drive the differentiation to the next stage. As the microcarriers used in this study were microporous, with a void fraction

greatly exceeding 90%, a large volume of residual medium from the previous differentiation stage is likely to remain in the interior of cell-laden microcarriers. It is not clear whether the residual components pose any significant effect on the outcome of differentiation. Because different signaling pathways are involved in committing cells in the different stages of differentiation to the next stage, it is possible that cytokines remaining from the previous step may have antagonistic effects on the ultimate levels of differentiation. The microcarrier concentration used in this study was low, and therefore the amount of residual components after medium replacement was also relatively small. However, in a differentiation bioprocess, with a higher microcarrier concentration, the effect of these residual cytokines may not be negligible. The potential adverse effects can be minimized by using solid microcarriers that do not have internal pores. One can also speculate that microporous microcarriers may act as slow release reservoirs for potential trophic factors; however, such a function remains as speculation.

Another aspect of microcarrier application is the recovery of the cultured or differentiated cell products. Dissociation of cells from microcarrier surface followed by cell-microcarrier separation is likely to be a necessity in clinical and drug testing applications. Viable MAPCs can be easily detached from microcarriers with high recovery efficiency after a mild trypsin treatment. Differentiated cells can also be harvested while still retaining their function and viability. For cell-bead separation, various methods have been studied from mesh filter to employment of temperature-sensitive microcarriers [243-245]. Development of effective cell dissociation and cell-microcarrier separation methods

will be a crucial advancement allowing microcarriers to be successfully applied in large scale stem cell expansion and directed differentiation processes.

We conclude that microcarrier suspension culture is a robust method for scale up of MAPC expansion and differentiation to the hepatic lineage. It will facilitate the transformation of the laboratory practice of stem cell culture to scalable bioprocesses generating hepatocyte-like cells at industrial scales for future clinical applications.

CHAPTER 5. EXPANSION AND HEPATIC DIFFERENTIATION OF HUMAN EMBRYONIC STEM CELLS ON MICROCARRIERS

5.1. Introduction

In the previous chapters, we discussed scalable culture systems for rMAPC in 2D, 3D, and microcarrier culture systems. In Chapter 5, we extend our findings obtained from the MAPC culture systems to hESC culture in microcarrier suspension system. Human ESCs, an allogeneic cell source with a greater potency than other types of stem cells, have been a promising candidate for regenerative therapies and drug toxicity screening. Many types of culture systems have been employed to cultivate hESCs. 2D cultivation in tissue culture plates is still the most common method, but the labor-intensive passaging procedure, limited surface area in tissue culture plates, and rapid depletion of culture medium limit the scale-up of 2D culture process for further clinical applications. Perfusion cultures featuring gas-permeable substrata were used for hESC maintenance, but low cell density requirement prevents its wide use. Stirred reactor systems are mostly used for differentiation of hESCs (Table 2). Human ESCs are cultured in suspension as embryoid bodies (EBs). ESCs start to spontaneously differentiate within EBs. Human ESC differentiation as EBs in stirred suspension culture may not be optimal due to cytokine gradient generated inside EBs. Also, there is a variation in EB sizes, which makes it difficult to provide homogeneous culture environment for the cells.

To this end, hESCs on microcarriers were maintained in monolayers and exposed more evenly to the culture environment. In addition, this allows the high density culture with high surface to volume ratio. Mouse ESCs have been expanded in microcarrier

suspension system [165-168], but hESC culture on microcarrier is more challenging because, unlike mESCs, (1) hESC are passaged as small clumps not as single cells, (2) LIF supplementation does not substitute the role of mouse embryonic fibroblast as a feeder layer for maintaining hESC undifferentiated.

In this chapter, we concisely show the potential of microcarrier culture as a scalable method for hESC expansion followed by directed hepatocyte differentiation in cell therapies and drug toxicity screening. Especially for drug toxicity screening, a popular cell source that has been used is rat hepatocytes because of the lack of human donor cells. This culture method can be easily adopted to produce large numbers of hepatocyte-like cells for drug screening system in the near future.

5.2. Materials and Methods

5.2.1. Cell lines

Human embryonic stem cell line HSF-6 (p71) was used in this study. Human ESCs were cultured as undifferentiated colonies in 6-well or 10 cm tissue culture plates, incubated at 37°C, in 22% O_2 and 10% CO_2. The tissue culture plates were pre-seeded with irradiated mouse embryonic fibroblasts (MEFs) as a feeder layer. hESCs on MEFs were cultured in hESC culture medium (80% (v/v) knockout DMEM (Gibco), 20% (v/v) knockout serum replacement (Invitrogen), 2 mM L-glutamine solution (Gibco), 0.1 mM MEM non-essential amino acids solution (Gibco), supplemented with 0.1 mM β-mercaptoethanol (Gibco) and 4 ng/ml bFGF (R&D)). Microcarrier surface was pre-coated with Matrigel®.

While on Matrigel, hESCs were cultured in conditioned medium (CM) (hESC culture medium without bFGF, pre-conditioned on MEFs, then supplemented with 4 ng/ml bFGF before the use). To passage the cells, collagenase (Invitrogen) was used to partially detach the cell colonies on MEF plate, followed by scraping and breaking into a desired clump size.

5.2.2. Human ESC expansion culture on microcarriers

Cytodex 1, a crosslinked dextran microbead with N, N-diethylamioethyl groups on the surface, was purchased from GE healthcare as dry powders. Cytodex 1 stock was prepared by washing 1g of microcarrier powder with PBS for 3-5 times. Swollen beads were sedimented in 100 ml fresh PBS and sterilized by autoclaving.

Prior to suspension culture, microcarriers were coated with Matrigel in knockout DMEM (1:20 dilution) at room temperature for 1 hr, washed twice with knockout DMEM and further equilibrated in CM for 1 hr. hESC cultured on 10 cm tissue culture plates (NUNC) were collected as small clumps, washed, and resuspended in CM at a concentration of cells from half 10 cm-plate (about 0.7-1.0x10^6 cells)/ml. Cells were added to 10 mg/ml Cytodex 1 microcarriers at the concentration of 0.4x10^6 cells/ml. The mixture was transferred into Corning Ultra Low Attachment 24-well plates at 0.5 ml/well, then placed on a rocker inside the incubator and incubated for 2 hrs at 37°C to allow initial cell attachment to the beads. The mixture was re-distributed into the 24-well plates at 0.17 ml/well, and the CM was filled up to 1 ml/well. Half of the medium was replaced every

day until the microcarriers were confluent with cells (>90% coverage, estimated visually). The cultures were maintained at 37°C, in 22% O_2 and 10% CO_2.

5.2.3. *In vitro* directed hepatic differentiation

hESCs were differentiated into hepatocytes by using a four step twenty days hepatic differentiation protocol with modifications. For static plate differentiation, cells were inoculated in an ultra-low attachment 24 well plate (Corning) following the method described in hESC expansion culture on microcarriers. After three days of expansion culture, when the cells were >90% confluent on the microcarrier surface, the cells with microcarriers were washed once with PBS and re-suspended in 1 ml of hepatic differentiation medium. The composition of differentiation basal medium was a 60/40 (v/v) mixture of low glucose Dulbecco's Modified Eagle media (DMEM) (Gibco, USA) and MCDB-201(Sigma) supplemented with 0.026 μg/ml ascorbic acid 3-phosphate (Sigma), linoleic acid bovine serum albumin (LA-BSA, Sigma) (final concentrations of 250 μg/ml BSA and 2.04 μg/ml linoleic acid), insulin-transferrin-selenium (ITS, Sigma) (final concentration 2.5 μg/ml insulin, 1.12 μg/ml transferrin, 0.0015 μg/ml sodium selenite), 0.4 μg/ml dexamethasone (Sigma), 4.3 μg/ml β-mercaptoethanol, supplemented with 100 IU/ml penicillin and 100 μg/ml streptomycin (Gibco). Furthermore, additional protein factors were added as described below. The cytokines and growth factor supplements were added as follows: (i) Day 0:Activin A (100 ng/ml), Wnt3a (50 ng/ml) , 2% (w/v) FBS (ii) Day 2: Activin A (100 ng/ml) and 2% (w/v) FCS (iii) Day 6:bFGF (10

ng/ml), BMP4 (50 ng/ml), and 0.5 (w/v) FCS (iv) Day 10: FGF8b (25 ng/ml), aFGF (50 ng/ml), FGF4 (10 ng/ml), and 0.5 (w/v) FCS (v) Day 14: HGF (20 ng/ml), Follistatin (100 ng/ml), and 0.5 (w/v) FCS. Differentiation experiments were carried out at 21% O_2 and 5% CO_2 37°C for twenty days with 50% media change, corresponding to the differentiation stage, every two days.

5.2.4. RNA isolation and RT-qPCR

Total RNA was isolated from rMAPC cell lysates using RNAeasy microkit (Qiagen) according to instructions provided in the kit. cDNA was synthesized from the extracted RNA using the Superscript III reverse transcriptase (Invitrogen) method. The PCR reaction mix consisted of cDNA samples, SYBR Green Mix PCR reaction buffer (Applied Biosystems) and primers (5 μM stocks, sequence in table 1). The RT-qPCR reaction was run on a Realplex mastercycler (Eppendorf) using the following program: 50°C for 2 min, 95°C for 10 min, and 40 cycles at 95°C for 15 sec and 60°C for 1 min followed by a dissociation protocol to obtain a melting curve. Transcription abundance relative to *GAPDH* was calculated as △Ct which is Ct(transcript of interest)-Ct(*GAPDH*) and transcript abundance in sample relative to day 0 was calculated as △Ct (day0)-△Ct(day of sample).

5.2.5. Cell viability staining

The “live/dead viability/cytotoxicity kit” (Invitrogen) was used to stain cells on microcarriers with calcein and ethidium. Component B was added first to DPBS (1:1000)

and then component A was added to DPBS with component B (1:2000). Cells were incubated with the staining solution for 15-30 min at 37°C. Cells were washed once with PBS and observed under inverted fluorescent microscope (Axiovert 200, Zeiss). Live and dead cells appear as green and red respectively.

5.2.6. Cell enumaration by nuclei counting

Microcarriers from 1 ml culture were centrifuged at 500 rpm for 30 sec to remove supernatant. After adding 300-500 µl counting staining solution (0.1% (w/v) crystal violet (Sigma) in 0.1 M citric acid solution (Sigma)), the sample was incubated for 1 hr at 37°C. Nuclei were released by gentle shearing using a Pasteur pipette in a vertical position. The nuclei were counted with a hemacytometer.

For fixed cell staining, cells-microcarriers in 1 ml culture were stained by adding a drop or two of fixative staining solution (0.5% (w/v) crystal violet in 40% ethanol and 60% PBS) for 1-2 min. Stained cells-microcarriers were washed with PBS twice to remove the staining solution from the supernatant.

5.2.7. DiI staining of MEFs

MEFs were labeled using Vibrant™ DiI cell-labeling solution (Invitrogen). MEFs were allowed to attach to the tissue culture plates before staining. Labeling solution was added to the MEF culture medium at concentration of 5 µl/ml. The culture was incubated at

37°C for 30-40 minutes, and then washed three times with the MEF culture medium (10 min incubation per wash).

Table 7. List of primers used in Chapter 5.

Cell Lineage	Gene	Forward Primer	Reverse Primer
Pluripotency	*OCT4*	GATGGCGTACTGTGGGCCC	TGGGACTCCTCCGGGTTTTG
	SOX2	GGGAAATGGGAGGGGTGCAAAAGAGG	TTGCGTGAGTGTGGATGGGATTGGTG
	NANOG	GGATGGTCTCGATCTCCTGA	TCCCAATCCCAAACAATACG
Hepatic lineage	*AFP*	CCTACAATTCTTCTTTGGGCT	AGTAACAGTTATGGCTTGGA
	ALBUMIN	AGACTGCCTTGTGTGGAAGACT	CTGAGCAAAGGCAATCAACA
	AAT	TTAAAGGCAAATGGAAGAAGCC	TATTTCATCAGCAGCACCA
	TAT	CTCTACAATTTGTTGCCAGAG	TTCTGAAGATGACGTTTGCTG

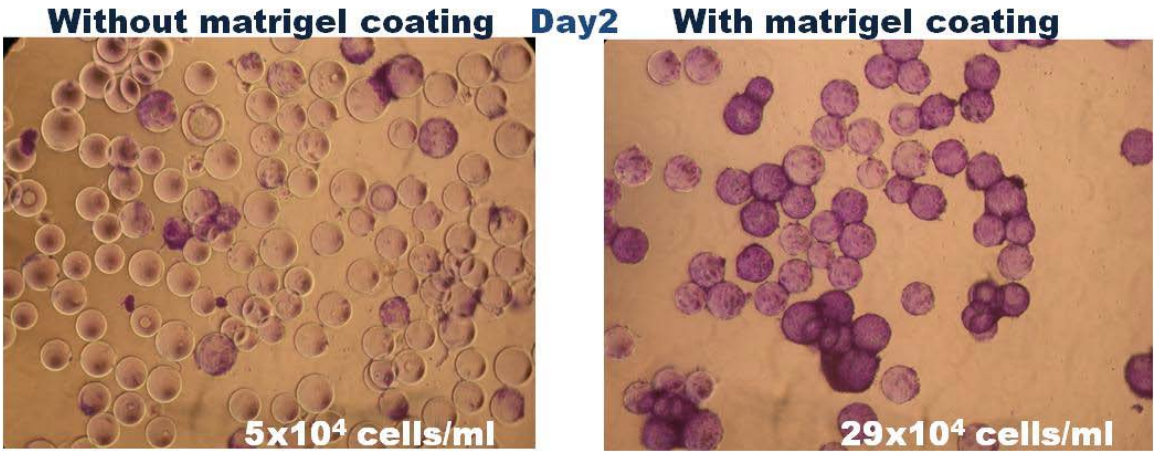

Figure 36. Matrigel coating enhances hESC attachment on microcarriers.

5.3. Results

5.3.1. Initial attachment of hESCs on microcarriers

Initial attachment of cells to the surface is a critical step to evenly distribute the cells and further proliferate on microcarriers. hESCs, not being able to grow as single cells, have to be passaged as small clumps. In addition, in order to culture hESCs undifferentiated, an appropriate extracellular matrix (ECM) is required. Currently hESCs are mostly cultured on feeder cells (MEFs) or on Matrigel. First, we coated Cytodex 1 microcarriers with Matrigel to explore whether Matrigel actually helps hESCs attachment and growth on the microcarriers.

With Matrigel coating, hESC clumps attach better to the microcarriers. Fewer cells were grown on uncoated microcarriers due to the poor initial attachment after two days of culture (Figure 36). The results suggested that Matrigel coating is necessary for more efficient culture hESCs on microcarriers.

hESC were broken into small clumps of 10-100 cells when they were harvested. hESCs were inoculated onto microcarriers at a seeding concentration of 0.4 $x10^6$ cells/ml culture medium and incubated at 37°C for 2 hours on a rocker in order to increase the frequency of direct contact between microcarriers and cells, before further diluted to reach final seeding concentration of $8x10^4$ cells/ml. With the seeding density we used, there were approximately 0-5 clumps attached to each bead after 2 hour incubation. An average of 2.2 clumps was attached to a Matrigel coated microcarrier (Figure 37).

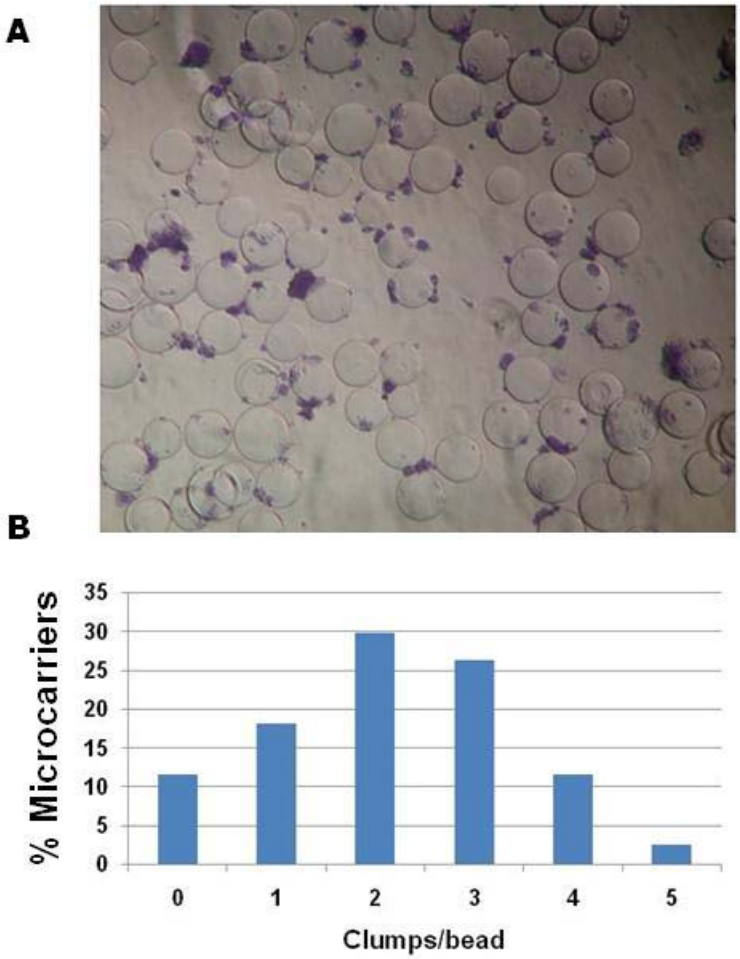

Figure 37. Initial attachment of hESC on microcarriers 2hrs after inoculation. (a) Small clumps attached to the surface. (b) Number of clumps distribution on a microcarrier.

Before hESCs inoculation for microcarrier cultue, hESCs were cultured on MEFs. Since MEFs, with a fibroblastic nature, easily attached to the surface, we tested whether MEFs preferentially attached to the microcarriers during the initial attachment phase and affect hESC culture. MEFs were pre-labeled with DiI, a lipid dye that labels cell membrane for a relatively long term. Compared to hESC clumps, few MEFs attached to the

microcarriers, and they did not grow out on to the surface as they were pre-irradiated cells (Figure 38).

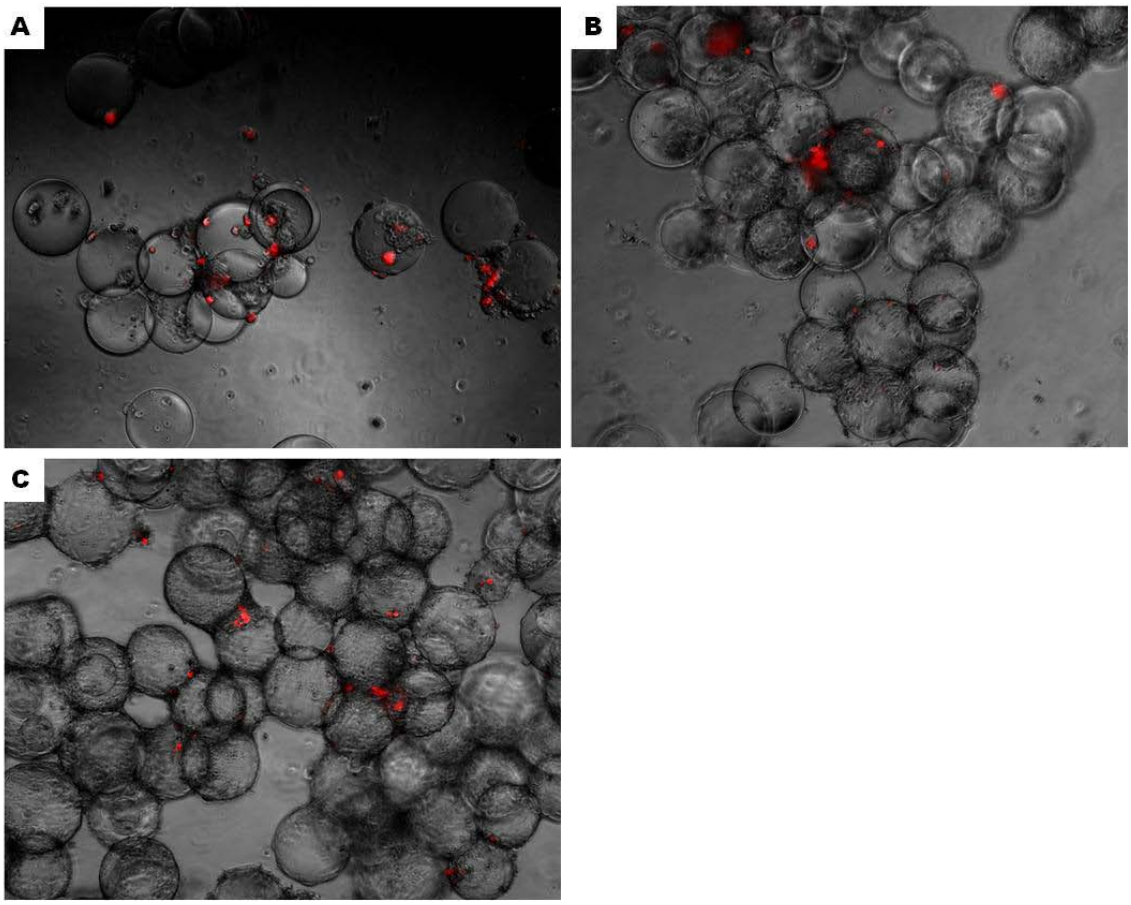

Figure 38. MEF attachment on microcarriers during hESC culture. (a) Day 0 (b) Day 2 (c) Day4 (Red: MEF).

5.3.2. hESCs expansion on microcarriers

The cell-laden microcarriers were cultured in an ultra low attachment 24-well plate with a hydrophilic and neutrally-charged surface. hESCs propagated on microcarriers to reach confluence four days after seeding (Figure 39). hESC-microcarrer agglomerated in culture. Calcein-ethidium staining of cells on microcarriers (day4) show that cells retained high viability for four days (Figure 39e). The cell concentration increased from $8x10^4$ cells/ml to $80x10^4$ cells/ml after four days of culture equivalent to 10-fold cell expansion (Figure 39f). The population doubling time was about 29 hr in average for four days. Unlike MAPC culture, hESCs did not form multiple layers after day 3. Once the culture reached confluence, the cells of the outer layer started to dissociate and single cells were observed in the culture (Figure 39d).

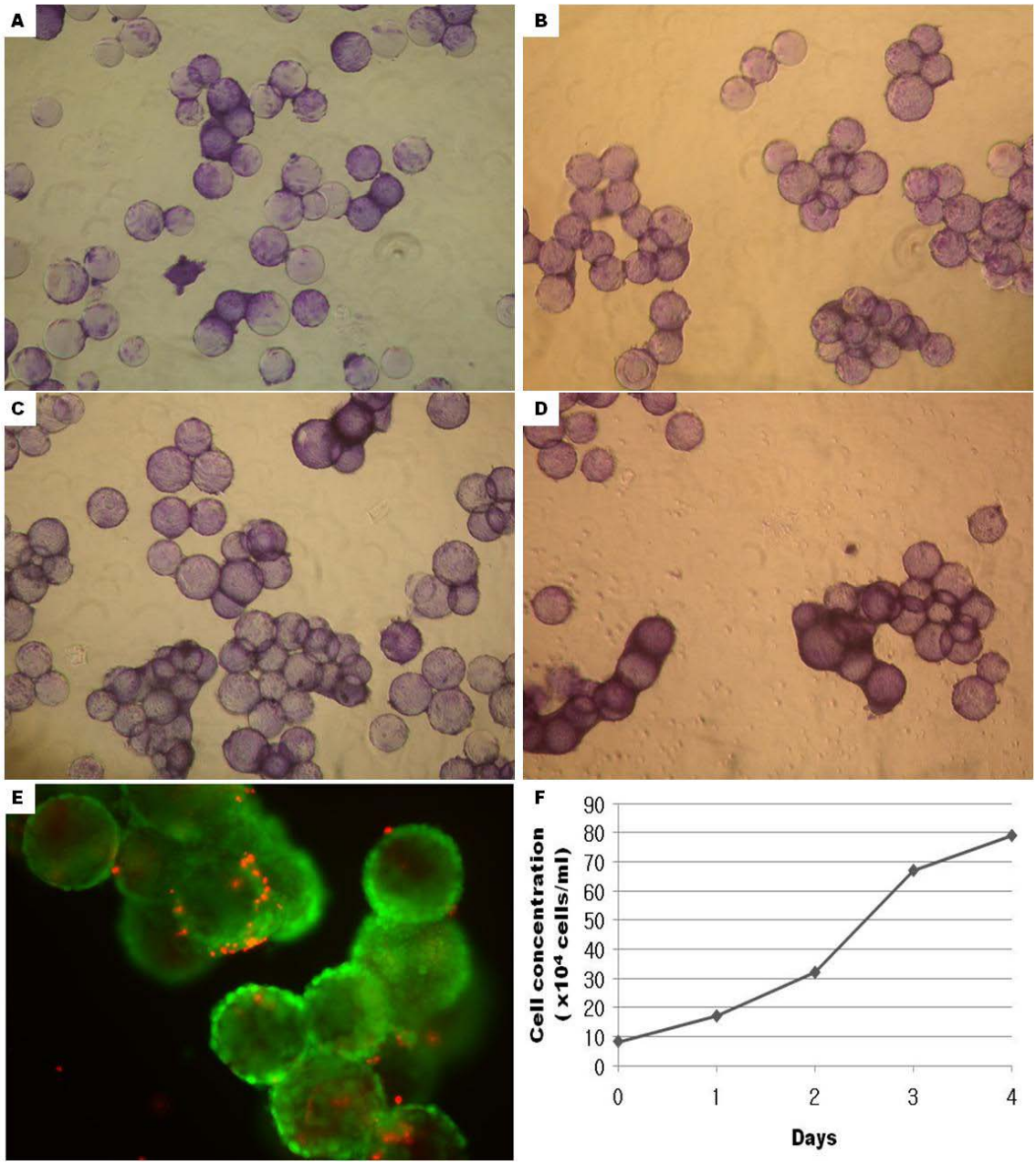

Figure 39. Cultivation of hESC on microcarriers. Crystal violet staining on (a) day 1, (b) day 2, (c) day 3, and (d) day 4. (e) Viability staining of cells on microcarriers on day 4. (f) Growth kinetics of cells during four day culture.

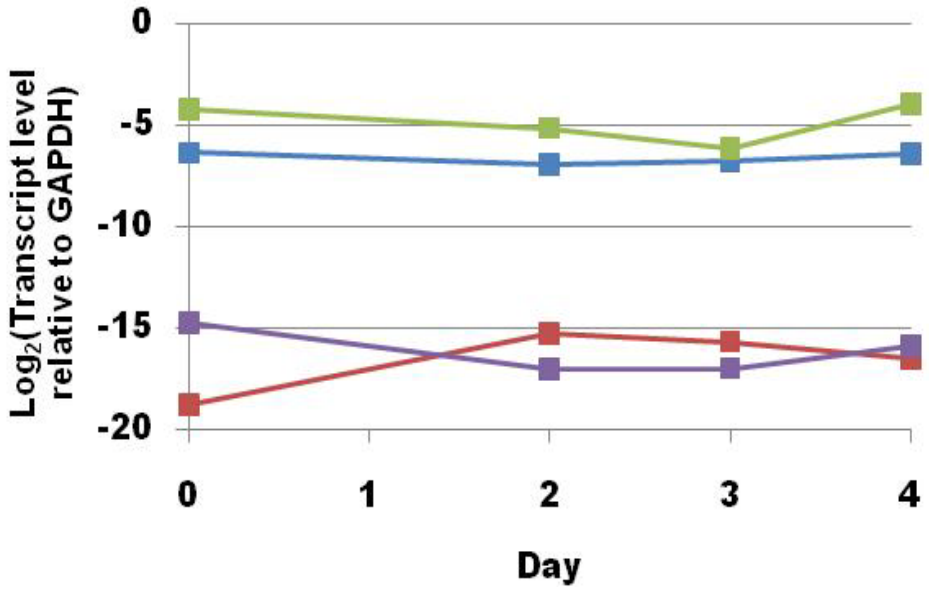

Figure 40. Maintenance of potency by RT-qPCR (*OCT4; SOX2; NANOG; AFP*).

5.3.3. Maintenance of undifferentiated hESCs on microcarriers

We evaluated the retention of pluripotency-related markers on hESCs expanded on microcarriers for four days. The expression levels of key pluripotency transcripts, *OCT4, REX1*, *SOX2, and NANOG* were assessed by RT-qPCR on day 0, day 2, day 3, and day 4. Transcript level of *OCT4* (ΔCT6-7) and *SOX2* (ΔCT4-5) were sustained during hESC proliferation (Figure 40). However, *NANOG* was expressed in a very low level. *AFP*, which expression is indicative of early differentiation, remained undetectable during four days of expansion culture (Figure 40). The results showed that hESCs in microcarrier suspension culture were expanded >10-fold while maintaining stable pluripotency gene expression.

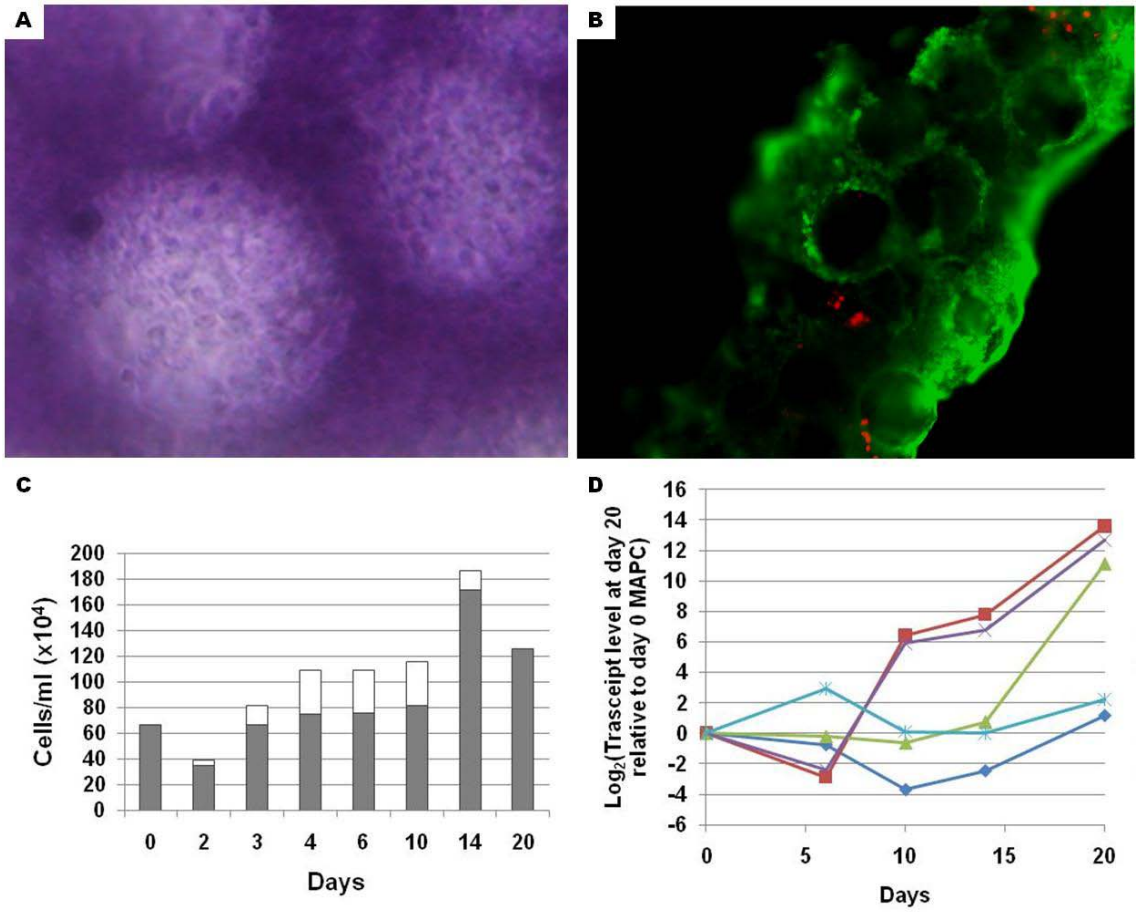

Figure 41. Directed hepatic differentiation for twenty days. (a) Crystral violet staining (day 20). (b) Viability staining (day 20; green (live) and red (dead) merged). (c) Cell concentration change for 20 days (■ live; □ dead). (d) RT-qPCR of *OCT4* and hepatic markers (*OCT4*; *AFP*; *ALBUMIN*; *AAT*; *TAT*).

5.3.4. Directed hepatic differentiation of hESCs on microcarriers

While hESCs remained on microcarriers, directed differentiation to hepatic lineage was carried out. hESCs were expanded on microcarriers first using the same cell concentration described in 4.2.2. Upon reaching 80-90% confluent, hESCs-laden-microcarriers were washed with PBS once and resuspended in differentiation medium as

prescribed by differentiation protocol in 4.2.3. The viable cell concentration increased slightly from $6.7x10^5$ cells/ml to $7.6x10^5$ cells/ml after treatment in Activin A and Wnt3a for six days. The concentration again increased up to $8.2x10^5$ cells/ml on day 10, further increased to $17.6x10^5$ cells/ml on day 14, and then decreased to $12.6x10^5$ cells/ml at the end of differentiation. The increase of dead cells was observed during first ten days (Figure 41c). Morphological changes of the cells seen in the culture were similar to those seen in static liver differentiation; cells became octagonal shape towards the end of differentiation (Figure 41a). After twenty days of hepatic differentiation, cells still retained high viability (Figure 41b).

We also monitored gene expression involved during hepatic differentiation. Transcript levels of the hepatic genes, *AFP*, *ALBUMIN*, and *AAT* was increased significantly (by 12-14 CTs) by day 20 of the hepatic differentiation (Figure 41d). However, the expression level of Tat was not detected.

5.4. Discussion

Current hESC expansion mostly relies on labor-intensive 2D culture techniques, which prevents a scale-up of hESC culture to meet the needs of clinical applications. Microcarriers enable culture of anchorage-dependent cells in suspension, thus allow high density culture in stirred reactor systems. In this study, we expanded hESCs as undifferentiated on microcarriers and used these for inducing hepatic cells.

The initial cell distribution on microcarriers greatly affects subsequent growth kinetics. Occasional mixing resulted in a better distribution of cells on the microcarriers. Unlike MAPCs which attach fast to microcarriers without any surface coating in a short incubation time, hESC clumps do not attach well onto microcarrier surface. The surface of Cytodex 1 microcarriers was modified with Matrigel to enhance the hESC clump attachment. Upon inoculating into a Matrigel coated Cytodex 1 microcarrier culture, hESCs attach to microcarriers and proliferate at a growth rates of 29 hr population doubling time. The doubling time we observed here fall within a range of the previously reported doubling times (31-33hr) of hESCs cultured on Matrigel plates or on Matrigel coated microcarriers [181, 246]. Since hESCs-microcarriers agglomerate into larger cells masses, and the cells grow in multiple layers on and in between microcarriers in the agglomerated mass, it is conceivable that the chemical environment in those tightly packed aggregates is not homogeneous. Inefficient transport of nutrients and metabolic wastes may cause inconsistency in cell growth and differentiation.

The high cell density seen on microcarriers maintained the potency of hESCs over the four-day culture period. The cells continued to express the stable levels of *OCT4* and *SOX2* transcripts, transcription factors expressed in ESCs essential for the maintenance of pluripotency. However, the *OCT4* transcript expression of all the cells (including day 0 starting cells) was lower by 3-4 delCTs when compared to typical *OCT4* expression of hESCs, and *NANOG* was expressed at a very low level. It is possible that hESCs were already partially differentiated to start with. We did not detect increased expression of

AFP, an early endoderm gene associated with differentiation (Figure 40). Our findings suggest that hESCs can be cultured on Matrigel-coated microcarriers maintaining pluripotency transcript level for a short term. Further pluripotency assessments such as evaluating OCT4, NANOG, and SOX2 expression at protein level, EB formation and teratoma formation should be performed to support the maintenance function of microcarriers on hESC culture.

In order to utilize this culture method for a long-term and large-scale culture, harvesting and passaging of hESCs are the challenges to overcome. At harvest, cells were detached from microcarriers by collagenase first, and then trypsinized with 2% chicken serum. hESCs harvested by this method usually have 70-80% viability (data not shown), which still has a room to increase the yield in large-scale culture system. hESCs, even under the conventional culture conditions, are known to be difficult to passage as single cells; the clonal efficiency of single cells is less than 7% [194]. As serial passaging would be necessary for a long-term culture, increase of seeding efficiency is a bottleneck to highly efficient production.

In this study, hESCs were seeded onto microcarriers as a mixture of small clumps and single cells, which makes the attachment efficiency low. It will be important to control the clump size in the future. Seeding efficiency is sensitive to the size of clumps; single cell or large clusters do not attach well [181]. Many studies have been discussed ways to improve the seeding efficiency. Low oxygen tension is known to increase the clonal

efficiency of H1 and H9 hESC lines [194]. Inhibition of Rho-associated kinase (ROCK) increased clonal survival of individual cells [247]. Surface modification with appropriate ECM may help the cell seeding and growth on microcarriers.

With the experience from MAPC differentiation on microcarriers, we used microcarrier culture systems for hepatocyte differentiation of hESCs. Cell concentration profiles recapitulated the cell concentration changes seen during rMAPC or hESC hepatic differentiations; the number of dead cells increased over first ten days, and cells proliferated during day 10-14 corresponding to hepatoblast proliferation phase. At the end of the differentiation, the cell concentration reached $1.2x10^6$ cells/ml, which is high even for a reactor culture system. The expression of hepatic genes, *AFP*, *ALBUMIN*, and *AAT*, were significantly up-regulated towards the end of hepatic differentiation (Figure 41). The extent of differentiation into hepatocyte-like cells on microcarriers, as judged by level of the expression of these genes, was inconsistent with the previous hESC-microcarrier-based hepatic differentiation, and was slightly lower than that seen in differentiation in 2D or in 3D in culture dishes (n=1). This could be due to the cells that initially expressed lower level of *OCT4* transcript than typical hESCs or to the culture system that needs further optimization. Although there was inconsistency in the results, these results still suggest that hepatic differentiation on microcarriers can provide hepatic cells in a larger scale.

Forming agglomeration of cell-microcarriers, this culture system may work as quasi-3D differentiation system with few layers of cells to improve nutrient transport. It may be beneficial to employ in hepatic differentiation since 3D aggregate differentiation was found to produce more mature hepatocytes (Subramanian et al, manuscript in preparation). Further investigation is needed to compare 3D aggregate differentiation and agglomerated microcarrier differentiation to study actual effects.

We conclude that microcarrier suspension culture is a scalable culture method for hESC expansion and subsequent directed differentiation to the hepatic lineage. It will facilitate the transformation of the laboratory practice of stem cell culture to scalable bioprocesses generating hepatocyte-like cells at industrial scales for future clinical applications.

CONCLUSIONS AND FUTURE DIRECTIONS

Throughout this thesis, different types of cultivation methods including the conventional 2D culture in dishes and the bioreactor culture were explored to expand and differentiate rat MAPCs more efficiently.

In Chapter 2, it was demonstrated that even though hypoxia and low density culture is required for isolation of high Oct4 expressing MAPC, once the culture has been established MAPC can be cultured at a higher cell density and under normoxic level with maintaining their potency. Hypoxia promotes the MAPC proliferation, but is not a critical factor in maintaining Oct4 expression and potency of rodent MAPC. This study provides evidences that MAPC can be readily cultured at a higher cell density (1000 cells/cm^2) and under low oxygen level (5% O_2) for long term culture. With a seeding density of 1000 cells/cm^2, MAPCs do not grow completely confluent on the tissue culture surface after two days. Long-term cell culture at very high cell densities or lower oxygen levels (<3%) should be studied further to optimize 2D MAPC culture and explore the effects of more physiologically relevant or more exhausting culture conditions. These findings open the possibility for easy scale up of rodent MAPC cultures that will allow testing their usefulness in preclinical models of tissue repair or bioengineering applications.

Then the culture system was switched from a conventional tissue plate culture to a bioreactor culture. As described in Chapter 3, we have developed a suspension based culture platform with 70 fold cell expansion of rat MAPCs as aggregates to obtain a final

cell concentration of 10^6 cells/ml. During the spinner culture, MAPCs were maintained undifferentiated retaining their potency-related gene expressions and differentiation capability. Interestingly, aggregates give rise to clumps of cells (30-300 μm in diameter) due to shear stress. If these clumps can be continuously generated and maintained at a certain size with a stable level of self-renewal capability and potency, it will be beneficial for easily providing more homogeneous culture for larger scale applications. More studies need to be done to control the sizes of these clumps and the consequent influence on stem cell expansion and differentiation. Further, we have also demonstrated that these aggregates can be maintained undifferentiated in spinner culture for a longer term with appropriate medium replacements. For a long-term culture of MAPC aggregates, optimization of the frequency of medium replacement and the upper limit of cell concentration need to be defined for further optimization.

In addition, we demonstrated the differentiation of these spinner expanded MAPC aggregates and clumps into 'hepatocyte-like' cells that has applications in *in vitro* hepatoxicity screening and as a model for studies related to liver development and regeneration. The protocol developed for rat MAPC differentiation to hepatocytes can be readily applicable for human ESC or iPSC differentiations, with minor modifications for more use in clinical applications.

Every culture system has up and down sides of its intrinsic properties, and the successful employment of it is usually cell type dependent. We explored another stirred vessel

culture technique using microcarriers. As shown in Chapter 4, microcarrier suspension culture is a robust method for scale up of MAPC expansion and differentiation to the hepatic lineage. This method allowed an over 80-fold expansion of MAPC during 4 day culture. Cells differentiated on microcarriers expressed genes specific to hepatic cells such as *Albumin, Aat, Tat,* and *Hnf4α* and showed a degree of functionality confirmed by albumin and urea secretion. Microcarrier suspension culture system provides more homogeneous environment to allow a major fraction of cells differentiate and express the hepatic phenotype. Recently in our lab, Subramanian et al. (manuscript in preparation) found that MAPC hepatic differentiation as 3D aggregates produce more mature hepatocyte-like-cells in a static culture. Driven by this finding, we combined 3D and microcarrier culture for hepatic differentiation in order to first, expand hepatic progenitor cells on microcarriers and then mature the cells using the aggregate differentiation. However, we did not observe further hepatic maturation in our culture. Endothelium-like cells seem to proliferate and dominate the cell populations during the aggregate culture. The control of different cell populations and time of aggregation in the later phase of differentiation process need to be investigated for further utilizing 3D culture system for stem cell differentiation in spinner culture. 3D hepatic differentiation may need to be performed in advance in the spinner culture as a proof of concepts on its maturation effect.

We also extended our experience in microcarrier culture to hESC culture, and demonstrated that hESCs can be expanded and differentiated on microcarriers using a

modified protocol. hESCs attach to Matrigel-coated microcarriers as small clumps and expand maintain a stable pluripotency-related gene expression. hESCs also can be differentiated into hepatocyte-like cells on microcarriers. There is still a need to optimize and increase the efficiency of hESC microcarrier culture system, but at least it shows a potential of microcarrier use in hepatic differentiation to generate hepatocyte-like cells in a larger scale.

Overall, we conclude that both 3D aggregate and microcarrier culture systems are efficient and robust methods to generate differentiation competent (or undifferentiated) or directed differentiated rat MAPCs at a large scale. We envision this study laying the foundation for the development of a scalable culture platform for expansion of human MAPCs, ESCs, and iPSCs, and their differentiation into functional somatic cell types in the future. With further optimization of culture parameters in more controlled reactors, it will facilitate the translation of the laboratory practice of stem cell culture to scalable bioprocesses generating stem cells or stem cell-derived cells at industrial scales for future clinical applications.

REFERENCES

1. Weissman, I.L., *Translating stem and progenitor cell biology to the clinic: barriers and opportunities.* Science, 2000. **287**: p. 1442-6.
2. Lakshimipathy, U., Verfaillie, C., *Stem cell plasticity.* Blood Rev, 2005. **19**(1): p. 29-38.
3. Niwa, H., *How is pluripotency determined and maintained?* Development, 2007. **134**(4): p. 635-46.
4. Wagers, A., Weissman, IL., *Plasticity of adult stem cells.* Cell, 2004. **116**(5): p. 639-48.
5. Evans, M., Kaufman, MH., *Establishment in culture of pluripotential cells from mouse embryos.* Nature, 1981. **292**(5819): p. 154-6.
6. Thomson, J., et al., *Embryonic stem cell lines derived from human blastocysts.* Science, 1998. **282**(5391): p. 1145-7.
7. Palmieri, S.L., et al., *Oct-4 transcription factor is differentially expressed in the mouse embryo during establishment of the first two extraembryonic cell lineages involved in implantation.* Dev. Biol., 1994. **166**(1): p. 259-267.
8. Niwa, H., Miyazaki J, Smith AG, *Quantitative expression of Oct-3/4 defines differentiation, dedifferentiation or self-renewal of ES cells.* . Nat Genet, 2000. **24**(4): p. 372-6.
9. Taga, T., Kishimoto T., *Gp130 and the interleukin-6 family of cytokines.* Annu. Rev. Immunol., 1997. **15**: p. 797-819.
10. Cartwright, P., et al., *LIF/STAT3 controls ES cell self-renewal and pluripotency by a Myc-dependent mechanism.* Development, 2005. **132**(5): p. 885-96.
11. Niwa, H., et al., *Self-renewal of pluripotent embryonic stem cells is mediated via activation of STAT3.* Genes Dev., 1998. **12**(13): p. 2048-60.
12. Liu, N., et al., *Molecular mechanisms involved in self-renewal and pluripotency of embryonic stem cells.* J. Cell. Physiol., 2007. **211**(2): p. 279-86.
13. Itskivitz-Eldor, J., et al., *Differentiation of human embryonic stem cells into embryoid bodies compromising the three embryonic germ layers.* Mol. Med., 2000. **6**(2): p. 88-95.
14. Takahashi, K., Yamanaka S, *Induction of pluripotent stem cells from mouse embryonic and adult fibroblast cultures by defined factors.* Cell, 2006. **126**(4): p. 663-76.
15. Aoi, T., et al., *Generation of pluripotent stem cells from adult mouse liver and stomach cells.* Science, 2008.

16. Lowry, W., et al., *Generation of human induced pluripotent stem cells from dermal fibroblasts.* Proc Natl Acad Sci USA, 2008. **105**: p. 2883-2888.

17. Okita, K., Ichisaka T, Yamanaka S, *Generation of germ-line competent induced pluripotent stem cells.* Nature, 2007. **448**(7151): p. 313-7.

18. Park, I., et al., *Generation of human-induced pluripotent stem cells.* Nat. Protoc., 2008. **3**(7): p. 1180-6.

19. Yu, J., et al. , *Induced pluripotent stem cell lines derived from human somatic cells.* Science, 2007. **318**(5858): p. 1917-20.

20. Blelloch, R., et al., *Generation of induced pluripotent stem cells in the absence of drug selection.* Cell Stem Cell, 2007. **1**: p. 245-247.

21. Nakagawa, M., et al., *Generation of induced pluripotent stem cell wihout Myc from mouse and human fibroblasts.* Nat. Biotechnol., 2008. **25**(1): p. 101-6.

22. Lin, T., et al., *p53 induces differentiation of mouse embryonic stem cells by supressing Nanog expression.* Nat. Cell Biol., 2005. **7**(2): p. 165-71.

23. Rowland, B., Bernards R, Peeper DS, *The Klf4 tumour suppressor is a transcriptional repressor of p53 that acts as a context-dependent oncogene.* Nat. Cell Biol. , 2005. **7**(11): p. 1074-82.

24. Matsui, T.K., T. Morikawa, Y. Tohya, K. Katsuki, M. Ito, Y. Kamiya, A. Miyajima, A. , *K-Ras mediates cytokine-induced formation of E-cadherin-based adherens junctions during liver development.* . Embo J, 2002. **21**: p. 1021-30.

25. Yamanaka, S., *Induction of pluripotent stem cells from mouse fibroblast by four transcription factors.* Cell Prolif., 2008. **41 Suppl 1**: p. 51-6.

26. Park, I., et al., *Reprogramming of human somatic cells to pluripotency with defined factors.* Nature, 2008. **451**(7175): p. 141-6.

27. Wernig, M., et al., *In vitro reprogramming of fibroblasts into a pluripotent ES-cell-like state.* Nature, 2007. **448**(7151): p. 318-24.

28. Richards, M., et al., *The transcriptome profile of human embryonic stem cells as defined by SAGE.* Stem Cells, 2004. **22**(1): p. 51-64.

29. Nishikawa, S., Goldstein, RA., Nierras, CR., *The promise of human induced pluripotent stem cells for research and therapy.* Nature Reviews, 2008. **9**: p. 725-9.

30. Vierbuchen, T., Ostermeier A, Pang ZP, Kokubu Y, Sudhof TC, Wernig M, *Direct conversion of fibroblasts to functional neurons by defined factors.* Nature, 2010. **463**: p. 1035-41.

31. Okita, K., et al., *Generation of mouse induced pluripotent stem cells without viral vectors.* Science, 2008. **332**(5903): p. 949-53.

32. Kaji, K., et al., *Virus-free induction of pluripotency and subsequent excision of reprogramming factors.* Nature, 2009. **458**: p. 771-775.

33. Hanna, J., et al., *Direct reprogramming of terminally differentiated mature B lymphocytes to pluripotency.* Cell, 2008. **133**: p. 250-264.

34. Kim, J., Sebastiano V, Wu G, Arauzo-Bravo MJ, Hubner K, Bermemann C, Ortmeier C, Zenke m, Fleischmann BK, Zaehres H, Scholer HR, *Oct4-induced pluripotency in adult neural stem cells.* Cell, 2009. **136**: p. 411-419.

35. Yoon, Y.S., et al., *Clonally expanded novel multipotent stem cells from human bone marrow regenerate myocardium after myocardial infarction.* J Clin Invest, 2005. **115**(2): p. 326-38.

36. D'Ippolito, G., et al., *Marrow-isolated adult multilineage inducible (MIAMI) cells, a unique population of postnatal young and old human cells with extensive expansion and differentiation potential.* J Cell Sci, 2004. **117**: p. 2971-81.

37. Kucia, M., et al., *Morphological and molecular characterization of novel population of CXCR4+ SSEA-4+ Oct-4+ very small embryonic-like cells purified from human cord blood: preliminary report.* Leukemia, 2007. **21**(2): p. 297-303.

38. Kucia, M., et al., *A population of very small embryonic-like (VSEL) CXCR4(+)SSEA-1(+)Oct-4+ stem cells identified in adult bone marrow.* Leukemia, 2006. **20**(5): p. 857-69.

39. Kogler, G., et al., *A new human somatic stem cell from placental cord blood with intrinsic pluripotent differentiation potential.* J Exp Med, 2004. **200**(2): p. 123-35.

40. Gupta, S., et al., *Isolation and characterization of kidney-derived stem cells.* J Am Soc Nephrol, 2006. **17**(11): p. 3028-40.

41. Bonnet, A.-A.a., *Nonhematopoietic/endothelial SSEA-1+ cells define the most primitive progenitors in the adult murine bone marrow mesenchymal compartment.* Blood, 2007. **109**(3): p. 1298-306.

42. Cantz, T., et al., *Absence of OCT4 expression in somatic tumor cell lines.* Stem Cells, 2008. **26**: p. 692-7.

43. Lin, H., et al., *Stem cell regulatory function mediated by expression of a novel mouse Oct4 pseydogene.* Biochem. Biophys. Res.Commun., 2007. **355**: p. 111-6.

44. Pain, D., et al., *Multiple retropseudogenes from pluripotent cell-specific gene expression indicates a potential signature for novel gene identification.* J of Biological Chemistry, 2005. **280**: p. 6265-8.

45. Suo, G., et al., *Oct4 pseudogenes are transcribed in cancers.* Biochem. Biophys. Res.Commun., 2005. **337**: p. 1047-51.

46. Robertson, M., et al., *Nanog retrotransposed genes with functionally conserved open reading frames.* Mammalian Genome, 2006. **17**: p. 732-43.

47. Booth, H., and Holland, PWH., *Eleven daughters of NANOG.* Genomics, 2004. **84**: p. 229-238.

48. Nobuhiko, M., and Kosaka, M., *Novel variants of Oct-3/4 gene expressed in mouse somatic cells.* J of Biological Chemistry, 2008. **283**: p. 30997-31004.

49. Liedtke, S., et al., *Oct4 and its pseudogenes confuse stem cell research.* Cell Stem Cell, 2007. **1**: p. 364-6.

50. Jiang, Y., et al., *Multipotent progenitor cells can be isolated from postnatal murine bone marrow, muscle, and brain.* Exp Hematol, 2002. **30**(8): p. 896-904.

51. Reyes, M., Dudek, A., Jahagirdar, B., Koodie, L., Marker, PH., Verfaillie, CM., *Origin of endothelial progenitors in human postnatal bone marrow*. J. Clin. Invest., 2002. **109**: p. 337-346.

52. Breyer, A., Estharabadi, N., Oki, M., Ulloa, F., Nelson-Holte, M., Lien, L., Jiang, Y., *Multipotent adult progenitor cell isolation and culture procedures.* Exp. Hematol., 2006. **34**: p. 1596-1601.

53. Subramanian, K., Graerts M, Pauwelyn KA, Park Y, Owens DJ, Muijtjens M, Ulloa-Montoya F, Jiang Y, Verfaillie CM, Hu WS, *Isolation procedure and characterization of multipotent adult progenitor cells from rat bone marrow*, in *Cellular Programming and Reprogramming*. 2010, Humana Press. p. 55-78.

54. Ulloa-Montoya, F., Kidder BL, Pauwelyn KA, Chase LG, Luttun A, Crabbe A, Geraerts M, Sharov AA, Piao Y, Ko MSH, Hu WS, Verfaillie C, *Comparative transcriptome analysis of embryonic and adult stem cells with extended and limited differentiation capcity.* Genome Biology, 2007. **8**: p. R163.

55. Kunath, T., et al., *Imprinted X-inactivation in extra-embryonic endoderm cell lines from mouse blastcysts.* Development, 2005. **132**(7): p. 1649-61.

56. Jiang, Y., Henderson D, et al, *Neuroectodermal differentiation from mouse multipotent adult progenitor cells.* Proc Natl Acad Sci USA, 2003. **100 Suppl1**: p. 11854-60.

57. Schwartz, R., Reyes, M., Koodie, L., Jiang, Y., Blackstad, M., Lund, T., Lenvik, T., Hounson, S., Hu, WS., Verfaillie, CM., *Multipotent adult progenitor cells from bone marrow differentiate into functional hepatocyte-like cells.* J. Clin. Invest., 2002. **109**: p. 1291-1302.

58. Aranguren, X.L., et al., *In vitro and in vivo arterial differentiation of human multipotent adult progenitor cells.* Blood, 2007. **109**(6): p. 2634-42.

59. Chazaud, C., et al., *Early lineage segregation between epiblast and primitive endoderm in mouse blastocysts through the Grb2-MAPK pathway.* Dev Cell, 2006. **10**(5): p. 615-24.

60. Serafini, M., et al., *Hematopoietic reconstitution by multipotent adult progenitor cells: precursors to long-term hematopoietic stem cells.* J Exp Med, 2007. **204**(1): p. 129-39.

61. Guyton, A., Hall, JE., *The liver as an organ*, in *Text book of medical physiology*. 2000, W.B Saunders.

62. Zorn, A. *Liver development*. 2008 [cited; StemBook:[Available from: http://www.stembook.org.

63. Hoodless, P., et al., *FoxH1 (Fast) functions to specify the anterior primitive streak in the mouse.* Genes Dev., 2001. **15**(10): p. 1257-71.

64. Lowe, L., et al., *Genetic dissection of nodal function in patterning the mouse embryo.* Development, 2001. **128**(10): p. 1831-43.

65. Norris, D., et al., *The Foxh1-dependent autoregulatory enhancer controls the level of Nodal signals in the mouse embryo.* Development, 2002. **129**(14): p. 3455-68.

66. Shen, M., *Nodal signaling: developmental roles and regulation.* Development, 2007. **134**(1023-34).

67. Zorn, A., Wells, JM, *Molecular basis of vertebrate endoderm development.* Int Rev Cytol, 2007. **259**: p. 49-111.

68. Waldrip, W., et al., *Smad2 signaling in extraembryonic tissues determines anteriorposterior polarity of the early mouse embryo.* Cell, 1998. **92**(6): p. 797-808.

69. Chen, Y.P., F.C. Brandes, N. Afelik, S. Solter, M. Pieler, T., *Retinoic acid signaling is essential for pancreas development and promotes endocrine at the expense of exocrine cell differentiation in Xenopus.* . Dev Biol, 2004. **271**(144-160).

70. Dessimoz, J.O., R. Kordich, J.J. Grapin-Botton, A. Wells, J.M. , *FGF signaling is necessary for establishing gut tube domains along the anterior-posterior axis in vivo.* Mech Dev, 2006. **123**(41-55).

71. Kumar, M.J., N. Melton, D. Grapin-Botton, A., *Signals from lateral plate mesoderm instruct endoderm toward a pancreatic fate.* Dev Biol 2003. **259**: p. 109-122.

72. McLin, V.A.R., S.A. Zorn, A.M. , *Repression of Wnt/{beta}-catenin signaling in the anterior endoderm is essential for liver and pancreas development.* Development, 2007. **134**(2207-17).

73. Roberts, D.J.J., R.L. Burke, A.C. Nelson, C.E. Morgan, B.A. Tabin, C., *Sonic hedgehog is an endodermal signal inducing Bmp-4 and Hox genes during induction and regionalization of the chick hindgut.* Development, 1995. **121**: p. 3163-3174.

74. Stafford, D.H., A. Mueller, P.R. Prince, V.E., *A conserved role for retinoid signaling in vertebrate pancreas development.* Dev Genes Evol, 2004. **214**: p. 432-441.

75. Tiso, N.F., A. Pauls, S. Bortolussi, M. Argenton, F. , *BMP signalling regulates anteroposterior endoderm patterning in zebrafish.* Mech Dev 2002. **118**: p. 29-37.

76. Wells, J., Melton, DM., *Vertebrate endoderm development.* Annu Rev Cell Dev Biol, 1999. **15**: p. 393-410.

77. Jung, J., et al., *Initiation of mammalian liver development from endoderm by fibroblast growth factors.* Science, 1999. **284**(5422): p. 1998-2003.

78. Lough, J., Sugi, Y., *Endoderm and heart development.* Dev Dyn, 2000. **217**(4): p. 327-42.

79. Gualdi, R., et al., *Hepatic specification of the gut endoderm in vitro: cell signaling and transcriptional control.* Genes Dev., 1996. **10**(13): p. 1670-82.

80. Rossi, J., et al., *Distinct mesodermal signals, including BMPs from the septum transversum mesenchyme, are required in combination for hepatogenesis from the endoderm.* Genes Dev., 2001. **15**(15): p. 1998-2009.

81. Cascio, S., Zaret, KS., *Hepatocyte differentiation initiates during endodermalmesenchymal interactions prior to liver formation.* Development, 1991. **113**(1): p. 217-25.

82. Solloway, M., Robertson, EJ., *Early embryonic lethality in Bmp5;Bmp7 double mutant mice suggests functional redundancy within the 60A subgroup.* Development, 1999. **126**(8): p. 1753-68.

83. Bort, R.M.-B., J.P. Beddington, R.S. Zaret, K.S. , *Hex homeobox gene-dependent tissue positioning is required for organogenesis of the ventral pancreas.* Development, 2004. **131**(797-806).

84. Matsumoto, K.Y., H. Rossant, J. Zaret, K.S. , *Liver organogenesis promoted by endothelial cells prior to vascular function. .* Science, 2001. **294**: p. 559-563.

85. Tatsumi, N.M., R. Katsu, K. Yokouchi, Y., *Neurturin-GFRalpha2 signaling controls liver bud migration along the ductus venosus in the chick embryo.* Dev Biol Stand, 2007. **307**(14-28).

86. Sosa-Pineda, B., et al., *Hepatocyte migration during liver development requires Prox1.* Nat Genet, 2000. **25**(3): p. 254-5.

87. Berg, T.R., C.B. Lee, L. Estrada, J. Sala, F.G. Choe, A. Veltmaat, J.M. De Langhe, S. Lee, R. Tsukamoto, H., *Fibroblast growth factor 10 is critical for liver growth during embryogenesis and controls hepatoblast survival via beta-catenin activation.* . Hepatology, 2007. **46**(1187-97).

88. Yanai, M.T., N. Hasunuma, N. Katsu, K. Endo, F. Yokouchi, Y. , *FGF signaling segregates biliary cell-lineage from chick hepatoblasts cooperatively with BMP4 and ECM components in vitro.* Dev Dyn, 2008. **237**: p. 1268-1283.

89. Moumen, A.I., A. Patane, S. Sole, C. Comella, J.X. Dono, R. Maina, F. , *Met signals hepatocyte survival by preventing Fas-triggered FLIP degradation in a PI3k-Akt-dependent manner.* . Hepatology, 2007. **45**: p. 1210-17.

90. Hentsch, B.L., I. Li, R. Hartley, L. Lints, T.J. Adams, J. M. Harvey, R.P. , *Hlx homeo box gene is essential for an inductive tissue interaction that drives expansion of embryonic liver and gut.* . Genes Dev., 1996. **10**: p. 70-79.

91. Wandzioch, E.K., A. Jacobsson, M. Friedman, S.L. Carlsson, L. , *Lhx2-/- mice develop liver fibrosis.* . Proc Natl Acad Sci USA, 2004. **101**: p. 16549-54.

92. Weinstein, M.M., S.P. Liu, Y. Brodie, S.G. Tang, Y. Li, C. Mishra, L. Deng, C.X. , *Smad proteins and hepatocyte growth factor control parallel regulatory pathways that converge on beta1-integrin to promote normal liver development.* Mol Cell Biol 2001. **2**: p. 5122-31.

93. Beg, A., et al., *Embryonic lethality and liver degeneration in mice lacking the RelA component of NF-kappa B.* Nature, 1995. **376**: p. 167-70.

94. Bonnard, M., et al., *Deficiency of T2K leads to apoptotic liver degeneration and impaired NF-kappaB-dependent gene transcription.* Embo J, 2000. **19**: p. 4976-85.

95. Doi, T.S.M., M.W. Takahashi, T. Yoshida, T. Sakakura, T. Old, L. J. Obata, Y. , *Absence of tumor necrosis factor rescues RelA-deficient mice from embryonic lethality.* Proc Natl Acad Sci USA, 1999. **96**: p. 2994-99.

96. Eferl, R.S., M. Hilberg, F. Fuchsbichler, A. Kufferath, I. Guertl, B. Zenz, R. Wagner, E.F. Zatloukal, K., *Functions of c-Jun in liver and heart development.* J Cell Biol, 1999. **145**: p. 1049-61.

97. Johnson, L.G., D. Cichowski, K. Mercer, K. Murphy, E. Schmitt, E. Bronson, R.T. Umanoff, H. Edelmann, W. Kucherlapati, R. Jacks, T. , *K-ras is an essential gene in the mouse with partial functional overlap with N-ras.* Genes Dev., 1997. **11**: p. 2468-81.

98. Reimold, A.M.E., A. Clauss, I. Perkins, A. Friend, D.S. Zhang, J. Horton, H.F. Scott, A. Orkin, S.H. Byrne, M.C. , *An essential role in liver development for transcription factor XBP-1.* Genes Dev., 2000. **14**: p. 152-7.

99. Rosenfeld, M.E.P., L. Shiojiri, N. Fausto, N. (2000). , *Prevention of hepatic apoptosis and embryonic lethality in RelA/TNFR-1 double knockout mice.* Am J Pathol, 2000. **156**: p. 997-1007.

100. Suzuki, A.I., A. Miyashita, H. Nakauchi, H. Taniguchi, H. , *Role for growth factors and extracellular matrix in controlling differentiation of prospectively isolated hepatic stem cells.* . Development, 2003. **130**(2513-24).

101. Dudas, J., et al., *Prospero-related homeobox 1 (Prox1) is a stable hepatocyte marker*

during liver development, injury and regeneration, and is absent from oval cells. Histochem Cell Biol, 2006. **126**(5): p. 549-562.

102. Kamiya, A.K., T. Ito, Y. Matsui, T. Morikawa, Y. Senba, E. Nakashima, K. Taga, T. Yoshida, K. Kishimoto, T. Miyajima, A. , *Fetal liver development requires a paracrine action of oncostatin M through the gp130 signal transducer.* . Embo J, 1999. **18**(2127-36).

103. Michalopoulos, G.K.B., W.C. Mule, K. Luo, J. , *HGF-, EGF-, and dexamethasone-induced gene expression patterns during formation of tissue in hepatic organoid cultures.* . Gene Expr, 2003. **11** p. 55-75.

104. Tan, X.Y., Y. Zeng, G. Apte, U. Thompson, M.D. Cieply, B. Stolz, D.B. Michalopoulos, G.K. Kaestner, K.H. Monga, S.P. , *beta-Catenin deletion in hepatoblasts disrupts hepatic morphogenesis and survival during mouse development.* Hepatology, 2008. **47**: p. 1667-79.

105. Zaret, K.S., *Regulatory phases of early liver development: paradigms of organogenesis.* Nat Rev Genet, 2002. **3**(7): p. 499-512.

106. Herrera, M., Bruno S, Buttiglieri S, Tetta C, Gatti S, Deregibus MC, Bussolati B, Camussi G, *Isolation and characterization of a stem cell population from adult human liver.* Stem Cells, 2006. **24**: p. 2840-2850.

107. Lazaro, C., et al., *Generation of hepatocytes from oval cell precursors in culture.* Cancer Res, 1998. **58**: p. 5514-22.

108. Rogler, L., *Selective bipotential differentiation of mouse embryonic hepatoblasts in vitro.* Am J Pathol, 1997. **150**: p. 591-602.

109. Schmelzer, E., et al., *The phenotypes of pluripotent human hepatic progenitors.* Stem Cells, 2006. **24**(1852-58).

110. Tanimizu, N., et al., *Isolation of hepatoblasts based on the expression of Dlk/Pref-1.* J Cell Sci, 2003. **116**: p. 1775-1786.

111. Tanimizu, N., et al., *Long-term culture of hepatic progenitors derived from mouse Dlk+ hepatoblasts.* J Cell Sci, 2004. **117**: p. 6425-34.

112. Zhang, L., et al., *The stem cell niche of human livers: symmetry between development and regeneration.* Hepatology, 2008. **48**: p. 1598-1607.

113. Clotman, F.J., P. Plumb-Rudewiez, N. Pierreux, C.E. Van der Smissen, P. Dietz, H.C. Courtoy, P.J. Rousseau, G.G. Lemaigre, F.P. , *Control of liver cell fate decision by a gradient of TGF beta signaling modulated by Onecut transcription factors.* Genes Dev., 2005. **19**(1849-54).

114. Clotman, F.L., V.J. Reber, M. Cereghini, S. Cassiman, D. Jacquemin, P. Roskams, T. Rousseau, G.G. Lemaigre, F.P., *The onecut transcription factor HNF6 is required for normal development of the biliary tract.* Development, 2002. **129**: p. 1819-28.

115. Katoonizadeh, A., et al., *Liver regeneration in acute severe liver impairment: a clinicopathological correlation study.* Liver Int, 2006. **26**: p. 1225-33.

116. Roskams, T., et al., *Neuroregulation of the neuroendocrine compartment of the liver.* Anat Rec A Discn Mol Cell Evol Biol, 2004. **280**: p. 910-23.

117. Thorgeirsson, S., et al., *Hepatic stem cell compartment: activation and lineage commitment.* Proc Soc Exp Biol Med, 1993. **204**: p. 253-60.

118. Fujio, K., et al., *Expression of stem cell factor and its receptor, c-kit, during liver generation from putative stem cells in adult rat.* Lab Invest, 1994. **70**: p. 511-6.

119. Monga, S., et al., *Expansion of hepatic and hematopoietic stem cells utilizing mouse embryonic liver explants.* Cell Transplant, 2001. **10**: p. 81-89.

120. Hamazaki, T., et al., *Hepatic maturation in differentiating embryonic stem cells in vitro.* FEBS Lett., 2001. **497**: p. 15-19.

121. Heo, J., et al., *Hepatic precursors derived from murine embryonic stem cells contribute to regeneration of injured liver.* Hepatology, 2006. **44**: p. 1478-86.

122. Jones, E., et al., *Hepatic differentiation of murine embryonic stem cells.* Exp Cell Res, 2002. **272**: p. 15-22.

123. Cai, J., Zhao Y, Liu Y, Ye F, Song Z, Qin H, Meng S, Chen Y, Zhou R, Song X, Guo Y, Ding M, Deng H, *Directed differentiation of human embryonic stem cells into functional hepatic cells.* Hepatology, 2007. **45**: p. 1229-1239.

124. Soto-Gutierrez, A., et al., *Reversal of mouse hepatic failure using an implanted liver-assist device containing ES cell-derived hepatocytes.* Nat Biotechnol, 2006. **24**: p. 1412-19.

125. Teratani, T., et al., *Direct hepatic fate specification from mouse embryonic stem cells.* Hepatology, 2005. **41**: p. 836-46.

126. Yamamoto, H., et al., *Differentiation of embryonic stem cells into hepatocytes: biological functions and therapeutic application.* Hepatology, 2003. **37**: p. 983-93.

127. Yin, Y., et al., *AFP(+), ESC-derived cells engraft and differentiate into hepatocytes in vivo.* Stem Cells, 2002. **20**: p. 338-346.

128. Gadue, P., et al., *Wnt and TGF-beta signaling are required for the induction of an in vitro model of primitive streak formation using embryonic stem cells.* Proc Natl Acad Sci USA, 2006. **103**: p. 16806-11.

129. Basma, H., Soto-Guitierrez A, Yannam GR, Liu L, Ito R, Yamamoto T, Ellis E, Carson SD, Sato S, Chen Y, Muirhead D, Navarro-Alvarez N, Wong RJ, Roy-Chowdhury J, Platt JL, Mercer DF, Miller JD, Strom SC, Kobayashi N, Fox IJ, *Differentiation and transplantation of human embryonic stem cell-derived hepatocytes.* Gastroenterology, 2009. **136**: p. 990-999.

130. D'Amour, K., et al., *Efficient differentiation of human embryonic stem cells to definitive endoderm.* . Nat Biotechnol, 2005. **23**: p. 1534-1541.

131. Kubo, A.S., K. Shannon, J.M. Kouskoff, V. Kennedy, M. Woo, S. Fehling, H.J. Keller, G. , *Development of definitive endoderm from embryonic stem cells in culture.* Development, 2004. **131**: p. 1651-1662.

132. Yasunaga, M.T., S. Torikai-Nishikawa, S. Nakano, Y. Okada, M. Jakt, L.M. Nishikawa, S. Chiba, T. Era, T. , *Induction and monitoring of definitive and visceral endoderm differentiation of mouse ES cells.* . Nat Biotechnol, 2005. **23**(1542-50).

133. Hay, D., Zhao D, Fletcher J, Hewitt ZA, McLean D, Urruticoechea-Uriguen A, Black JR, Elcome C, Ross JA, Wolf R, Cui W, *Efficient differentiation of hepatocytes from human embryonic stem cells exhibiting markers recapitulating liver development in vivo.* Stem Cells, 2008. **26**: p. 894-902.

134. Agarwal, S., Holton KL, Lanza R, *Efficient differentiation of functional hepatocytes from human embryonic stem cells.* Stem Cells, 2008. **26**: p. 1117-1127.

135. Baharvand, H.H., S.M. Shahsavani, M. , *Differentiation of human embryonic stem cells into functional hepatocyte-like cells in a serum-free adherent culture condition.* . Differentiation, 2007.

136. Chen, X., et al., *Bioreactor expansion of human adult bone marroe-derived mesenchymal stem cells.* Stem Cells, 2006. **24**: p. 2052-59.

137. Gouon-Evans, V.B., L. Gadue, P. Nierhoff, D. Koehler, C.I. Kubo, A. Shafritz, D.A. Keller, G. , *BMP-4 is required for hepatic specification of mouse embryonic stem cell-derived definitive endoderm.* Nat Biotechnol, 2006. **24**(1402-11).

138. Hamazaki, T., et al., *Hepatic maturation in differentiating embryonic stem cells in vitro.* FEBS Lett, 2001. **497**(1): p. 15-9.

139. Yamada, T., et al., *In vitro differentiation of embryonic stem cells into hepatocyte-like cells identified by cellular uptake of indocyanine green.* Stem Cells, 2002. **20**(2): p. 146-54.

140. Rambhatla, L., et al., *Generation of hepatocyte-like cells from human embryonic stem cells.* Cell Transplant, 2003. **12**(1): p. 1-11.

141. Sancho-Bru, P., Najimi M, Caruso M, Pauwelyn K, Canz T, Forbes S, Roskams T, Ott M, Gehling U, Sokal E, Verfaillie CM, Muraca M, *Stem and progenitor cells for liver repopulation: can we standardise the process from bench to bedside?* Gut, 2009. **58**: p. 594-603.

142. Si-Tayeb, K., Noto FK, Nagaoka M, Li JX, Battle MA, Duris C, North PE, Dalton S, Duncan SA, *Highly efficient generation of human hepatocyte-like cells from induced pluripotent stem cells.* Hepatology, 2010. **51**: p. 297-305.

143. Song, Z., Cai J, Liu YX, Zhao DX, Yong J, Duo SG, Song XJ, Guo YS, Zhao Y, Qin H, Yin XL, Wu C, Che J, Lu SC, Ding MX, Deng HK, *Efficient generation of hepatocyte-like cells from human induced pluripotent stem cells.* Cell Research, 2009. **19**: p. 1233-1242.

144. Dalgetty, D., et al., *Progress and future challenges in stem cell-derived liver technologies.* Am J Pathol, 2009. **297**: p. 241-8.

145. Papoutsakis, E., *Fluid-mechanical damage of animal cells in bioreactors.* Trends Biotechnol., 1991. **9**: p. 427-437.

146. Bancel, S., Hu WS., *Confocal laser scanning microscopy examination of cell distrubution in macroporous microcarriers.* Biotechnol Prog, 1996. **12**(3): p. 398-402.

147. Lanza, R., Langer R., Vacanti J., *Tissue engineering bioreactors*, in *Principles of tissue engineering*. 2000, Elsevier Science (USA).

148. Prewett, T., et al., *Three dimensional modeling of T-24 human bladder carcinoma cell line: a new simulated microgravity culture system.* J. Tissue Cult. Methods, 1993. **15**: p. 29-36.

149. Schwarz, R., et al. , *Cell culture for three-dimensional modeling in rotating-wall vessels: an application of simulated microgravity.* J. Tissue Cult. Methods, 1992. **14**: p. 51-58.

150. Portner, R., et al., *Bioreactor design for tissue engineering.* J of Bioscience and bioengineering, 2005. **100**: p. 235-245.

151. Stojkovic, M., et al., *Derivation, growth and applications of human embryonic stem cells.* Reproduction, 2004. **128**(3): p. 259-67.

152. Cabrita, G.J., Ferreira, B. S., da Silva, C. L., Goncalves, R., Almeida-Porada, G., and Cabral, J. M., *Hematopoietic stem cells: from the bone to the bioreactor.* Trends in biotechnology, 2003. **21**: p. 233-240.

153. Noll, T., Jelinek, N., Schmid, S., Biselli, M., and Wandrey, C., *Cultivation of hematopoietic stem and progenitor cells:*

biochemical engineering aspects. Adv. Biochem. Eng. Biotechnol., 2002. **74**: p. 111-128.

154. Schubert, H., Garrn, I., Berthold, A., Knauf, W. U., Reufi, B., Fietz, T., and Gross, U. M., *Culture of haematopoietic cells in a 3-D bioreactor made of Al2O3 or apatite foam.* J. Mater. Sci. Mater. Medicine., 2004. **15**: p. 331-334.

155. Gilbertson, J., Sen A, Behie LA, Kallos MS, *Scaled-up production of mammalian neural precursor cell aggregates in computer-controlled suspension bioreactors.* Biotechnol Bioeng, 2006(94): p. 783-792.

156. McLeod, M., et al., *Transplantation of bioreactor-produced neural stem cells into the rodent brain.* Cell Transplant, 2006. **15**: p. 689-97.

157. Sen, A., Kallos, M. S., and Behie, L. A., *New tissue dissociation protocol for scaled-up production of neural stem cells in suspension bioreactors.* Tissue Engineering, 2004. **10**: p. 904-13.

158. Youn, B., et al., *Large-scale expansion of mammary epithelial stem cell aggregates in suspensio bioreactors.* Biotechnol Prog, 2005. **21**: p. 984-993.

159. Youn, B., et al., *Scale-up of breast cancer stem cell aggregate cultures to suspension bioreactors.* Biotechnol Prog, 2006. **22**(801-810).

160. Xie, Y., et al., *Three-dimensional flow perfusion culture system for stem cell proliferation inside the critical-size b-tricalcium phosphate scaffold.* Tissue Eng., 2006. **12**: p. 3535-3543.

161. Zhao, F., Pathi P, Grayson W, Xing Q, Locke BR, Ma T, *Effects of oxygen transport on 3D human mesenchymal stem cell metabolic activity in perfusion and static cultures: experiments and mathematical model.* Biotechnol Prog, 2005. **21**: p. 1269-1280.

162. Zhao, F., Ma, T., *Perfusion bioreactor system for human mesenchymal stem cell tissue engineering: dynamic cell seeding and construct development.* Biotechnol Bioeng, 2005. **91**: p. 482-493.

163. Zhao, F., et al. , *Effects of shear stress on 3D human mesenchymal stem cell construct development in a perfusion bioreactor system: experiments and hydrodynamic modelling.* Biotechnol Bioeng, 2007. **96**(584-595).

164. Bracchini, A., et al., *Three-dimensional perfusion culture of human bone marrow cells and generation of osteoinductive grafts.* Stem Cells, 2005. **23**: p. 1066-72.

165. Cormier, J., et al., *Expansion of undifferentiated murine embryonic stem cells as aggregates in suspension culture bioreactors.* Tissue Eng., 2006. **12**: p. 3233-45.

166. Fok, E., Zanstra PW, *Shear-controlled single step-mouse embryonic stem cell expansion and embryoid body-based differentiation.* Stem Cells, 2005. **23**: p. 1333-1342.

167. zur Nieden, N., et al., *Embryonic stem cells remain highly pluripotent following long term expansion as aggregates in suspension bioreactors.* J. Biotechnol., 2007.

168. Abranches, E., et al., *Expansion of mouse embryonic stem cells on microcarriers.* Biotechnol Bioeng, 2007. **96**: p. 1211-21.

169. LI, Y., et al., *Expansion of human embryonic stem cells in defined serum-free medium devoid of animal-derived products.* Biotechnol Bioeng, 2005. **91**: p. 688-98.

170. Lu, J., et al., *Defined culture conditions of human embryonic stem cells.* Proc Natl Acad Sci USA, 2006. **103**: p. 5688-93.

171. Ludwig, T., et al., *Derivation of human embryonic stem cells in defined conditions.* Nat Biotechnol, 2006. **24**: p. 185-7.

172. Schroeder, M., Neibruegge S, Werner A, Willbold E, Burg M, Ruediger M, Field LJ, Lehmann J, Zweigerdt R, *Differentiation and lineage selection of mouse embryonic stem cells in a stirred bench scale bioreactor with automated process control.* Biotechnol Bioeng, 2005. **92**: p. 920-933.

173. Dang, S., et al., *Efficiency of embryoid body formation and hepatopoietic development from embryonic stem cells in different culture systems.* Biotechnol Bioeng, 2002. **78**: p. 442-53.

174. Gerecht-Nir, S., et al., *Three-dimensional porous alginate scaffolds provide a conducive environment for generation of well-vascularized embryoid bodies from human embryonic stem cells.* Biotechnol Bioeng, 2004. **86**: p. 493-502.

175. Liu, H., Roy K., *Biomimetric three-dimensional cultures significantly increase hematopoietic differentiation efficacy of ESCs.* Tissue Eng., 205. **11**: p. 319-330.

176. Bauwens, C., Yin T, Dang S, Peerani R, Zandstra PW, *Development of a perfusion fed bioreactor for embryonic stem cell-derived cardiomyocyte generation: oxygen-mediated enhancement of cardiomyocyte output.* Biotechnol Bioeng, 2005. **90**: p. 452-461.

177. Gerecht-Nir, S., et al., *Bioreactor cultivation enhances the efficiency of human embryoid body formation and differentiation.* Biotechnol Bioeng, 2004. **86**: p. 493-502.

178. King, J., Miller WM, *Bioreactor development for stem cell expansion and controlled differentiation.* Current opinion in chemical biology, 2007. **11**: p. 394-398.

179. Cameron, C., Hu WS, Kaufman DS, *Improved development of human embryonic stem cell-derived embryoid bodies by stirred cessel cultivation.* Biotechnol Bioeng, 2006. **94**: p. 938-948.

180. Lock, L., Tzanakakis ES, *Expansion and differentiation of human embryonic stem cells to endoderm progeny in a microcarrier stirred-suspension culture.* Tissue Engineering Part A, 2009. **15**: p. 2051-2063.

181. Nie, Y., Bergendahl V, Hei D, Jones JM, Palecek SP, *Scalable culture and cryopreservation of human embryonic stem cells on microcarriers.* Biotechnol Prog, 2009. **25**: p. 20-31.

182. Oh, S., Chen AK, Mok Y, Chen XL, Lim UM, Chin A, Choo ABH, Reuveny S, *long-term microcarrier suspension cultures of human embryonic stem cells.* Stem Cell Research, 2009. **2**: p. 219-230.

183. Zhao, E., et al., *Enrichment of cardiomyocytes derived from mouse embryonic stem cells.* J Heart Lung Transplant, 2006. **25**: p. 664-674.

184. Li, Q., Liu Q, Cai H, Tan WS, *A comparative gene-expression analysis of CD34+ hepatopoietic stem and progenitor cells grown in static and stirred culture systems.* Cell Mol Biol Lett, 2006. **11**.

185. Liu, Y., Liu T, Fan X, Ma X, Cui Z, *Ex vivo expansion of hematopoietic stem cells derived from umblical cord blood in rotating wall vessel.* J Biotechnol, 2006. **124**: p. 592-601.

186. Frith, J., et al., *Dynamic three-dimensional culture methods enhance mesenchymal stem cell properties and increase therapeutic potential.* Tissue Eng Part C Methods, 2009.

187. Yu, Y., et al., *Ex vitro expansion of human placenta-derived mesenchymal stem cells in stirred bioreator.* Appl Biochem Biotechnol, 2009. **159**(1): p. 110-8.

188. Frauenschuh, S., Reichmann E, Ibold Y, Goetz PM, Sittinger M, Ringe J, *A microcarrier-based cultivation system for expansion of primary mesenchymal stem cells.* Biotechnology Progress, 2007. **23**: p. 187-193.

189. Jiang, Y., Jahagirdar, BN., Reinhardt, RL., Schwartz, RE., Keene, CD., Ortiz-Gonzalez, XR., Reyes, M., Lenvik, T., Lund, T., Blackstad, M., Du, J., Aldrich, S., Lisberg, A., Low, WC., Largaespada, DA., Verfaillie, CM., *Pluripotency of mesenchymal stem cells derived from adult marrow.* Nature, 2002. **418**: p. 41-49.

190. Muguruma, Y., et al, *In vivo and in vitro differentiation of myocytes from human bone marrow-derived multipotent progenitor cells.* Exp Hematol, 2003. **31**(12): p. 1323-1330.

191. Ross, J., Hong, Z., Willenbring, B., Zeng, L., Isenberg, B., Lee, EH., Reyes, M., Keirstead, S., Weir, EK., Tranquillo, RT., Verefaillie, CM., *Cytokine induced differentiation of adult multipotent progenitor cells into fuctional smooth muscle cells.* J. Clin. Invest., 2006. **116**: p. 3139-3149.

192. Zeng, L., Rahrmann E, Hu Q, Lund T, Sandquist L, Felton M, O'Brien TD, Zhang J, Verfaillie C, *Multipotent adult progenitor cells from swine bone marrow.* Stem Cells, 2006. **25**(9): p. 2387.

193. Javazon, E., Beggs KJ, Flake AW, *Mesenchymal stem cells: paradoxes of passaging.* Exp. Hematol, 2004. **32**: p. 414-425.

194. Forsyth, N., Musio A, Vezzoni P, Simpson A, Noble BS, McWhir J, *Physiologic oxygen enhances human embryonic stem cell clonal revocery and reduces chromosomal abnormalities.* Cloning Stem Cells, 2006. **8**: p. 16-23.

195. Gibbons, J., Hewitt E, Gardner DK, *Effects of oxygen tension on the establishment and lactate dehydrogenase activity of murine embryonic stem cells.* Cloning Stem Cells, 2006. **8**: p. 117-122.

196. Ezashi, T., Das P, Roberts RM, *Low O_2 tensions and the prevention of differentiation of hES cells.* Proc Natl Acad Sci USA, 2005. **102**: p. 4783-4788.

197. Zandstra, P., Nagy A, *Stem cell bioengineering.* Annu. Rev. Biomed. Eng., 2001. **3**: p. 275-305.

198. Ogawa, M., *Differentiation and proliferation of hematopoietic stem cells.* Blood, 1993. **81**(11): p. 2844.

199. Lennon, D., Edmison JM, Caplan AI, *Cultivation of rat marrow-derived mesenchymal stem cells in reduced oxygen tension: effects on in vitro and in vivo osteochondrogenesis.* J Cell Physiol, 2001. **187**: p. 345-55.

200. Breyer, A., Estharabadi N, Oki M, Ulloa F, Nelson-Holte M, Lien L, Jiang Y, *Multipotent adult progenitor cell isolation and culture procedure.* Exp Hematol, 2006. **34**(11): p. 1596-1601.

201. Pesce, M., Scholer HR, *Oct-4: gatekeeper in the beginnings of mammaliam development.* Stem Cells, 2001. **19**(4): p. 271-278.

202. Wiesener, M., Jurgensen JS, Rosenberger C, Scholze CK, Horstrup JH, Warnecke C, Mandriota S, Bechmann I, Frei UA, Pugh CW, *Widespread hypoxia-inducible expression of HIF-2a in distinct cell populations of different organs.* FASEB J, 2003. **17**: p. 271-273.

203. Covello, K., Kehler J, Yu HW, Gordan JD, Arsham AM, Hu CJ, Labosky PA, Simon MC, Keith B, *HIF-2 alpha regulates Oct-4: effects of hypoxia on stem cell function, embryonic development and tumor growth.* Genes Dev., 2006. **20**(5): p. 557-570.

204. Boyer, L., Lee TI, Cole MF, Johnstone SE, Levine SS, Zucker JP, Guenther MG, Kumar RM, Murray HL, Jenner RG, et al, *Core transcriptional regulatory circuitry in human embryonic stem cells.* Cell, 2005. **122**: p. 947-956.

205. Khan, W., et al, *Hypoxic conditions increase hypoxia-inducible transcription factor 2 alpha and enhance chondrogenesis in stem cells from the infrapatellar fat pad of osteoarthritis patients.* Arthritis Res Ther, 2007. **9**(3).

206. Pauwelyn, K., Sancho-Bru P, Subramanian K,et al., *Differentiation of rat multipotent adult progenitor cells towards the hepatic lineage by recapitulating liver embryology.* Hepatology, 2007. **46**(4): p. 804A.

207. D'Ippolito, G., Diabira S, Howard GA, Roos BA, Schiller PC, *Low oxygen tension inhibits osteogenic differentiation and enhances stemness of human MIAMI cells.* Bone, 2006. **39**: p. 513-522.

208. Grayson, W., Zhao F, Izadpanah R, Bunnell B, Ma T, *Effects of hypoxia on human mesenchymal stem cell expansion and plasticity in 3D constructs.* J Cell Physiol, 2006. **207**: p. 331-339.

209. Grayson, W., Zhao F, Bunnell B, Ma T, *Hypoxia enhances proliferation and tissue formation of human mesenchymal stem cells.* Biochem. Biophys. Res.Commun., 2007. **358**(3): p. 948-953.

210. Li, X., Yang L, Liu T, Ma X, Cui Z, *Effects of hypoxia on rat mesenchymal stem cells.* Cell Res, 2008. **18**.

211. Goncalo, J., Ferreira BS, da Silva CL, Goncalves R, Almeida-Porada G, Cabral JMS, *Hematopoietic stem cells: from the bone to the bioreactor.* Trends in biotechnology, 2003. **21**(5): p. 233-240.

212. Michiels, C., Minet E, Mottet D, Raes M, *Regulation of gene expression by oxygen: NF-kappaB and HIF-1, two extremes.* Free Radic Biol Med, 2002. **33**: p. 1231-42.

213. Mostafa, S., et al, *Oxygen tension modulates the expression of cytokine receptors, transcription factors, and lineage-specific markers in cultured human megakaryocytes.* Exp Hematol, 2001. **29**: p. 873-883.

214. Griffith, L.G. and M.A. Swartz, *Capturing complex 3D tissue physiology in vitro.* Nat Rev Mol Cell Biol, 2006. **7**(3): p. 211-24.

215. Keller, P.J., F. Pampaloni, and E.H. Stelzer, *Life sciences require the third dimension.* Curr Opin Cell Biol, 2006. **18**(1): p. 117-24.

216. Pampaloni, F., E.G. Reynaud, and E.H. Stelzer, *The third dimension bridges the gap between cell culture and live tissue.* Nat Rev Mol Cell Biol, 2007. **8**(10): p. 839-45.

217. Yamada, K.M. and E. Cukierman, *Modeling tissue morphogenesis and cancer in 3D.* Cell, 2007. **130**(4): p. 601-10.

218. Liu, T., et al., *Hepatic Differentiation of Mouse Embryonic Stem Cells in Three-dimensional Polymer Scaffolds.* Tissue Eng Part A, 2009.

219. Ong, S.M., et al., *Engineering a scaffold-free 3D tumor model for in vitro drug penetration studies.* Biomaterials, 2009.

220. Ng, E.S., et al., *Forced aggregation of defined numbers of human embryonic stem cells into embryoid bodies fosters robust, reproducible hematopoietic differentiation.* Blood, 2005. **106**(5): p. 1601-3.

221. Kelm, J.M., et al., *Method for generation of homogeneous multicellular tumor spheroids applicable to a wide variety of cell types.* Biotechnol Bioeng, 2003. **83**(2): p. 173-80.

222. Kurosawa, H., *Methods for inducing embryoid body formation: in vitro differentiation system of embryonic stem cells.* J Biosci Bioeng, 2007. **103**(5): p. 389-98.

223. Ralston, A. and J. Rossant, *Genetic regulation of stem cell origins in the mouse embryo.* Clin Genet, 2005. **68**(2): p. 106-12.

224. Guan, K., et al., *Pluripotency of spermatogonial stem cells from adult mouse testis.* Nature, 2006. **440**(7088): p. 1199-203.

225. Kurosawa, H., et al., *A simple method for forming embryoid body from mouse embryonic stem cells.* J Biosci Bioeng, 2003. **96**(4): p. 409-11.

226. Hevehan, D.L., E.T. Papoutsakis, and W.M. Miller, *Physiologically significant effects of pH and oxygen tension on granulopoiesis.* Exp Hematol, 2000. **28**(3): p. 267-75.

227. Mostafa, S.S., W.M. Miller, and E.T. Papoutsakis, *Oxygen tension influences the differentiation, maturation and apoptosis of human megakaryocytes.* Br J Haematol, 2000. **111**(3): p. 879-89.

228. Purpura, K.A., et al., *Soluble Flt-1 regulates Flk-1 activation to control hematopoietic and endothelial development in an oxygen-responsive manner.* Stem Cells, 2008. **26**(11): p. 2832-42.

229. Rizzino, A., *Sox2 and Oct-3/4: A Versatile Pair of Master Regulators that Orchestrate the Self-renewal and Pluripotency of Embryonic Stem Cells by Functioning as Molecular Rheostats.* Wiley Interdiscip Rev Syst Biol Med, 2009. **1**(2): p. 228-236.

230. Ulloa-Montoya, F., *Characterization and comparative transcriptome analysis of multipotent adult progenitor cells*, in *Department of chemical engineering and materials science*. 2006, University of Minnesota: Minneapolis.

231. Allain, J., Dagher I, Mahieu-Caputo D, Loux N, Andreoletti M, Westerman K, Briand P, Franco D, Leboulch P, Weber A, *Immortalizatiion of a primate bipotent epithelial liver stem cell.* Proc Natl Acad Sci USA, 2002. **99**: p. 3639-3644.

232. Cai, J., Ito M, Weterman KA, Kobayashi N, Leboulch P, Fox IJ, *Construction of a non-tumorigenic rat hepatocyte cell line for transplantation: reversal of hepatocyte immortalization by site-specific excision of the SV40 T antigen.* J Hepatol, 2000. **33**: p. 701-708.

233. Wege, H., Chui MS, Le HT, Strom SC, Zern MA, *In vitro expansion of human hepatocytes is restricted by telomere-dependent replicative aging.* Cell Transplant, 2003. **12**: p. 897-906.

234. Fernandes, A., Fernandes TG, Diogo MM, *Mouse embryonic stem cell expansion in a microcarrier-based stirred culture system.* J Biotechnol, 2007. **132**: p. 227-236.

235. Chiu, B., Wan JZM, Abley D, *Induction of vascular endothelial phenotype and cellular proliferation from human cord blood stem cells cultured in simulated microgravity.* ACTA Astronautica, 2005. **56**: p. 918-922.

236. Kehoe, D., Jing DH, Lock LT, Tzanakakis ES, *Scalable stirred-suspension bioreactor culture of human pluripotent stem cells.* Tissue Engineering Part A, 2010. **16**: p. 405-421.

237. Yang, Y., Rossi FMV, Putnins EE, *Ex vivo expansion of rat bone marrow mesenchymal stromal cells on microcarrier beads in spin culture.* Biomaterials, 2007. **28**: p. 3110-3120.

238. Tao, T., Ji GY, Hu WS, *Human fibroblastic cells attach to controlled-charge and gelating-coated microcarriers at different rates.* J of Biotechnology, 1987. **6**(1): p. 9-12.

239. Walkup, M.H., et al., *Endothelial cell interactions with hepatic progenitor cells affect proliferation and differentiation.* Journal of the American College of Surgeons, 2007. **205**(3, Supplement 1): p. S64-S64.

240. Geraud, C., et al., *Liver sinusoidal endothelium: A microenvironment dependent differentiation program in rat including the novel junctional protein Leda-1*. Hepatology, 2010. **9999**(999A): p. NA: published online.

241. Suzuki, A.e.a., *In vitro production of functionally mature hepatocytes from prospectively isolated hepatic stem cells.* Cell Transplant, 2003. **12**(5): p. 469-73.

242. Dan, Y., et al., *Isolation of multipotent progenitor cells from human fetal liver capable of differentiatng into liver and mesenchymal lineages.* Proc Natl Acad Sci USA, 2006. **103**(26): p. 9912-7.

243. Billing, D., Clark JM, Ewell AJ, Carter CM, Gebb C, *the seperation of harvested cells from microcarriers: a comparison of methods.* Dev Biol Stand, 1983. **55**: p. 67.

244. Gao, N., Wang HJ, Yang EH *An experimental study on ferromagnetic nickel nanowires functionalized with antibodies for cell separation* Nanotechnology, 2010. **21**: p. 105107.

245. Yang, H., Seo JH, Kim BS *Serial Propagation of Cells on Thermo-Sensitive Microcarrier.* Tissue engineering and regerative medicine, 2009. **6**: p. 1262-1267.

246. Xu, C., et al., *Feeder free growth of undifferentiated human embryonic stem cells.* Nat Biotechnol, 2001. **19**: p. 971-974.

247. Watanabe, K., et al., *A ROCK inhibitor permits survival of dissociated human embryonic stem cells.* Nat Biotechnol, 2007. **25**: p. 681-6.

APPENDIX

List of Abbreviations used.

Abbreviation	*Full name*
ESC	Embryonic stem cell
iPSC	Induced pluripotent stem cells
HSC	Hematopoietic stem cells
MSC	Mesenchymal stem cells
ICM	Inner cell mass
MEF	Mouse embryonic fibroblast
SSEA	Stage specific embryonic antigen
TRA	Transfer region
Oct4	Octamer binding protein 4
Nanog	Homeobox transcription factor Nanog
LIF	Leukemia inhibitory factor
Stat	Singal transducer and activator of transcription
Myc	v-myc myelocytomatosis viral oncogene homolog
ECM	Extracellular matrix
Klf4	Kruppel like factor 4
Rex1	RNA exonuclease 1 homolog
Lin28	Lin-28 homolog
hBMSC	Human bone marrow derived stem cells
MAPC	Multipotent adult progenitor cells
MAIMI	Marrow isolated adult multilineage inducible
VSEL	Very small ES like
MRPC	Multipotent renal progenitor cells
USSC	Unrestricted somatic stem cells
EB	Embryoid bodies
MHC	Major histocompatibility complex
FBS	Fetal bovine serum
cMet	Cmet proto oncogene (hepatocyte growth factor receptor)
BMP	Bone morphogenic protein
NTRK3	Neurotrophic tyrosine kinase receptor 3
Sca1	Stem cell antigen 1
Afp	Alpha-fetoprotein
CK	Cytokeratin
MyoD	Myogenic differentiation
Myf5	Myogenic factor 5
Gfap	Glial fibrillary acidic protein

SDF	Stromal cell derived factor
HGF	Hepatocyte growth factor
Pax	Paired box
GlyA	Glycophorin A
Ter119	Erythoid cell marker
Thy	Thy-1 cell surface antigen
EPCAM	Epithelial cell adhesion molecule
c-kit	Hardy-Zuckerman 4 feline sarcoma viral oncogene homolog
Tef	Thryotrophic embryonic factor
Pitx2	Paired like homeodomain 2
VEGF	Vascular endothelial growth factor
Wnt3a	Wingless-type MMTV integration site family, member 3a
TGF	Transforming growth factor
SMC	Smooth muscle cells
Lhx1	LIM homeobox 1
PS	Primitive streak
Cer1	Cerberus 1, cysteine knot superfamily, homolog
Smad	SMAD family member
NF1	Nuclear factor1
STM	Septum transversum mesenchyme
OC2	One cut homeobox
c-Jun	Jun oncogene
K-ras	Kirstin rat sarcoma viral oncogene homolog
Xbp1	X-box binding protein 1
Tbx3	T-box 3
TNF	Tumor necrosis factor
Aat	Alpha1-antitypsin
G6p	Glucose-6-phosphatase
Arg1	Liver specific arginase
Pepck	Phosphoenolpyruvate carboxykinase
Tat	Tyrosine aminotransferase
C/EBP	CCAAT enhancer-binding protein alpha
Dlk	Delta-like kinase
Prox1	Prospero-related homeobox
C-Met	HGF-receptor
Cxcr4	CXC chemokine receptor 4
FGF	Fibroblast growth factor
Gata	GATA family of zinc finger-containing transcription factors
Gsc	Goosecoid
Hex	Hematopoietically expressed homeobox
Hnf	Hepatocyte nuclear factor

Sox	SRY-related homolog
Ttr	Transthyretin
Mixl1	Mix gene homologue
Flk1	VEGF-receptor II
Pdx1	Pancreatic duodenal homeobox gene
Sm22	Smooth muscle 22
αSMA	Alpha-smooth muscle actin
vWF	Von Willebrand factor
Cyp	Cytochrome P450
ASGPR	Asialoglycoprotein receptor
OSM	Oncostatin M
Mrp	Multidrug resistant protein
Bsep	Bile salt export pump
Cx32	Gap junction beta-1 protein
Tm4sf2	Transmembrane 4 superfamily, member 2
Krt	Keratin
Adh1C	Alcohol dehydrogenase 1C (class I), gamma polypeptide
ApoF	Apolipoprotein F
CPSase I	Carbamoyl-phosphate synthetase 1, mitochondrial
HepPar1	Hepatocyte Paraffin 1
STRV	Slow-turning lateral vessel
HARV	High-aspect-ratio vessel
DMEM	Dulbecco's Modified Eagle medium
PDGF	Platelet derived growth factor
EGF	Epidermal growth factor
PFA	Paraformaldehyde
Epas1	Endothelial PAS domain protein 1
Enos	Endothelial nitric oxide sunthase
Mgst	Microsomal glutathione S-transferase 1
Lmo3	LIM domain only 3
Tcfec	Transcription factor EC
Maf	Musculoaponeurotic fibrosarcoma oncogene homolog
Leda1	Liver endothelial differentiation associated protein 1
Cdx	Caudal related homeobox